

1. Report No. FHWA/TX-86/05+401-1		2. Government Accession No.		3. Recipient's Catalog No.	
4. Title and Subtitle VERY EARLY POST-TENSIONING OF PRESTRESSED CONCRETE PAVEMENTS				5. Report Date June 1985	
				6. Performing Organization Code	
7. Author(s) J. Scott O'Brien, Ned H. Burns, and B. Frank McCullough				8. Performing Organization Report No. Research Report 401-1	
9. Performing Organization Name and Address Center for Transportation Research The University of Texas at Austin Austin, Texas 78712-1075				10. Work Unit No.	
				11. Contract or Grant No. Research Study 3-8-84-401	
				13. Type of Report and Period Covered Interim	
12. Sponsoring Agency Name and Address Texas State Department of Highways and Public Transportation; Transportation Planning Division P. O. Box 5051 Austin, Texas 78763				14. Sponsoring Agency Code	
15. Supplementary Notes Study conducted in cooperation with the U. S. Department of Transportation, Federal Highway Administration. Research Study Title: "Prestressed Concrete Pavement Design—Design and Construction of Overlay Applications"					
16. Abstract  <p>Temperature and shrinkage cracks occur in long prestressed concrete pavements during the first night after casting, before the post-tensioning operation is performed. Previous post-tensioning schedules and current design criteria by ACI, PTI, and AASHTO do not guarantee that compression can be introduced before the cracks form.</p> <p>This report (1) presents a more detailed discussion of the problem of temperature and shrinkage cracking, (2) reviews some of the literature on early concrete strength and anchorage zone stresses, (3) describes tests on the capacity of anchorage zone for very early post-tensioning, and (4) recommends a post-tensioning schedule accompanied by design aids. Experimental test variables included slab thickness, strand spacing, anchor size, and time from casting.</p>					
17. Key Words  post-tension, anchorage zone, pavements, concrete strength, early, cracks			18. Distribution Statement  No restrictions. This document is available to the public through the National Technical Information Service, Springfield, Virginia 22161.		
19. Security Classif. (of this report) Unclassified		20. Security Classif. (of this page) Unclassified		21. No. of Pages 184	22. Price

VERY EARLY POST-TENSIONING OF PRESTRESSED CONCRETE PAVEMENTS

by

J. Scott O'Brien  
Ned H. Burns  
B. Frank McCullough

Research Report Number 401-1

Prestressed Concrete Pavement Design --  
Design and Construction of Overlay Applications  
Research Project 3-8-84-401

conducted for

Texas State Department of Highways  
and Public Transportation Research

in cooperation with the  
U.S. Department of Transportation  
Federal Highway Administration

by the

Center for Transportation Research  
Bureau of Engineering Research  
The University of Texas at Austin

June 1985

The contents of this report reflect the views of the authors, who are responsible for the facts and the accuracy of the data presented herein. The contents do not necessarily reflect the official views or policies of the Federal Highway Administration. This report does not constitute a standard, specification, or regulation.

## PREFACE

This report presents the results of tests performed to determine the very early post-tensioning capacity of prestressed concrete pavements and gives a method to determine the timing and the magnitude of post-tensioning force that can be applied. The purpose of this work is to determine if post-tensioning within 24 hours of casting will prevent early temperature and shrinkage cracks.

This work is a part of Research Project 3-8-84-401, entitled "Prestressed Concrete Pavement Design -- Design and Construction of Overlay Application." The study described was conducted at the Phil M. Ferguson Structural Engineering Laboratory as a part of the overall research program for the Center for Transportation Research, Bureau of Engineering Research of The University of Texas at Austin. The work was sponsored jointly by the Texas Department of Highways and Public Transportation and the Federal Highway Administration under an agreement with The University of Texas at Austin and the Texas Department of Highways and Public Transportation.

Special thanks to Marc Badoux, Tim Bradberry, Joe Maffei, Neil Cable, Troy Madeley, Alberto Mendoza, and to all the other Graduate Research Assistants who contributed many hours to helping with the testing procedure. Without their generous assistance this study would not have been possible.

This page replaces an intentionally blank page in the original.

-- CTR Library Digitization Team

## LIST OF REPORTS

Report No. 401-1, "Very Early Post-tensioning of Prestressed Concrete Pavements," by J. Scott O'Brien, Ned H. Burns and B. Frank McCullough, presents the results of tests performed to determine the very early post-tensioning capacity of prestressed concrete pavement slabs, and gives a method to determine the timing and the magnitude of post-tensioning force that can be applied within the first 24 hours after casting.

This page replaces an intentionally blank page in the original.

-- CTR Library Digitization Team

## ABSTRACT

Temperature and shrinkage cracks occur in long prestressed concrete pavements during the first night after casting, before the post-tensioning operation is performed. Previous post-tensioning schedules and current design criteria by ACI, PTI, and AASHTO do not guarantee that compression can be introduced before the cracks form.

This report (1) presents a more detailed discussion of the problem of temperature and shrinkage cracking, (2) reviews some of the literature on early concrete strength and anchorage zone stresses, (3) describes tests on the capacity of anchorage zone for very early post-tensioning, and (4) recommends a post-tensioning schedule accompanied by design aids. Experimental test variables included slab thickness, strand spacing, anchor size, and time from casting.

KEYWORDS: Post-tension, anchorage zone, pavements, concrete strength, early, cracks.

This page replaces an intentionally blank page in the original.

-- CTR Library Digitization Team

## SUMMARY

Temperature and shrinkage cracks may occur in long prestressed concrete pavements during the first night after casting, before the post-tensioning operation is performed. Previous post-tensioning schedules and current design criteria by ACI, PTI, and AASHTO do not guarantee that compression can be introduced before the cracks form.

This report (1) presents a more detailed discussion of the problem of temperature and shrinkage cracking, (2) reviews some of the literature on early concrete strength and anchorage zone stresses, (3) describes tests on the capacity of anchorage zone for very early post-tensioning, and (4) gives a method to determine the timing and the magnitude of post-tensioning force that can be applied, together with design aids. Experimental test variables included slab thickness, strand spacing, anchor size and time from casting.

Experimental data show that, with the typical pavement concrete mix design, partial post-tensioning may safely be applied within the first 12 to 24 hours after casting. A new post-tensioning schedule for early operation is furnished together with design aids for the engineer. Emphasis is placed on post-tensioning to keep sections uncracked.

This page replaces an intentionally blank page in the original.

-- CTR Library Digitization Team

## IMPLEMENTATION STATEMENT

This report presents the most important findings of an experimental investigation of very early post-tensioning of prestressed concrete pavements to prevent temperature and shrinkage cracks that form during the first night after casting. A suggested early post-tensioning strategy to prevent these cracks is presented together with design aids.

The study and the previous prestress demonstration projects show that the current ACI, PTI, and AASHTO allowable post-tensioning loads and the previous post-tensioning schedules are inadequate to insure crack prevention. By using the recommended post-tensioning schedule, it should be possible to keep a crack-free pavement during the initial curing period.

This page replaces an intentionally blank page in the original.

-- CTR Library Digitization Team

## TABLE OF CONTENTS

PREFACE . . . . .	iii
LIST OF REPORTS . . . . .	v
ABSTRACT . . . . .	vii
SUMMARY . . . . .	ix
IMPLEMENTATION STATEMENT . . . . .	xi
<b>CHAPTER 1. INTRODUCTION</b>	
Background . . . . .	1
History . . . . .	1
Problem of Early Cracking . . . . .	2
Objective and Scope . . . . .	2
Outline of Chapters . . . . .	3
<b>CHAPTER 2. CRACKING PROBLEM AND SOLUTIONS</b>	
Temperature and Shrinkage Cracks . . . . .	5
Causes . . . . .	5
Analysis of Stresses . . . . .	6
Solutions . . . . .	11
Shrinkage Coefficient . . . . .	11
Temperature Drop . . . . .	12
Friction Coefficient . . . . .	12
Slab Length . . . . .	14
Very Early Post-Tensioning . . . . .	14
Anchorage Zone . . . . .	14
Definition . . . . .	15
Stresses . . . . .	15

CHAPTER 3. LITERATURE REVIEW

Anchorage Zone Stresses . . . . .	17
Elastic Solutions . . . . .	17
Photoelasticity . . . . .	26
Testing . . . . .	26
Finite Element Analysis . . . . .	29
Other Solution . . . . .	29
Early Age Concrete Strength . . . . .	29
Friberg . . . . .	30
Maturity Factor . . . . .	30
Current Design Procedures . . . . .	33
ACI . . . . .	33
PTI . . . . .	35
AASHTO . . . . .	35
Previous Projects . . . . .	35

CHAPTER 4. EXPERIMENTAL PROGRAM

Purpose . . . . .	37
Description of Test . . . . .	37
General . . . . .	37
Experimental Parameters . . . . .	38
Other Parameters Measured . . . . .	43
Testing Apparatus . . . . .	45
Testing Scheme . . . . .	48
Series I . . . . .	48
Series II . . . . .	48
Series III . . . . .	48

CHAPTER 5. DISCUSSION OF TESTS

Specimen Designation . . . . .	51
Summary of Results . . . . .	51
Concrete Strength . . . . .	52
Behavior of Slabs . . . . .	52
Summary of Each Series . . . . .	63
Series I . . . . .	63
Series II . . . . .	66
Series III . . . . .	67

CHAPTER 6. DISCUSSION OF THE EFFECTS OF VARIABLES

General . . . . .	69
Concrete Strength . . . . .	69
Time Since Batch . . . . .	69
Maturity . . . . .	76
Comparison of Strength Gain . . . . .	76
Slab Tests . . . . .	76
Effects of Variables on Cracking Load . . . . .	83
Ultimate Load . . . . .	86
Comparison of Results to Expected Values . . . . .	86
Concrete Strength . . . . .	91
Cracking Load . . . . .	91

CHAPTER 7. RECOMMENDATIONS FOR FIELD USE

General . . . . .	101
Data Regression . . . . .	101
Design Aids . . . . .	101
Limitations . . . . .	103
Equation . . . . .	103
Table . . . . .	104
Graphs . . . . .	104
Reliability Study . . . . .	104
Calculation Procedure . . . . .	109
Example . . . . .	109
Solution . . . . .	110
Determine the Tensile Stress . . . . .	110
Determine $P_{cr}$ . . . . .	110
Determine $P_{allowable}$ . . . . .	110
Check . . . . .	111

CHAPTER 8. CONCLUSIONS AND RECOMMENDATIONS

General . . . . .	113
Conclusions . . . . .	113
Concrete Strength Conclusions . . . . .	113
Slab Cracking Load Conclusions . . . . .	113
Recommendations for Further Research . . . . .	114

REFERENCES . . . . .	115
----------------------	-----

APPENDICES

Appendix A. Concrete Batch Mix . . . . . 119

Appendix B. Detailed Test Results . . . . . 123

Appendix C. Design Aids Using Concrete Compression Strength . 163

## CHAPTER 1. INTRODUCTION

### BACKGROUND

In one of the first investigations of the use of prestressed concrete pavements for highways in the U.S, Friberg (Ref 1) stated the purpose for prestressed pavement:

Strength properties of concrete are not fully utilized in conventional concrete pavements. Stresses are limited to the concrete's relatively low strength in bending; as a result, pavement deflections as limited by strains are generally less than could be accommodated by subgrades. Effective compressive prestress in pavements might make possible thinner pavements, more effective pavement design, long uncracked slabs, and improved performance.

This statement, made in 1962, explains why research continues, in an effort to perfect the design and construction of prestressed concrete pavements.

### History

Investigation of prestressed concrete as a viable material for pavement began in 1943, in England, and continues today (Ref 2). During the 1940's and 1950's various systems of post-tensioning were applied to both highway pavements and airport runways.

Prestressed highway pavement was constructed in the United States in 1971, in Delaware (Ref 3). Later that year a 3,200-foot demonstration project was built at Dulles International Airport in Virginia. Another demonstration project consisting of 2.5 miles of prestressed pavement, was constructed in 1973 in Pennsylvania (Ref 4). Two other projects exist in the

U.S., one in Mississippi, built in 1976, and the other in Arizona, built in 1977.

### Problem of Early Cracking

One of the attractions of prestressed concrete pavement over conventional concrete pavement is the large reduction in the number of joints. The span between joints ranged from 400 to 760 feet in the four major U.S. projects.

However this increased length of span between joints causes a major problem. During the first night after casting, when the temperature drops, the pavement must contract. The distance from the middle of the slab to the nearest joint, where movement is possible, is so long that, as the concrete tries to move, tensile stresses build up because of the frictional resistance of the subgrade. Then, if these tensile stresses exceed the tensile strength of the concrete, a crack forms.

Cracks occurring during the first night after casting have been reported in the Mississippi, Arizona, and Virginia projects. Mississippi reported cracks in 24 of 58 slabs. Although most of the cracks were closed after post-tensioning, keeping sections uncracked is a primary reason for prestressing pavements.

### OBJECTIVE AND SCOPE

This study is part of an investigation to develop a design procedure for prestressed concrete pavement and construct two demonstration projects near Waco and Gainesville, Texas. In this study, a few solutions to the problem of temperature and shrinkage cracks are briefly mentioned, and one particular solution, very early post-tensioning, is studied in depth and discussed.

This report includes (1) a closer look at the problem of cracking, (2) an investigation of the nature of the stresses that result from post-tensioning, (3) experimental work on both the strength of concrete at very early ages and the post-tensioning force that will cause cracking near the

post-tension anchorage at very early ages, and (4) recommendations on early post-tensioning.

#### OUTLINE OF CHAPTERS

Chapter 2 takes a closer look at the problem of temperature and shrinkage cracks, including the causes for the cracks, the magnitude of the tensile stresses that develop, and a brief discussion of various ways to avoid the cracks. Chapter 2 also contains an introduction to anchorage zones and the types of stresses that develop in them.

Chapter 3 is a literature review of both anchorage zones stresses and early age concrete strength, includes the current design procedures for anchorage zones and allowable prestress loads.

Chapter 4 discusses the experimental program and describes the test set-up and testing technique, and includes an explanation of the experimental parameters.

Chapter 5 is a summary of the test results for both early age concrete strength and anchorage zone behavior.

Chapter 6 contains a discussion of the effects of the experimental parameters on the slab anchorage zone cracking load. Also, the cracking loads are compared to expected results.

Chapter 7 gives recommendations for field use through the use of design aids and a reliability study.

Chapter 8 contains the conclusions and recommendations.

This page replaces an intentionally blank page in the original.

-- CTR Library Digitization Team

## CHAPTER 2. CRACKING PROBLEM AND SOLUTIONS

This chapter describes the cause of temperature and shrinkage cracks, outlines some potential solutions, and discusses their feasibility. Also, anchorage zone stresses caused by post-tensioning are introduced.

### TEMPERATURE AND SHRINKAGE CRACKS

As previously mentioned, several projects in the past have reported cracking during the first night after concrete placement. It is important to understand the causes of these cracks before proceeding to solutions.

#### Causes

Two basic and simple factors lead to the cracking of slabs during the first night:

- (1) tensile stresses build-up in the slab and
- (2) these tensile stresses exceed the concrete tensile strength capacity.

The development of tensile stresses is due to frictional restraint of the concrete contraction caused by moisture and temperature changes.

The major factor in developing tensile stresses is the drop in temperature. In the basic process that leads to the development of these stresses,

- (1) the concrete temperature drops,
- (2) the slab tries to move due to thermal action,
- (3) friction between the slab and subgrade restrains the slab, and
- (4) the restraining force causes tension.

### Analysis of Stresses

As part of a Ph.D. dissertation at The University of Texas at Austin, Alberto Mendoza-Diaz has been working on the analysis and design of prestressed concrete pavements. Part of the analysis is concerned with the environmental effects on the pavement movement and stress. Mendoza-Diaz modified a computer program for jointed pavement developed by Vallejo and McCullough (Ref 5), to consider prestressed concrete pavement.

When the slab temperature drops and moisture is lost during drying shrinkage of the concrete the slab contracts, with the local movement increasing from zero at the center of the slab to a maximum at the slab edge. The frictional forces present cause restraint to the movement and the build-up of tensile stresses, which increase from zero at the free edge to a maximum at the center of the slab length. The relationship of movement, restraint, and stress may be seen in Fig 2.1. Figure 2.2 shows a free body diagram of a slab element.

Stress in the slab is calculated by finding the strain and multiplying by Young's modulus. The strain depends on the amount of free movement and the amount of restraint. The rate of movement,  $\frac{dz}{dx}$ , of a slab element is expressed by

$$dz = dx \left( \alpha \Delta T - \frac{F_c}{E} \right)$$

where

- $\alpha$  = thermal coefficient of expansion for concrete, °F,
- $\Delta T$  = change in concrete temperature, °F,
- $F_c$  = concrete stress due to restraint, psi, and
- $E$  = Young's Modulus for concrete, psi.

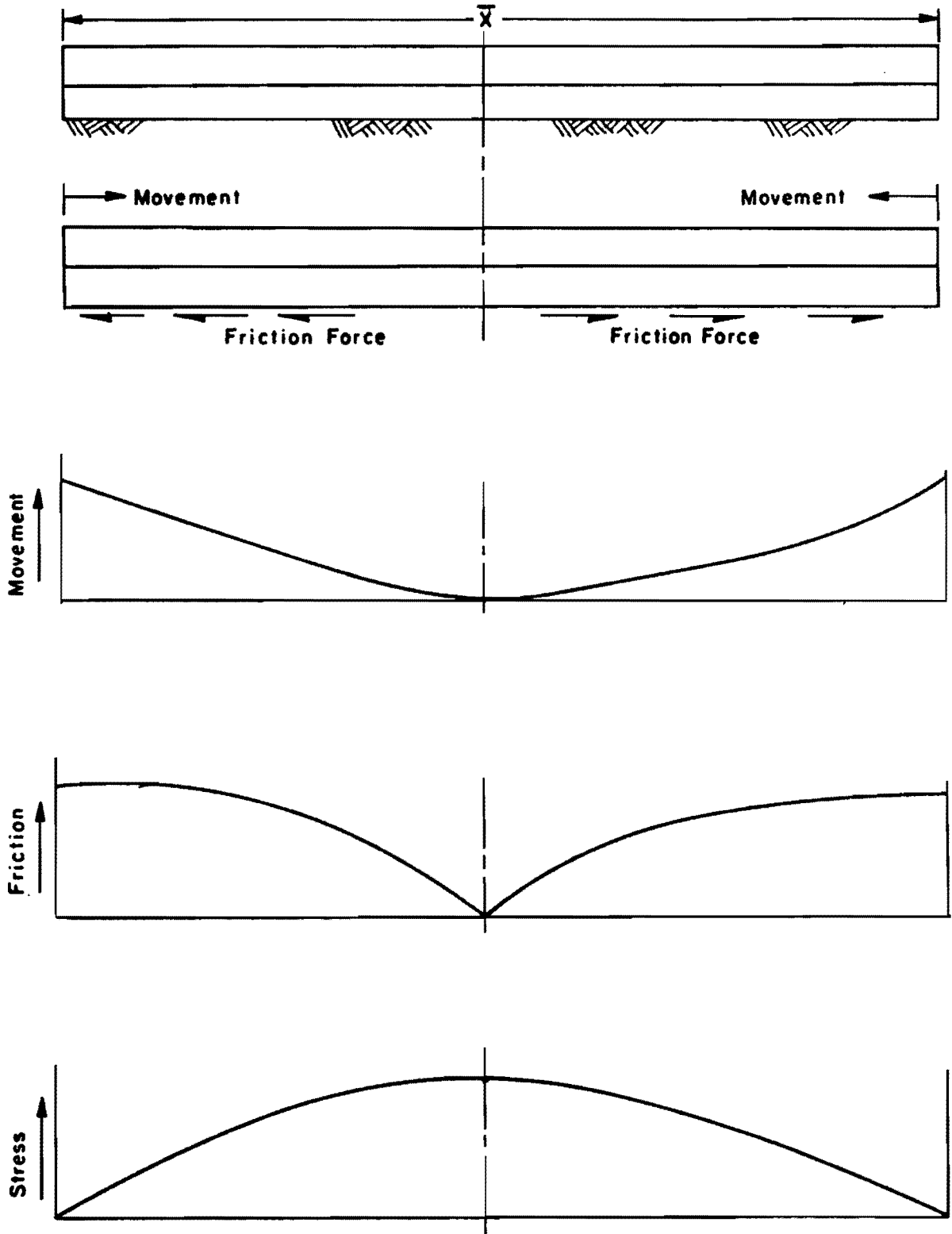


Fig 2.1. Effects of the restraint provided by the subbase on the concrete slab (from Ref 5).

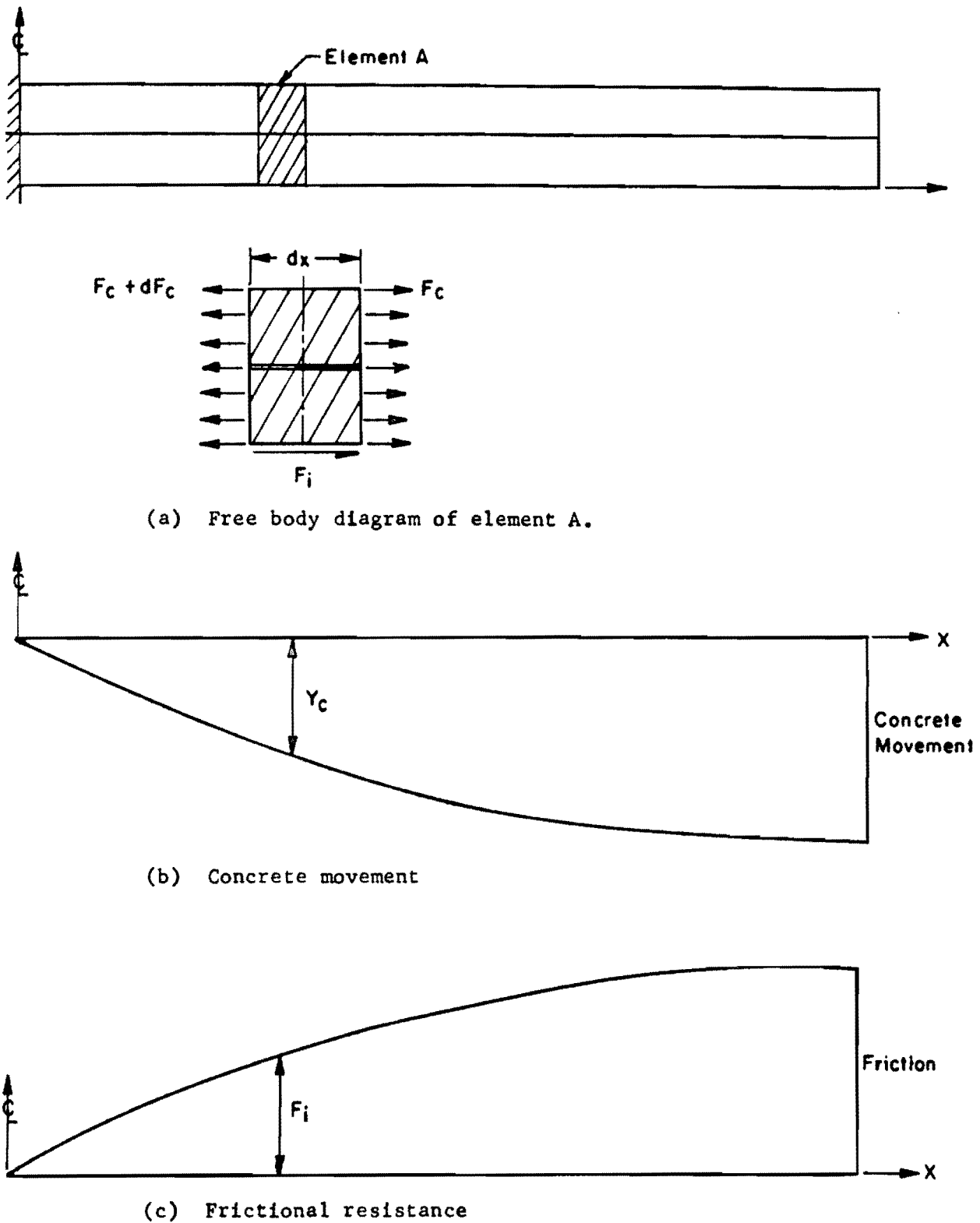


Fig 2.2. Free body diagram of an element in the slab (from Ref 5).

The stress due to restraint is expressed by

$$F_c = \int_x^L \mu_x \gamma t \, dx$$

where

- $\mu$  = friction coefficient,
- $\gamma$  = concrete density, lb/in.<sup>3</sup>, and
- $t$  = slab thickness, in.

The frictional resistance is a function of movement, as shown in Figs 2.1 and 2.2.

The movement at any point  $Y$  may be calculated by

$$Z(Y) = \int_0^Y \left[ \alpha \Delta T - \frac{\int_x^L \mu_x \gamma t \, dx}{dx} \right] dx$$

This equation does not consider shrinkage; however the computer program from Ref 5 does.

Mendoza-Diaz studied the maximum stresses that developed in the slabs as a function of daily placement time, and time since placement for reasonable daily temperature cycles. He found that the peak tensile stresses develop 18 hours after a noon placement. In Fig 2.3, tensile stress values are plotted against drop in concrete temperature for 18 hours after placement for 440 and 240-foot slabs. The difference in stress between the 6-inch and 8-inch slabs is negligible so Fig 2.3 may be considered to apply to both thicknesses. The friction coefficient used was 0.96, which is a conservative design value from tests run at The University of Texas. These figures may be used to estimate stresses for a change in concrete temperature at times other than 18 hours from casting because shrinkage accounts for a very small percentage of the total stress. Shrinkage effects contribute 6 and 8 percent of the total

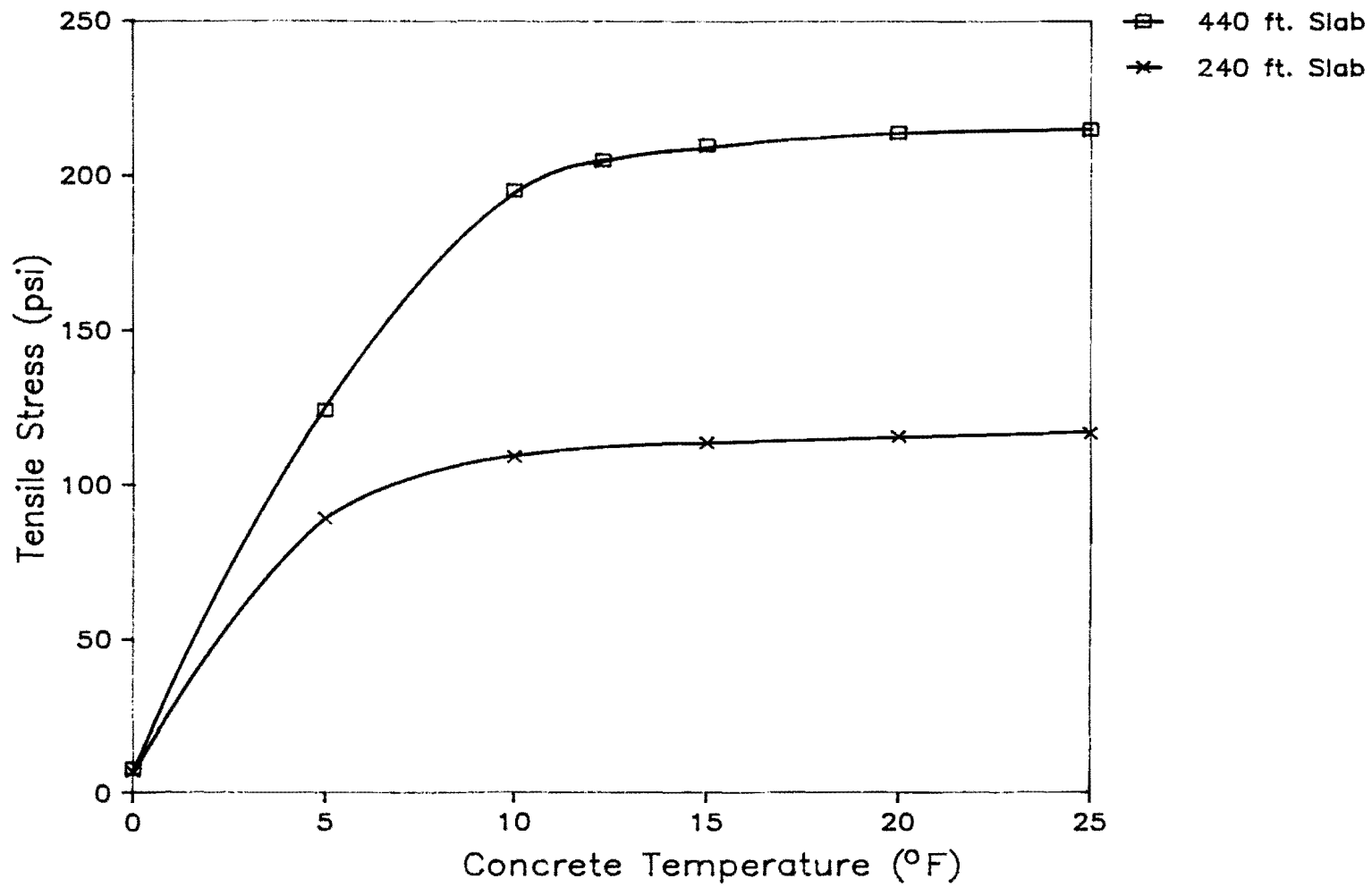


Fig 2.3. Tensile stresses in 240 and 440 foot slabs for a drop in concrete temperature and shrinkage in the first 18 hours.

stress at a  $\Delta T$  of  $5^{\circ}\text{F}$  for the 440 and 240-foot slabs, respectively, and 4 and 6 percent of the total stress at a  $\Delta T$  of  $10^{\circ}\text{F}$  for the 440 and 240 foot slabs, respectively, at 18 hours from casting.

## SOLUTIONS

There are several solutions to the problem of first night temperature and shrinkage cracks in prestressed pavement. Based on the two basic factors leading to cracking discussed earlier, either the tensile stresses must be reduced, or the concrete tensile stress capacity must be increased to prevent cracking.

The tensile stresses are a function of

- (1) the magnitude of  $\Delta T$ ,
- (2) the shrinkage coefficient of concrete,
- (3) the friction coefficient between the slab and the subgrade, and
- (4) slab length.

If one or more of these factors could be reduced or eliminated, the problem of first night temperature and shrinkage cracks could be prevented.

### Shrinkage Coefficient

The amount of shrinkage in the concrete pavement during the first 24 hours is very small. Both theory and experience show that the stresses that develop due to shrinkage during this time period are practically negligible. Theory shows that shrinkage contributes about 5 percent of the tensile stress for daily temperature cycles of about  $20^{\circ}\text{F}$  (Ref 5), and practice shows shrinkage to contribute about 10 percent (Refs 6, 7 and 8).

Due to the relatively small effect of shrinkage, shrinkage compensating cements would not be beneficial. Also, shrinkage compensating concrete expands and then contracts. Since stress is due to the movement, the stresses would not be eliminated and possibly not even reduced.

### Temperature Drop

Tensile stresses begin to build when the temperature drops and the slab tries to contract but is restrained. If the temperature remained constant, and shrinkage stresses were negligible, the stresses would be almost zero. If the temperature increased, the concrete would develop compressive stresses, which would not be a problem.

Placing the concrete during the night, when temperatures are lower, would eliminate temperature decreases and high tensile stresses would not develop. This idea was proposed for one of the Texas demonstration projects but was rejected because of possible high cost, potential construction difficulties, and possible safety problems.

If these potential problems were eliminated, night casting would be a valid solution, but it is not being considered for the immediate future.

### Friction Coefficient

If friction between the slab and subgrade were very low, the slab could move freely without developing high tensile stresses. Figure 2.4 shows tensile stresses for various slab lengths and various friction coefficients (FC). A daily concrete temperature cycle of 18°F was used for the calculations to check tensile stresses.

Although there are materials which reduce the friction coefficient, practical construction problems make this solution less than ideal. Three of the four previous U.S. projects have reported construction difficulties with friction coefficients of 0.5 to 0.6. The Mississippi, Arizona, and Pennsylvania projects all reported that the low friction caused sliding when the pavers began spreading the concrete (Refs 6, 7, and 8). The Arizona project reported (Ref 7) that a major problem encountered during the placement of the prestressed slabs was the displacement of the polyethylene. The top layer of sheeting continued to slide over the bottom layer as the paver was moved ahead and would fold just ahead of the concrete under the spreader.

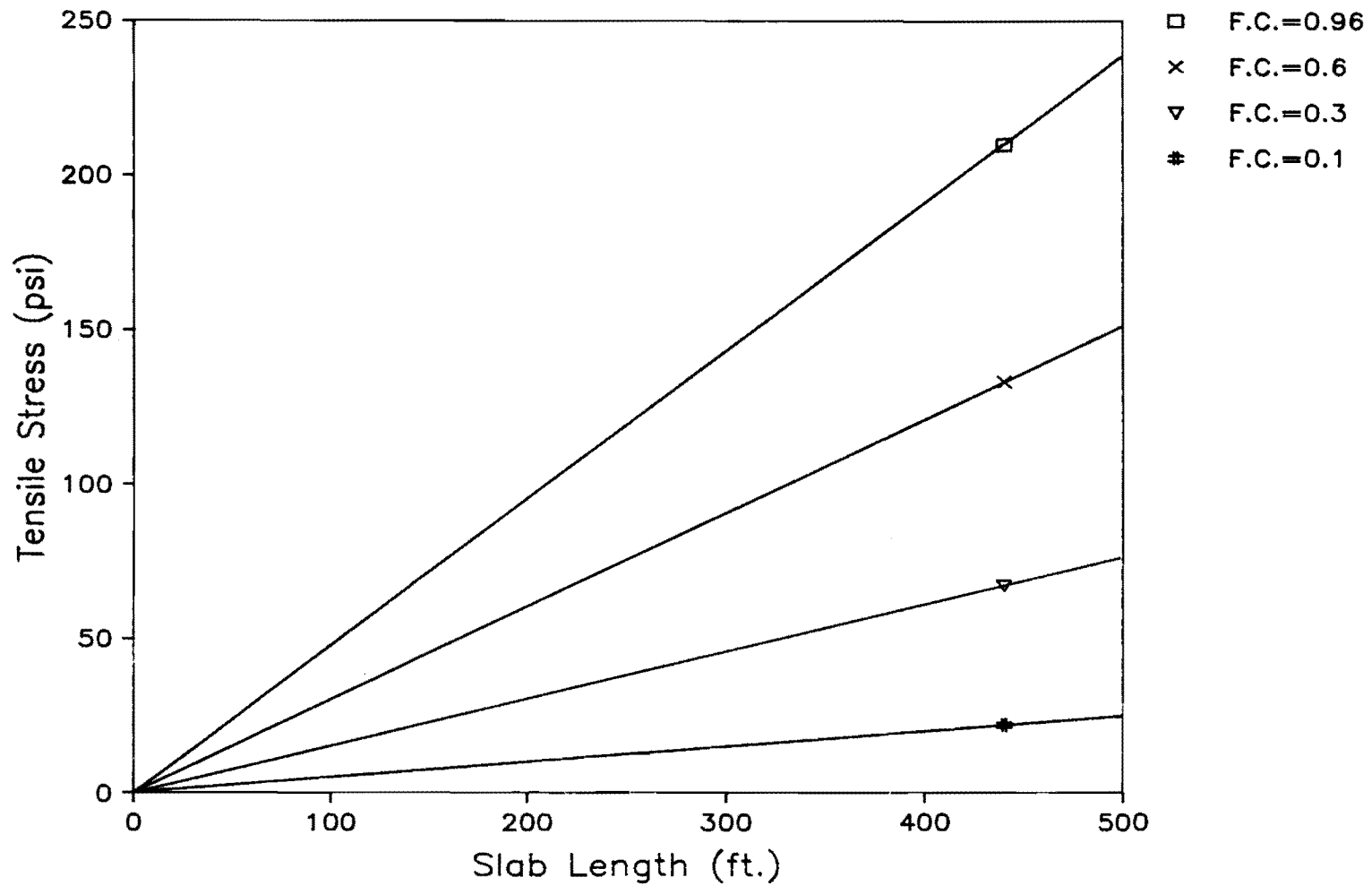


Fig 2.4. Tensile stress build up in slabs of various length for the friction coefficients shown in the legend, and an 18°F daily concrete temperature cycle.

### Slab Length

Reducing the slab length would reduce the resistance to movement and lower the tensile stresses. Figure 2.4 shows the maximum tensile stresses that develop in a slab for a daily concrete temperature cycle of 18°F for various friction coefficients as compared to slab length. Although shorter slabs develop lower stresses, solving the cracking problem by reducing the slab length is not advisable because long slabs, and few joints, is one of the primary advantages of prestressed concrete pavements.

### Very Early Post-Tensioning

Introducing compressive stresses into the pavement before enough tensile stresses develop to crack the slab is potentially a good solution to the cracking problem. The tensile stresses that develop for a given drop in concrete temperature for 240 and 440-foot slabs are shown in Fig 2.3. The maximum tensile stress that develops for a 240-foot slab and a 440-foot slab are about 120 psi and 220 psi, respectively. These stresses are almost fully developed with a drop in concrete temperature of 10°F.

If the temperature drop can be kept to a minimum and a light compression can be applied before high tensile stresses develop, cracking of the concrete can be avoided. It is not necessary to overcome 100 percent of the tensile stress. If the solution keeps tensile stress below the concrete tensile capacity, the solution is valid.

Information on the properties of concrete in the first 24 hours after batching is limited and, to the knowledge of the authors, there is no information on post-tensioning normal strength concrete in the first 24 hours. The need for information in these two areas led to the experimental work in this study.

### ANCHORAGE ZONE

Early transition to avoid the temperature and shrinkage cracks could cause cracking the slab near the post-tensioning anchorage, if the post-tensioning force is too high. This section gives a definition of the

anchorage zone and introduces the types of stresses that are present in the anchorage zone.

#### Definition

St. Venant's principle states that when a concentrated force is applied to a body, the force becomes uniformly distributed at some point within the body. The zone in which this transformation from a concentrated load to a uniformly distributed load occurs is called the anchorage zone.

#### Stresses

The manner in which the stresses in the anchorage zone are distributed is extremely complex. Three different types of stresses exist:

- (1) Bearing Stress - the magnitude of the applied load divided by the bearing area.
- (2) Bursting Stress - tensile stress along the line of loading, normal to it and away from the loading point.
- (3) Spalling Stress - tensile stress along the loaded surface, parallel to it and away from the loading point.

Bursting stresses appear to cause the most serious problem in post-tensioning. Cracks along the tendon path have been reported in post-tensioned box girders (Ref 9) and are also evident in post-tensioned slabs (Ref 10).

A more detailed discussion of the anchorage zone stresses is contained in the next chapter.

This page replaces an intentionally blank page in the original.

-- CTR Library Digitization Team

## CHAPTER 3. LITERATURE REVIEW

Two areas of concern in this study are the anchorage zone stresses and early age concrete properties. An understanding of each of these areas is critical in predicting the prestress force that will cause a failure in prestressed concrete pavements. This chapter presents a summary of some of the most significant literature written on these two topics.

### ANCHORAGE ZONE STRESSES

A fairly extensive amount of work has been done in the area of anchorage zone stress analysis, including elastic solutions, photoelasticity, lab test results, finite element analyses, and others.

#### Elastic Solutions

Since the purpose of early post-tensioning is to prevent temperature and shrinkage cracking, anchorage zone cracking will be considered the first mode of failure. The concrete will be assumed to act in the elastic range because the analyzed section will be uncracked. The first work in anchorage zone analysis using elastic solutions was done by Yves Guyon. Others followed his work by building upon it and expanding it to new applications. This section explains Guyon's work and briefly mentions some of the following work.

Guyon. Guyon pioneered the study of anchorage zone stresses and recorded his findings in his 1963 text book on prestressed concrete (Ref 11). Guyon modelled the anchorage zone as a two-dimensional elastic problem; stresses due to prestress force begin as a concentration at the loaded face and then spread to become uniformly distributed stress on the post-tensioned member. The distance into the member at which the uniformly distributed load is first attained is defined as the "lead in length".

Guyon saw that the lead in zone, or anchorage zone, stresses must pass progressively from the discontinuous distribution at the surface (AD in

Fig 3.1) to the continuous surface (BC). In order to do this, transverse stresses and shear stresses must develop along longitudinal planes in both the horizontal and vertical directions. For equilibrium of Fig 3.1(b) the following three criteria must be met:

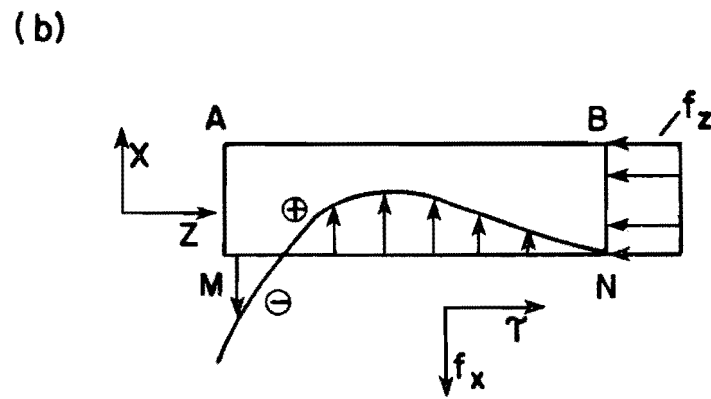
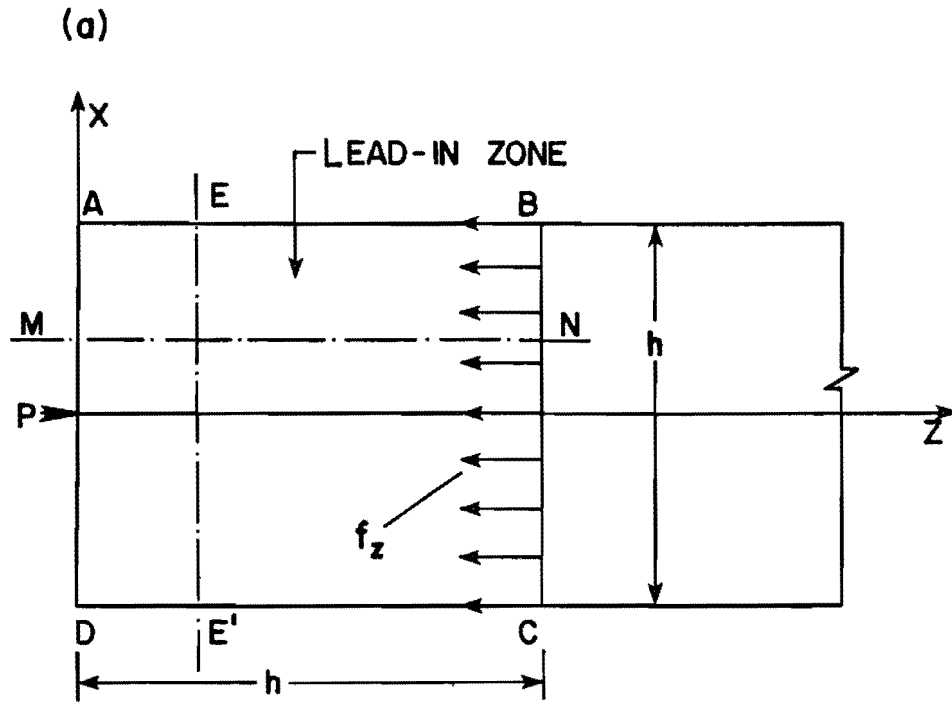
- (1) The resultant of  $f_x$  must equal zero, so  $f_x$  must be in compression at one section and tension at another.
- (2) The sum of the moments of stress  $f_x$  about a point on MN must equal the sum of the moments of forces acting on MA and NB.
- (3) The resultant of  $\tau$  must equal the resultant of the horizontal forces applied to ABNM.

The proportions of ABCD prohibit the use of conventional laws of strength of materials to calculate the stresses. The shapes of the curves describing the general distribution of stresses  $f_x$  and  $\tau$  are shown in Fig 3.2. The actual distribution of these stresses is very complex.

It is not necessary to perform a complete analysis of the anchorage zone; only an analysis along the critical planes is needed. Guyon lists the rules for the analysis on critical planes by breaking the problem down into several loading cases. For the purpose of this study, only two loading cases apply:

- (1) single axial force and
- (2) multiple symmetrical axial forces.

In the single axial force case, the force  $P$  is distributed over a distance  $2a'$  from  $a$  to  $b$  in Fig 3.3. The stresses pass from AB to CD along trajectories (such as 1, 2, 3 ...) which are isostatics issuing from the loaded area  $ab$ . The isostatics are originally parallel to  $P$  at both their origin and at the end of the anchorage zone, where stresses are uniformly distributed. Between these two faces, the isostatics must be S-shaped, with a point of inflection  $I$ . The S-shaped sections cannot carry compression without exerting transverse stresses, which act inward or outward depending on the convexity of the curve.



$f_x =$  BURSTING STRESS DISTRIBUTION

$$\sum F_x = 0 : \sum f_x^{\ominus} + \sum f_x^{\oplus} = 0$$

Fig 3.1. Equilibrium considerations within the lead-in zone (from Ref 9).

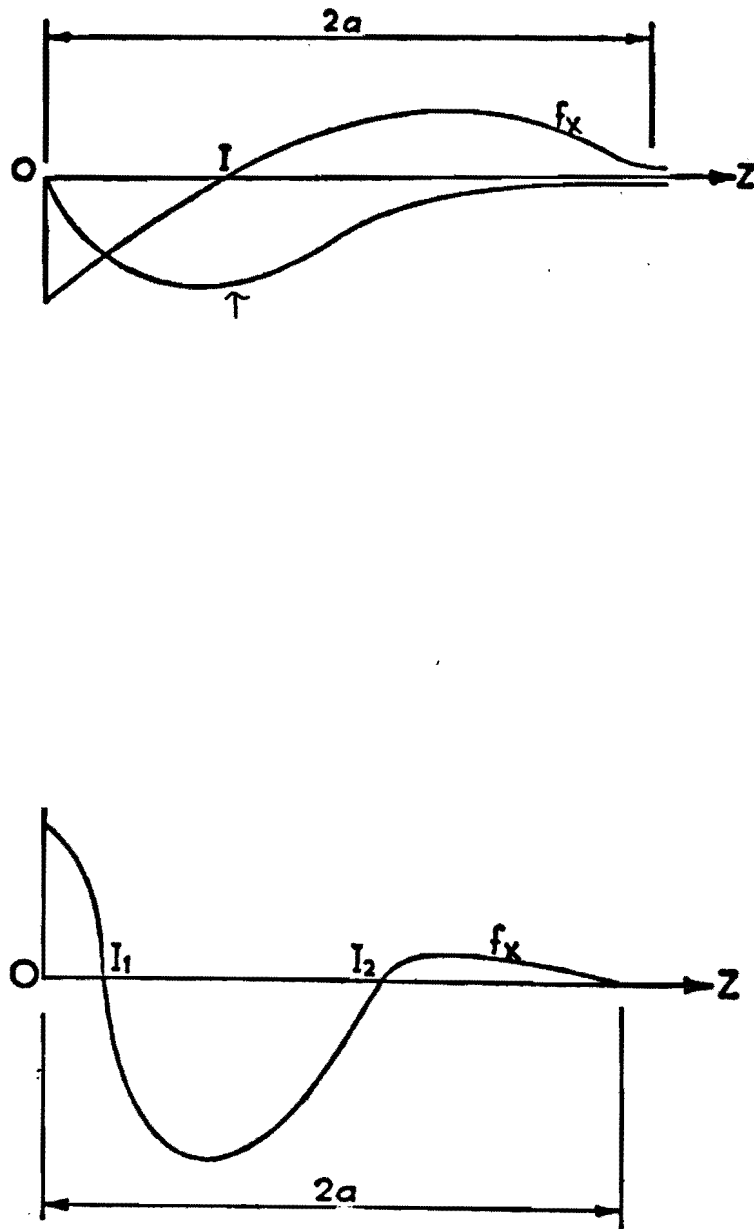


Fig 3.2. General stress distribution in lead-in zone (from Ref 11).

A second family of isostatics (bound by E and E' in Fig 3.3) forms normal to the thrust isostatics. Tension on these fibers increases from BC to OZ. Forces  $q_1$ ,  $q_2$ , and  $q_3$  add together and then decrease from OZ to AD. Transverse stresses are maximum on axis OZ, and by symmetry  $\tau$  is zero. Stress  $f_x$  is the only stress on axis OZ varying from AB to CD, where becomes zero or at least negligible. The tensile portion of  $f_x$  is referred to as the bursting stress.

Guyon looks at the variation of  $f_x$  along OZ by studying the case in which the isostatics are replaced by an average isostatic carrying a force  $P/2$  to the center of the upper or lower half of CD (see Fig 3.4). Taking  $R$  as the radius of curvature at any point, the transverse force equals  $\frac{P}{2R}$ , which equals  $f_x$  for a slab or beam thickness equal to unity.  $R$  is negative from face AB to the point of inflection I, making  $f_x$  compressive.  $R$  becomes infinite at point I so that  $f_x$  equals zero. From I to CD,  $R$  is positive and so  $f_x$  is tensile. Finally,  $R$  goes to infinity and therefore  $f_x$  goes to zero at CD. According to Guyon, the position of zero stress and the positions and values of the maximum compressive and tensile stresses all depend on the ratio  $a'/a$ .

Plots showing the position and value of the stresses are presented by Guyon in Ref 4. The distribution of  $f_x$  along the axis is shown in Fig 3.5 as a function of the average compression  $p$ , where  $p = \frac{P}{2a}$ . Figure 3.6 shows the same information in a different manner. Figure 3.7 shows some of the  $f_x$  isobars for varying degrees of concentration of force  $p$ . These figures reveal another zone of tensile stresses, called spalling stresses, at the face.

Tesar (Ref 12) performed some experiments with photoelasticity and obtained results very similar to Guyon's for ratios of  $a'/a = 0.1$ .

The multiple symmetrical axial force case is very similar to the case of a single axial force for bursting stresses, and may be analyzed for maximum bursting stresses using Figs 3.5 and 3.6. To satisfy equilibrium, however, the spalling stresses must increase and are maximum between the two forces (see Fig 3.8).

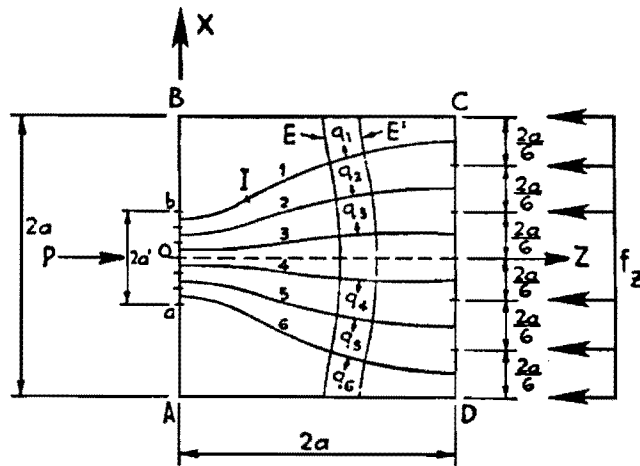


Fig 3.3. Guyon's basic theory. Note  $q = f_x$  (load per unit length in x-direction) (from Ref 11).

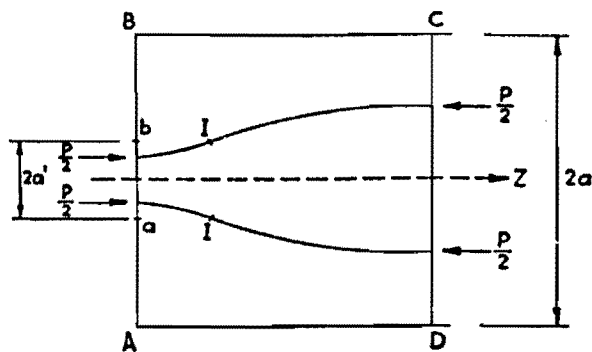


Fig 3.4. Isostatic lines of force through the lead-in zone (from Ref 11).

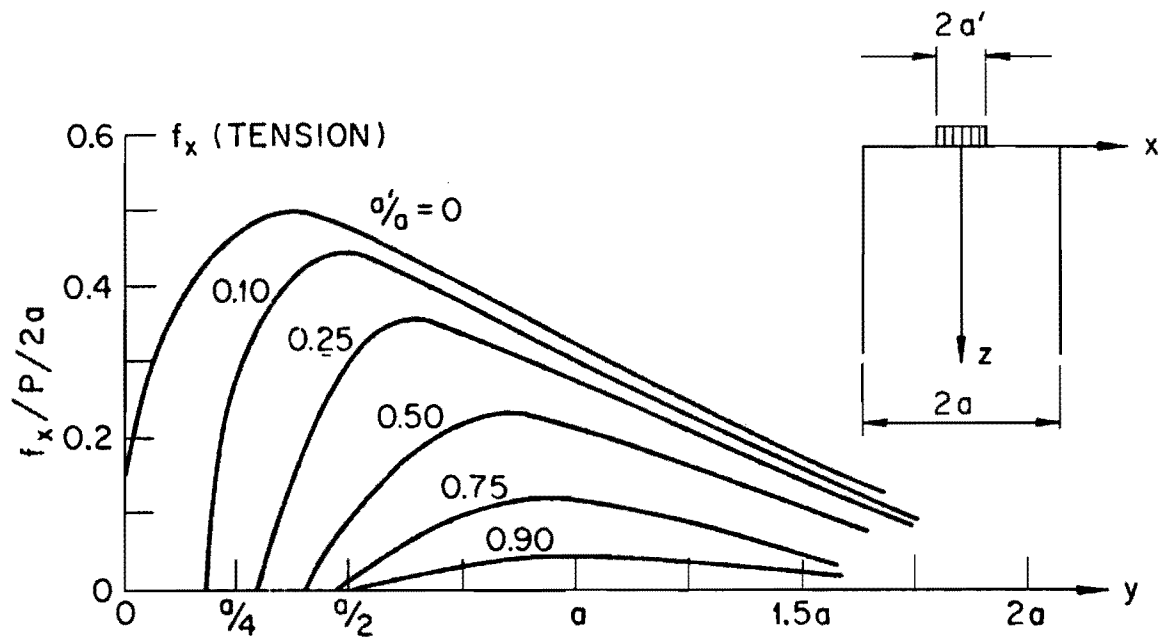
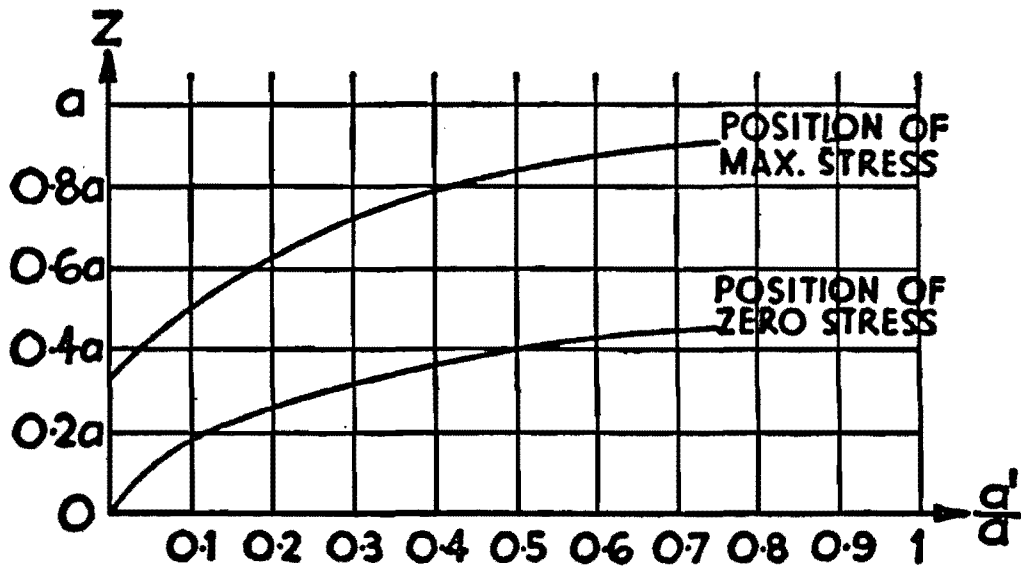
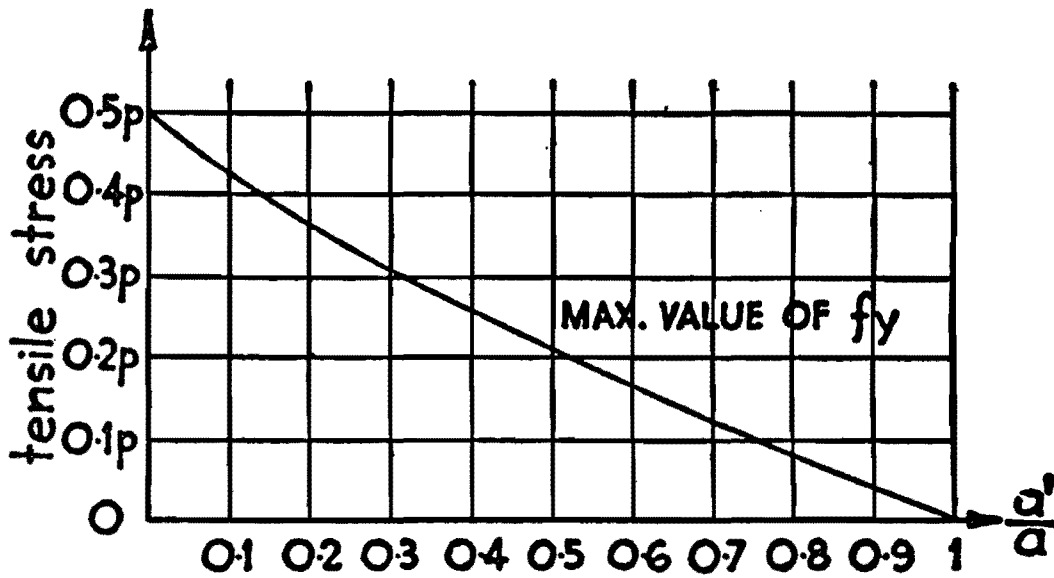


Fig 3.5. Bursting stresses for various loaded areas (from Ref 11).



(a)



(b)

Fig 3.6. Position of zeros and maximum bursting and magnitude of maximum bursting stress for various loaded areas (from Ref 11).

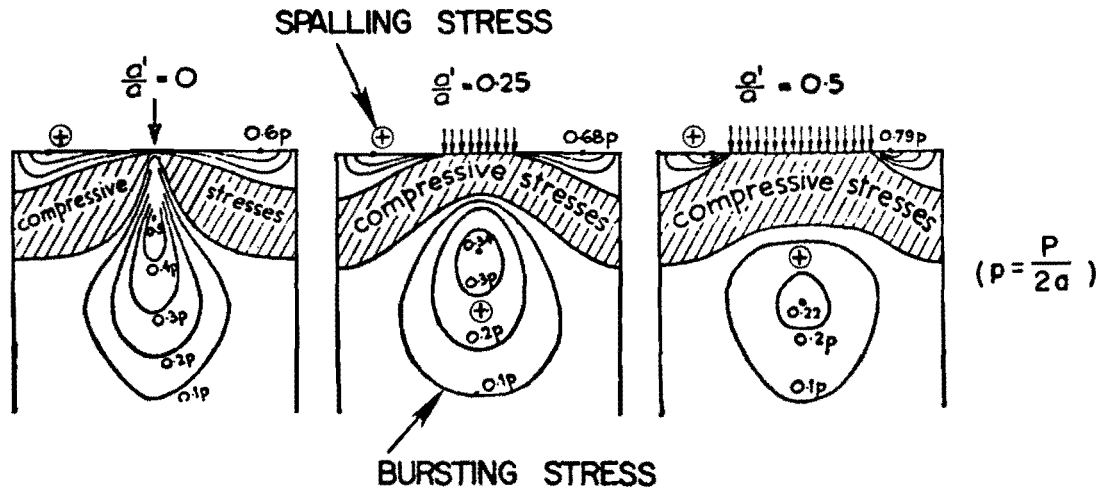


Fig 3.7. Bursting and spalling zones from Tesar's photoelastic tests (from Ref 11).

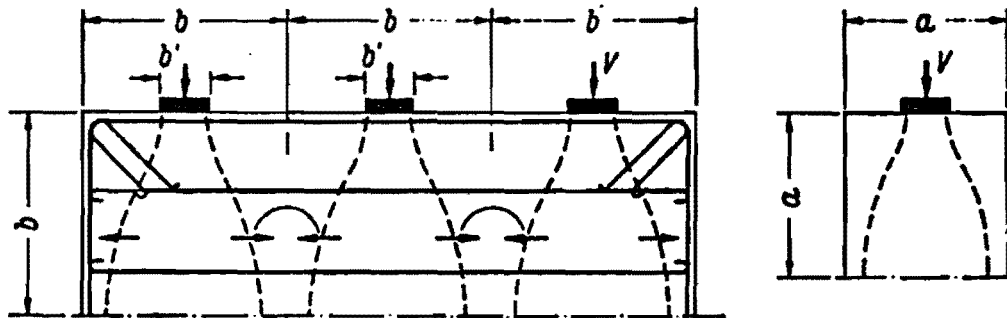


Fig 3.8. Multiple symmetrical axial force case (from Ref 31).

Guyon introduces two approximate methods for analyzing the single eccentric load case and the case where several eccentric loads exist. The single eccentric load case is called the "symmetric prism" method and is illustrated in Fig 3.9. In this method, an imaginary prism is used for bursting stress analysis. The prism has a width of  $2a_1$ , where  $a_1$  is the distance from the load to the nearest edge (see Fig 3.9). The rest of the analysis is similar to that for a single concentric load except for use of the imaginary prism rather than the full section.

The case of several eccentric loads is analyzed by Guyon's "successive resultant" method, shown in Fig 3.10. In this case the maximum bursting stress is assumed to lie on the axes of individual forces, on the axes of the resultant of two forces, and on the axis of the resultant of all the forces.

This first work in anchorage zone stress analysis by Guyon was followed by other studies in elastic solutions. Most of those reinforce Guyon's work by building upon it to expand the theories to new applications or design techniques.

Others. An extensive literature review was carried out in 1981 by William C. Stone at The University of Texas at Austin. The resulting report (Ref 9) presents an overview of the studies on anchorage zone stresses based on elasticity by Douglas and Trahair (Ref 13), Iyengar (Ref 14), and Gergely, Sozon, and Siess (Ref 15).

### Photoelasticity

Tesar (Ref 2) did some photoelastic studies on the anchorage zone stresses and got very good comparisons with Guyon's work for a ratio of  $a'/a = 0.1$  and fairly good results for the other cases. Tesar's work was followed by similar work by Christodoulides (Ref 16), Sargious (Ref 17), and Vaughn (Ref 18).

### Testing

Several anchorage zone testing programs have been performed, including those of Zielinski and Rowe (Refs 19 and 20), Taylor (Ref 21), and Friberg (Ref 1), and some at The University of Texas at Austin by Berezovytch and

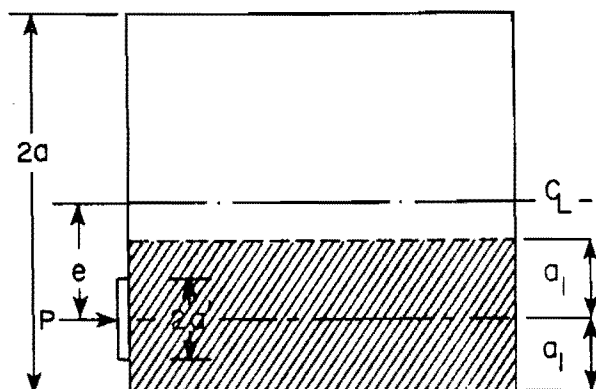


Fig 3.9. Guyon's symmetrical prism analogy (shaded areas indicate prism to be used for calculating bursting stresses for eccentric loading (from Ref 9).

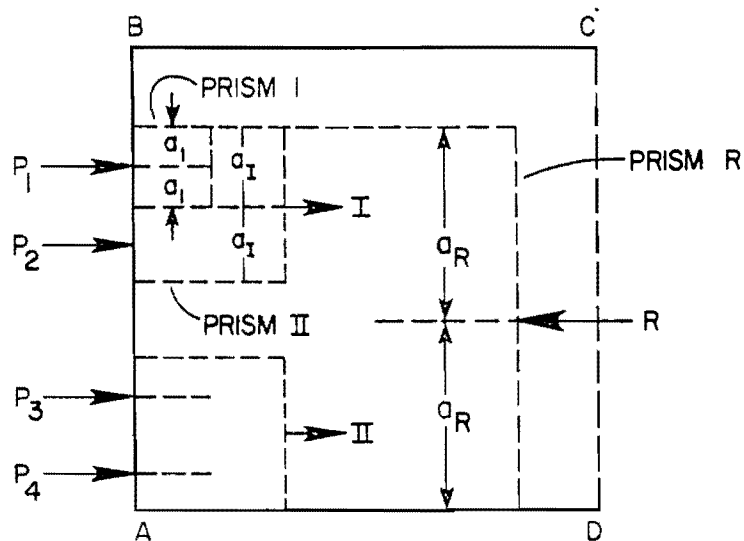


Fig 3.10. Guyon's successive resultant method for the case of multiple anchorages (from Ref 9).

Burns (Ref 10), Cooper, Gallaway, and Breen (Ref 22), and Stone and Breen (Ref 23). Some of the conclusions of interest to this study are:

- (1) For the specific case of a single symmetric load, the ratio of the loaded area to the cross section area was the most important factor in the transverse stress distribution. The smaller the ratio, the higher the stress (Ref 19).
- (2) The cracking load is not substantially affected by increasing the bearing area of the anchor (Ref 22).
- (3) The maximum bursting stress occurred on the axis of load and was greater than that predicted by Guyon using the symmetrical prism analogy (Ref 19).
- (4) The failure of a single anchor appeared to be caused by wedging the action of a cone of concrete under the bearing plate formed by shear forces due to the incompatible stiffness of the anchor unit and the concrete (Ref 21).
- (5) The cracking load is only slightly affected by the concrete strength (Refs 10 and 22).
- (6) The ultimate load clearly increases with increased slab thickness (Ref 10).
- (7) The anchor geometry did not appreciably affect either the distribution of transverse stresses or the ultimate load capacity (Ref 19).
- (8) The cracking load is not affected by increasing the percentage of reinforcement, although crack widths can be effectively controlled by the presence of reinforcement (Refs 10 and 22).
- (9) Spiral reinforcement appears to be effective in delaying early cracking as well as providing increased ultimate strength (Refs 10 and 23).
- (10) Transverse post-tensioning seems to be a very effective means of controlling (preventing) tendon path cracks (Refs 22 and 23).

### Finite Element Analysis

Stone performed extensive finite element analysis using both two-dimensional and three-dimensional programs (Ref 9). He found that the two-dimensional program results agreed closely with elastic analysis and photoelastic theory, and the three dimensional program results agreed very closely with test data and can be used to analyze the effects of variables. Stone writes (Ref 9):

The static, linear elastic, three-dimensional finite element analyses can be used to predict the state of stresses of the anchorage zone with reasonable accuracy up to the cracking load.

Since elasticity no longer applies after cracking, the linear elastic program cannot predict ultimate loads.

### Other Solutions

There are other analytical methods for anchorage stresses in addition to the ones mentioned. The reader is referred to Stone's more complete literature review for these additional methods (Ref 9).

### EARLY AGE CONCRETE STRENGTH

Knowledge of concrete properties, especially concrete strength, at very early ages is necessary to determine whether the early post-tensioning force may be applied without causing an anchorage zone failure. Little work has been done on normal strength concrete (3000 - 5000 psi 28-day strength) in the first 24 hours after casting. This section summarizes Friberg's work on early concrete properties and introduces the concept of using maturity factor, a function of time and concrete thermal history, as a strength indicator rather than time alone.

### Friberg

In the early 1960's at The University of Missouri, Rolla, Bengt F. Friberg coordinated several studies investigating the potential of prestressed concrete as a building material for pavements. Among those were studies on the properties of concrete at early ages, and stress distribution and failures under loads applied against an edge of a slab (Ref 1).

Friberg noted some interesting and very useful discoveries about the strength of concrete at early ages. Some of his findings were:

- (1) Concrete tensile strength increased much faster than compressive strength at early ages.
- (2) Modulus of elasticity reached mature values early, and critical limits of extensibility were low at early ages.
- (3) Prestress force could be applied early except at low temperatures.
- (4) Deformations, rather than strength, appeared to indicate the earliest age at which prestress could be applied.

Friberg studied compressive, tensile, and flexural strengths of concrete stored at 40°, 70°, and 100°F. The total number of specimens Friberg tested included 190 compression cylinders, 175 tensile splitting cylinders, and 165 beams loaded at third points. The concrete strength results are summarized in Figs 3.11 and 3.12.

### Maturity Factor

Recent studies show that concrete maturity, a temperature-time history of concrete, is a more accurate indicator of concrete strength than a time history alone (Refs 24, 25, and 26). Maturity is defined by Saul (Ref 24) as the temperature of the concrete above a datum temperature integrated over curing time. The following equation may be used to calculate maturity:

$$M = \int_0^t [T(t) - T_0] dt$$

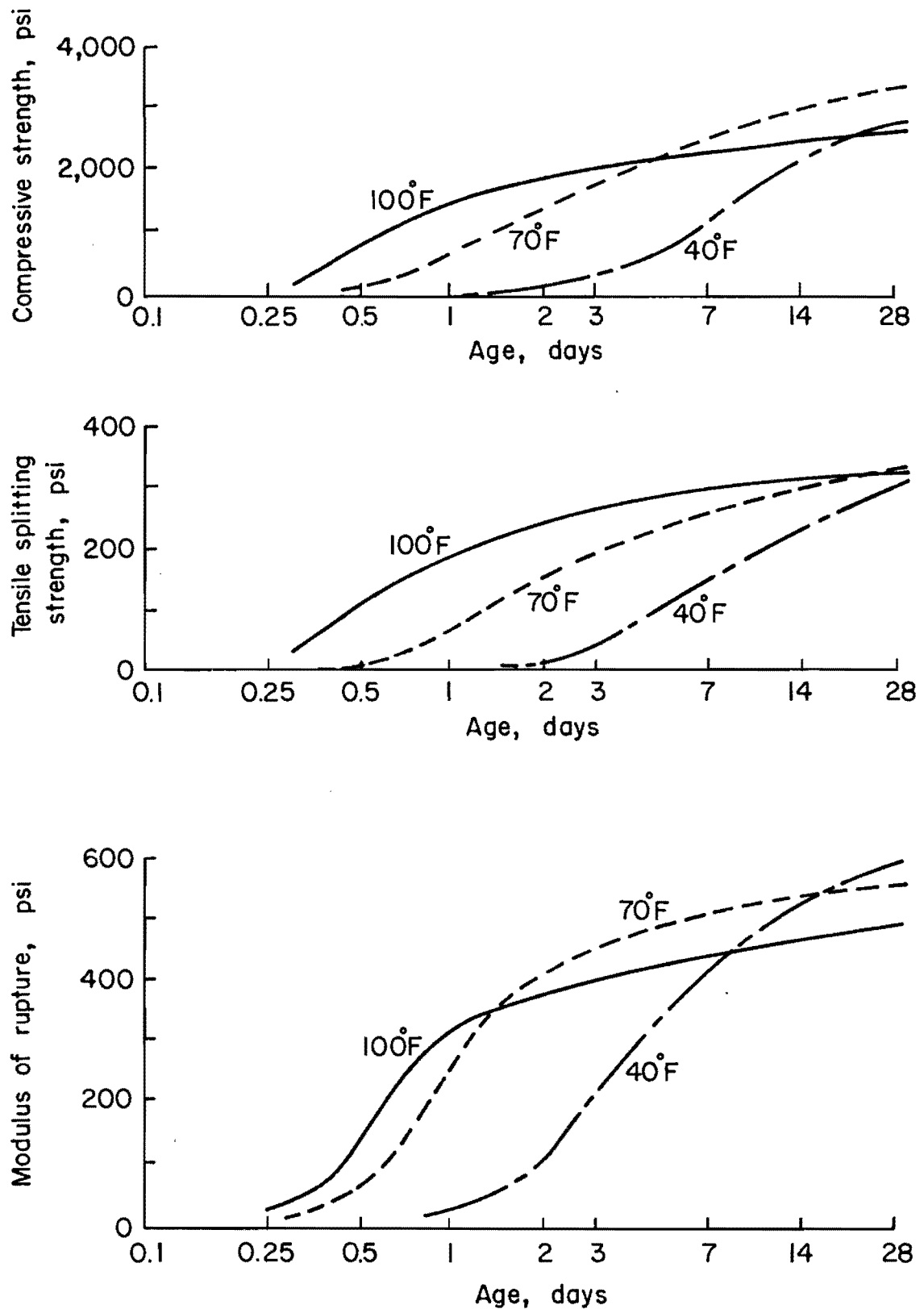


Fig 3.11. Results of Friberg's early age concrete strength tests (from Ref 1).

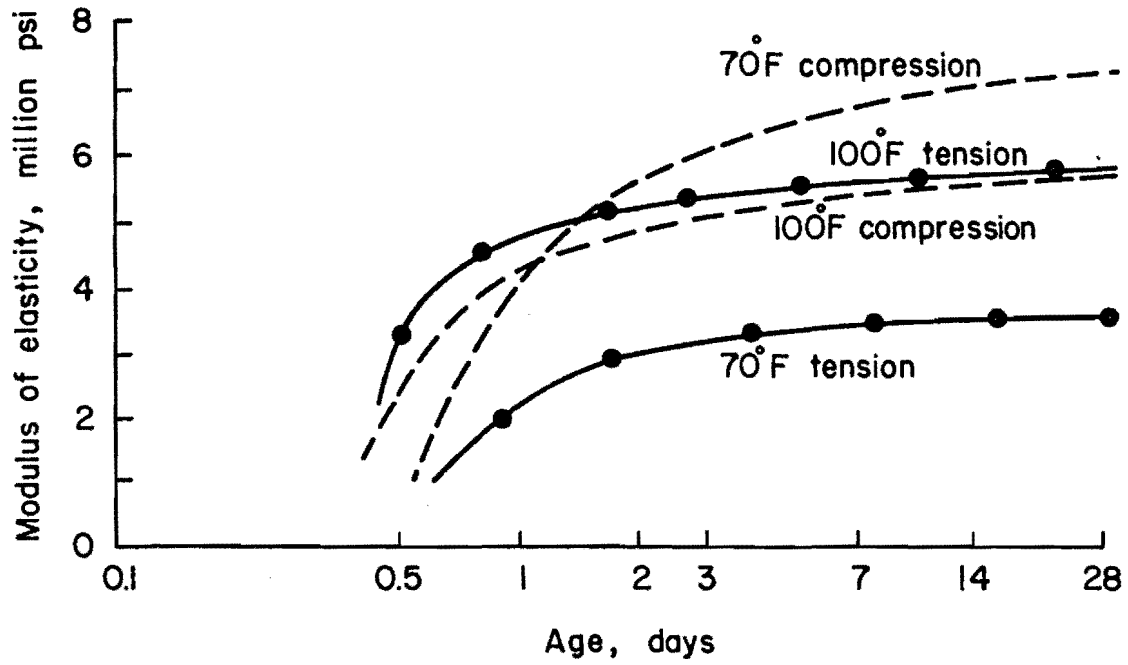


Fig 3.12. Results of Friberg's tests on the modulus of elasticity of concrete at early ages (from Ref 1).

where

- M = maturity at time t, hr - °F,  
 T(t) = temperature of concrete at time t, °F, and  
 T<sub>0</sub> = datum temperature, °F.

The accepted datum temperature is currently 14°F (-10°C).

By measuring the concrete temperature at a given time after casting, the maturity factor may be used to predict the concrete strength if a pre-established relationship between maturity and strength exists. The concept of maturity states that, for a given mix, the concrete will have equal strength at an equal maturity factor regardless of the thermal history.

#### CURRENT DESIGN PROCEDURES

Current building codes (ACI, PTI, and AASHTO) give little help in determining a practical allowable post-tensioning force. Each code uses an allowable bearing stress equation, which Stone and Breen report is very conservative in some applications and unconservative in others (Ref 30). This section reviews each of the three procedures and summarizes the post-tensioning schedules of the previous U.S. prestressed concrete highway pavement demonstration projects.

#### ACI

The ACI 318-83 Building Code (Ref 27), Section 18.13 on anchorage zones states that

- 18.13.1 - Reinforcement shall be provided where required in tendon anchorage zones to resist bursting, splitting, and spalling forces induced by tendon anchorages. Regions of abrupt changes in section shall be adequately reinforced.

- 18.13.2 - End blocks shall be provided where required for support bearing or for distribution of concentrated prestressing force.
- 18.13.3 - Post-tensioning anchorages and supporting concrete shall be designed to resist maximum jacking force for strength of concrete at time of prestressing.
- 18.13.4 - Post-tensioning anchorage zones shall be designed to develop the guaranteed ultimate tensile strength of prestressing tendons using a strength reduction factor of 0.90 for concrete.

The commentary section 18.13 adds to this by giving two formulas for permissible bearing stress. They are

- (1) immediately after tendon anchorage:

$$f_b = 0.8 f'ci \sqrt{A_2/A_1 - 0.2} \leq 1.25 f'ci$$

- (2) after allowance for prestress losses:

$$f_b = 0.6 f'ci \sqrt{A_2/A_1} \leq f'ci$$

where

- $A_1$  = bearing area of anchor plate of post-tensioning tendons;
- $A_2$  = maximum area of the portion of the anchorage surface that is geometrically similar to, and concentric with, the area of the anchor plate of the post-tensioning tendons; and

$f_b$  = permissible concrete bearing stress under the anchor plate or post-tensioning tendons with the end anchorage region adequately reinforced.

The commentary states that "the actual stresses are quite complicated around post-tensioning anchorages" but does not give any further guidance on the analysis or design of the anchorage zone.

#### PTI

The same allowable bearing stress equations recommended by ACI are recommended by PTI in Section 3.1.7 of the Post-tensioning Manual (Ref 28). References to bursting and spalling stresses are made in Section 5.4.1 but no analytical aids are provided.

#### AASHTO

The Standard Specifications for Highway Bridges (Ref 29), Section 1.6.6, B4, recommends a bearing stress of 3,000 psi, but one not exceeding 0.9  $f'_{ci}$ , where  $f'_{ci}$  is the concrete compressive strength at the time of stressing. This recommendation is even more conservative than ACI and PTI.

#### Previous Projects

Post-tensioning was performed in two or three stages in each of the previous U.S. demonstration projects for prestressed concrete pavements. The earliest any slab was stressed was one day after concrete placement. Each project based the allowable level of prestress on the compressive strength of the concrete. The jacking force schedule for each project based on compressive strength is presented in Table 3.1.

In many cases, this jacking schedule was inadequate to prevent temperature and shrinkage cracks. In order to improve upon the previous jacking schedules, a laboratory test program was set up and performed.

TABLE 3.1. POST-TENSIONING SCHEDULE FOR THE PREVIOUS U.S. DEMONSTRATION PROJECTS

---

Project Location	f'c (psi)	Jacking Force (kips)
Virginia	1000	10
	2000	20
	3000	29
Pennsylvania	1000	10
	2500	46.9
Mississippi	1000	14
	2500	33
Arizona	1100	9
	1500	13
	2000	19
	2500	26
	3000	31

---

## CHAPTER 4. EXPERIMENTAL PROGRAM

### PURPOSE

An experimental program was performed in order to discover the earliest possible time at which concrete slabs could be post-tensioned to overcome tensile stresses due to temperature and shrinkage effects without causing an anchorage zone failure. Although data from previous tests exist, no data were available for very early post-tensioning when concrete properties are not the same as for more mature concrete.

### DESCRIPTION OF TEST

#### General

The test slab design simulated the materials and cross section of two one-mile post-tensioned concrete pavement overlays, which are being constructed in 1985. These demonstration projects are part of the experimental study at The University of Texas at Austin for the development of a design procedure for prestressed concrete pavements. The test specimens consisted of several single strand full scale concrete slabs.

The slab width was determined by the strand spacing of the actual pavement design and the length was taken as 4 feet for convenience of form work. Four feet was more than adequate to develop the anchorage zone stresses. The thickness also corresponded to the actual pavement design.

The strand used was 0.6-inch-diameter, 270 ksi, seven wire coated strand manufactured in accordance with ASTM A-416. The strand was located 1/4 inch above mid-depth, simulating the actual design which called for strand placement 1/4 inch below mid-depth. The strand was placed above mid-depth rather than below so that the side with thinner cover was visible.

The slabs were reinforced with one number 4 bar above and one below the strand just in front of the anchor. To develop the bar, a closed hoop was

used in the narrow test slabs. The design calls for continuous bars in the two projects.

The forms were lined with polyethylene to be consistent with the actual slabs, which will be cast on polyethylene to reduce friction. The specimens could be easily removed from the forms because of this liner. A typical form for several slabs is shown in Fig 4.1. Figure 4.3 shows the anchor and reinforcing bars immediately in front of the anchor.

A readymix plant supplied the concrete mix designed in accordance with Item 360 of the Standard Texas Highway Department Specifications for slip form paving. The mix called for 5 sacks of Type I cement per cubic yard. Strength was specified as 650 psi minimum for center point load modulus of rupture tests at seven days. A more complete batch design may be found in Appendix A.

Concrete was placed using an overhead crane and bucket (Fig 4.3) and was finished and covered with wet burlap and plastic. Many test beams and cylinders were cast for concrete strength measurements (see Fig 4.4).

#### Experimental Parameters

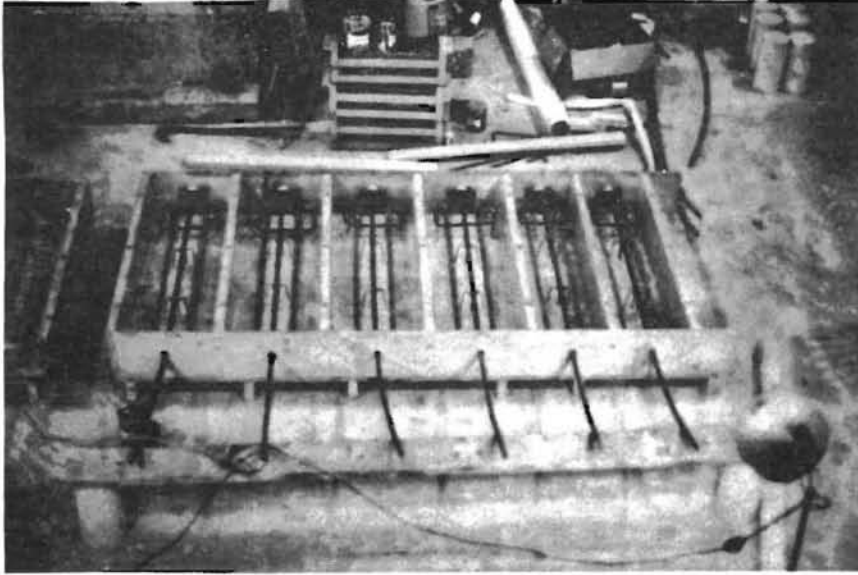
The variables considered in this testing program were selected according to the varying field conditions. Table 4.1 contains a summary of the variables for the actual pavement design.

Strand Spacing. As part of the overall investigation of prestressed concrete pavement performance, two different pavement lengths were chosen, 240 and 440 feet, to see which was more acceptable in terms of economy and pavement performance (including joints). The corresponding strand spacings to obtain the minimum prestress necessary for the 240 foot and 440 foot slabs were 24 and 16 inches, respectively, for one site and 18 and 12 inches, respectively, for the other.

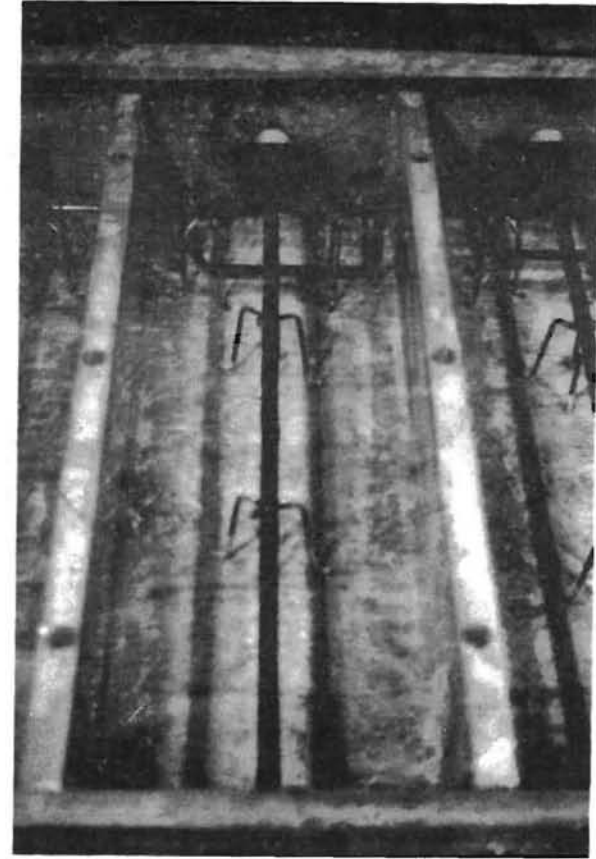
According to Guyon (Ref 11) the bursting stresses in a single strand specimen with slab width equal to  $2a$  are very similar to those of a multi-strand slab with strand spacing equal to  $2a$ . Based on this information, strand spacings were modeled by a single strand slab with widths of 12, 16,

TABLE 4.1. SUMMARY OF SOME OF THE DESIGN PARAMETERS FOR THE TWO TEXAS DEMONSTRATION PROJECTS

Location	Slab Length (ft)	Strand Spacing (in.)	Slab Thickness (in.)
Site 1	240	24	6
	440	16	6
Site 2	240	18	8
	440	12	8



(a)



(b)

Fig 4.1. Forms for test slabs ready for concrete placement.

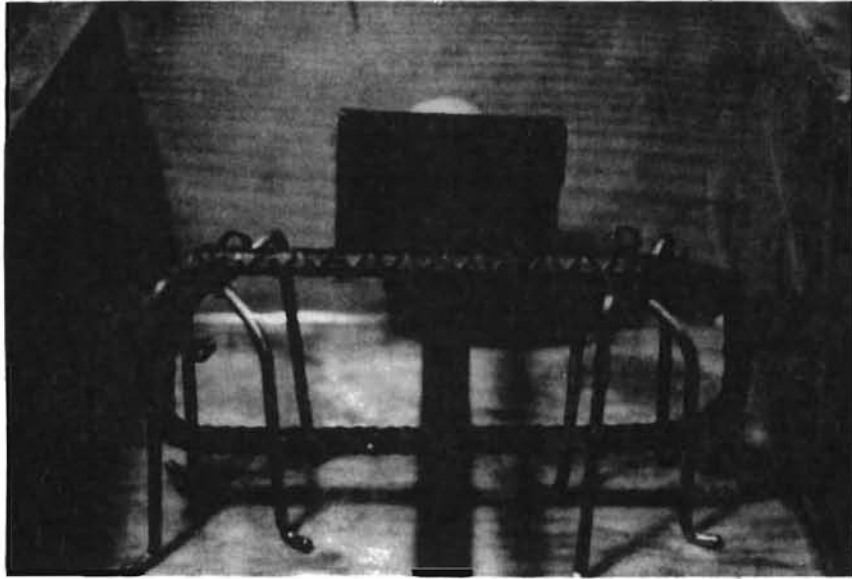


Fig 4.2. Reinforcement for test slabs.

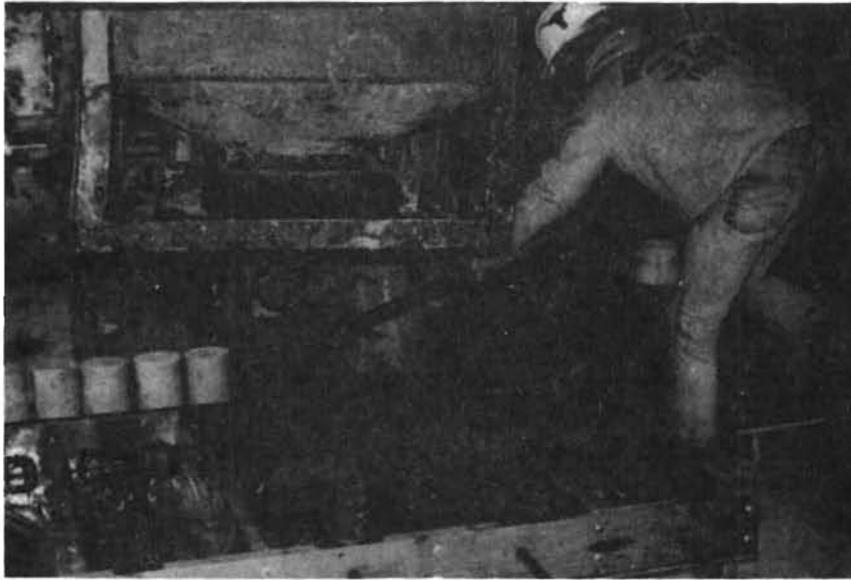


Fig 4.3. Concrete placement.

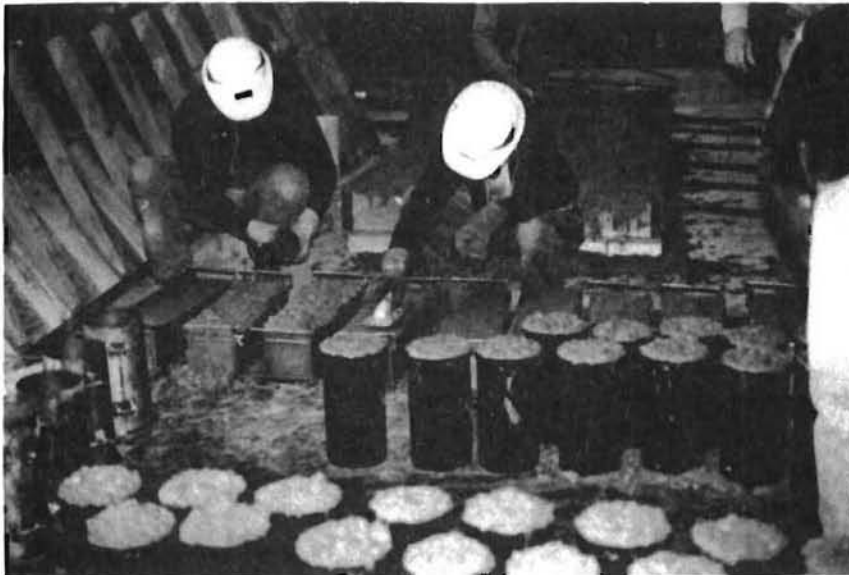


Fig 4.4. Preparing specimens for concrete strength tests.

and 24 inches. Actual widths were 11, 14-1/4 and 22-1/8 inches because of limiting geometry of a 4 foot by 8 foot sheet of plywood.

Slab Thickness. Slab thickness and prestress level depend on the supporting properties of the existing pavement structure, and loading and environmental conditions. Field conditions yielded design thicknesses of 6 and 8 inches 65 and 100 psi effective prestress level for for the two sites. These sets of design values were determined from fatigue analysis on the two experimental sites. Thicknesses of 6 and 8 inches were chosen for the test slabs.

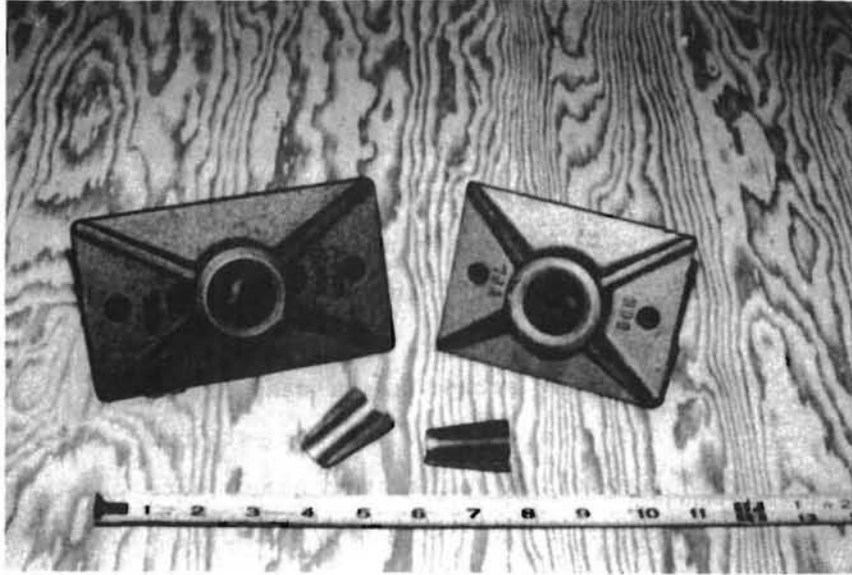
Anchor Size. Single strand anchor sizes range from 5-3/8 x 2-3/4 inches to 6 x 3-1/2 inches for 0.6 inch diameter strand, depending on the manufacturer (Ref 28). Two different anchor sizes were chosen to study the bearing area effect. Anchor 1 (A1) was 4-5/8 x 3-1/2 inches and anchor 2 (A2) was 6 x 3-1/2 inches. These were in the mid to large size range. The anchors are shown in Fig 4.5.

Time. Since the objective of the testing program was to determine the earliest possible time at which post-tension force could be applied, time after casting at which the slabs were tested was a very important variable. Time since concrete batching was also used as a more general indicator. The first crack on previous projects occurred during the first night, and, therefore, a 24-hour testing schedule was established. For the first two series, testing times of 6, 12, 18, and 24 hours after casting were chosen. For reasons that will become clear later, the times were revised to 4, 8, 12, and 16 hours for the third series.

#### Other Parameters Measured

Several parameters were not controlled, but were measured because they have an influence on the results of the study. This section describes those parameters.

Ambient Temperature. No attempt was made to control the ambient temperature as a variable, but it is of concern for curing conditions and it was recorded regularly throughout the testing period.



(a) Two anchors used in tests.



(b) Anchor with strand and grips in place.

Fig 4.5. Mono-strand anchorage used in tests.

Concrete Temperature. Concrete temperature was not controlled but was recorded. Thermal couples were placed in four slabs at the strand depth and concrete temperature was monitored throughout the testing period.

Concrete Maturity. As previously mentioned, concrete maturity is a more accurate indicator of concrete strength than time alone. Maturity was calculated using the concrete temperature and time after batching.

Concrete Strength. Concrete strength was measured using three different testing means; compressive strength, tensile strength and flexural strength.

Compressive strength was measured by testing three 6-inch-diameter by 12-inch-tall cylinders at each testing time. Tensile strength was measured using the 6-inch by 12-inch cylinders in a split cylinder test, and flexural strength was measured using the 6 x 6 x 22-inch beam in a modulus of rupture test with center point loading on an 18-inch span.

#### Testing Apparatus

This section describes the manner in which the slab anchorage zones were tested, including the means of load application and load measurement, and the loading technique.

Load Application. For each of the test specimens the strands were stressed using a hydraulic ram with a hand pump. Load was applied slowly directly to a stiff spreader beam to distribute the load over the area of the slab end face and to avoid concentrated loads and possible localized failures (see Figs 4.6 and 4.7).

Load Measurement. Loads were measured using a load cell and a strain indicator which were calibrated before and after the tests. A pressure gauge for the ram was used as a backup load measuring device (see Fig 6.7).

Loading Technique. After removing the forms, loads were applied slowly at small intervals. Due to the violent nature of some of the failures, crack observation was done after each load interval rather than during loading. For this reason there is slight uncertainty as to the exact load at which cracking occurred, but the intervals were small enough for the recorded cracking load accuracy to be within 1-kip.

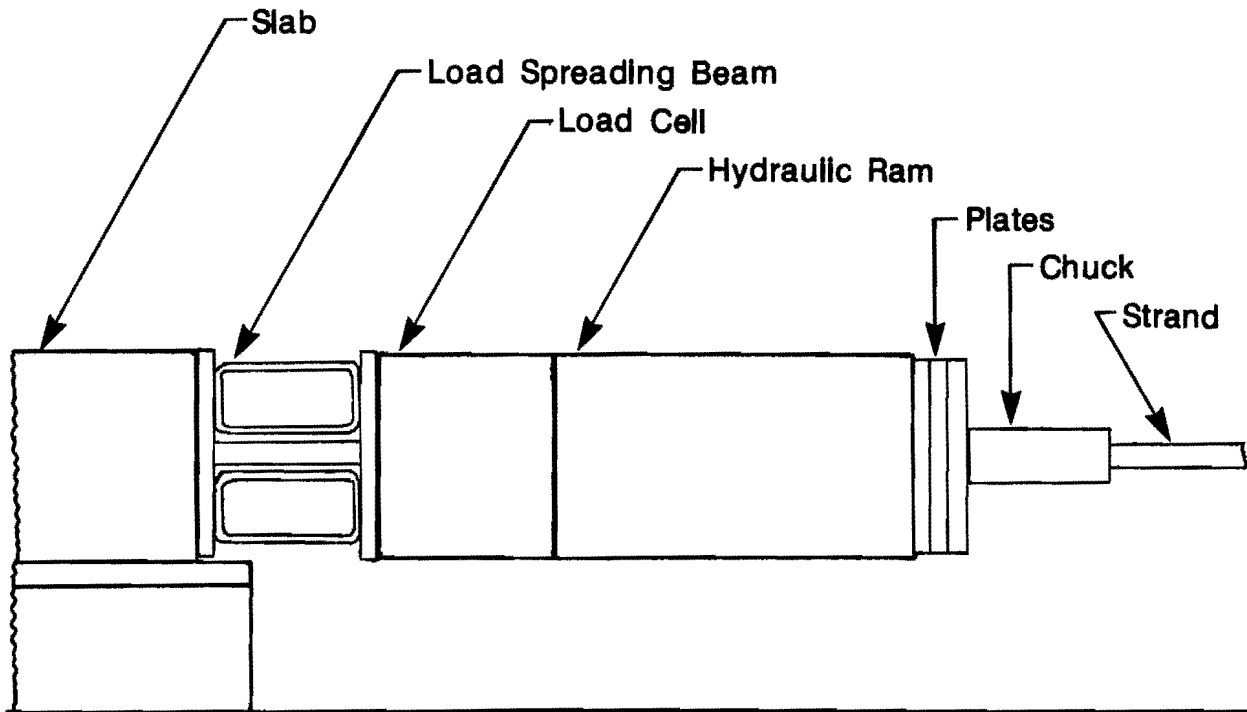
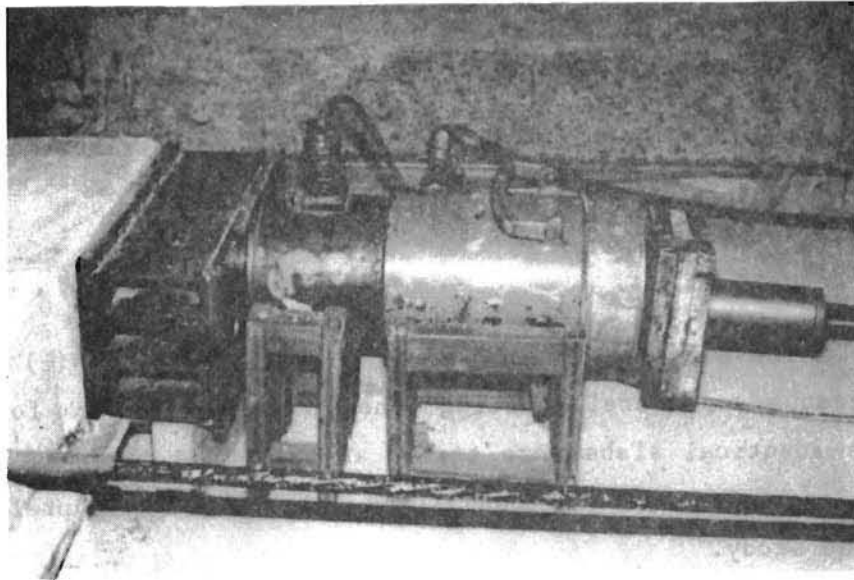
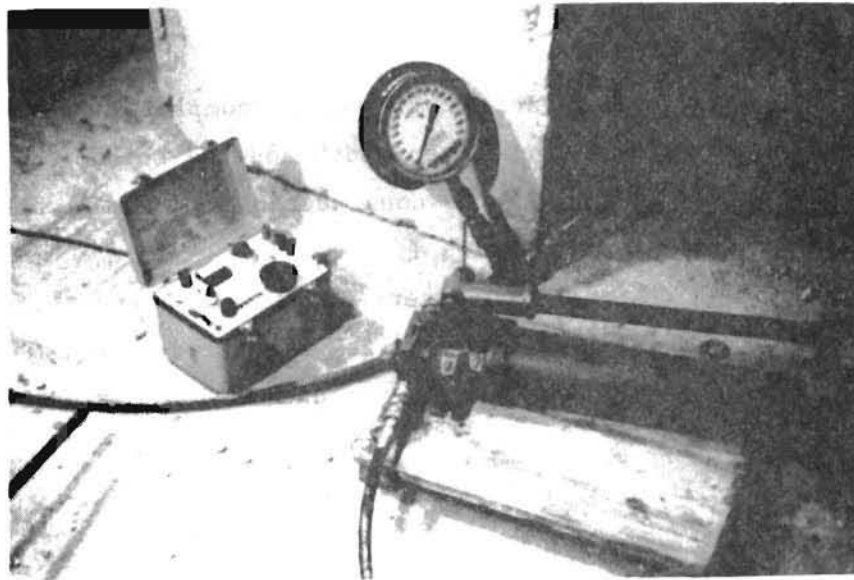


Fig 4.6. Test slab loading apparatus.



(a) Load application.



(b) Strain indicator and pressure guage for load reading.

Fig 4.7. Application of post-tensioning force to slabs.

## TESTING SCHEME

Testing was completed in three different series. Each series had a certain purpose and set-up. The following sections describe the purpose and set-up of each series.

### Series I

Purpose. The purpose of test Series I was threefold: (1) to test the loading apparatus and overall testing scheme; (2) to check for scatter in data (three identical slabs were tested at each time to find out the range of cracking loads and ultimate loads); and (3) to set some preliminary data points for the study.

Set-up. The test slabs of Series I were all 6 inches thick, 16 inches wide, and contained a small anchor.

### Series II

Purpose. The purpose of Series II was to complete the testing of 6-inch-thick slabs by varying the specimen width and the anchor size. Only one slab with each set of variables was constructed and tested because little scatter of data was observed in Series I.

Set-up. The test slabs in this series were all 6 inches thick and had widths of 16 and 24 inches. The anchor size was varied. The small anchor is designated anchor one (A1), and the larger anchor is designated anchor two (A2).

### Series III

Purpose. There were three purposes of Series III. The first was to include the variables slab thickness and strand spacing. The second was to repeat tests of Series I because of the poor quality of the concrete for the first tests. This will be discussed later. The final purpose was to test one double strand slab.

Set-up. All slabs contained the small anchor plate, because the second series of tests showed that the size of the anchor did not affect the results substantially. Five 6-inch slabs were cast. Four were 16 inches wide and one 32 inches wide. The 32-inch slab contained two strands which were stressed simultaneously for comparison with the single strand slabs.

Ten 8-inch-thick slabs were cast and tested. Four were 24 inches wide, four were 16 inches wide, and two were 12 inches wide. All 8-inch-slabs contained one strand each.

This page replaces an intentionally blank page in the original.

-- CTR Library Digitization Team

## CHAPTER 5. DISCUSSION OF TESTS

The testing process was completed in three series. After the first two series, the effects of the variables that had been studied were evaluated and some slight changes were made.

### SPECIMEN DESIGNATION

The slabs were numbered to show all the variables. An example of slab markings follows:

I - 606 - 16A1 - 1

where

- I = series,
- 6 = thickness (inches),
- 06 = time since casting (hours),
- 16 = slab width (inches),
- A1 = anchor 1 = small anchor (3-1/2 x 4-5/8 inches)  
anchor 2 = large anchor (3-1/2 x 6 inches), and
- 1 = indicator of test if all other variables are the same. This applies to Series I only.

### SUMMARY OF RESULTS

This section presents the test results in a summarized form, including tables of concrete strength and slab cracking loads, and discussions of

typical slab behavior. For a more detailed discussion of the slab tests, see Appendix B.

### Concrete Strength

The concrete was supplied by a readymix plant with the design mix as discussed previously. The poor concrete quality of Series I led to a slow strength gain and lower ultimate strength than the other two series. Outside temperatures near freezing, apparent lack of fine aggregate, and high slump all contributed to the poor quality.

The concrete quality of Series II and III was by far superior to that of Series I. The result in improved rate of strength gain was phenomenal.

Concrete strength data is presented in Table 5.1. Time since batching, maturity and concrete compressive, tensile, and flexural strengths for all three series are presented. Concrete placement began 30 minutes after batching for each of the three series and lasted one hour for Series I and II and one and one half hours for Series III. Concrete strengths are presented in graphical form in Chapter 6.

### Behavior of Slabs

With the fairly high concrete strengths that occurred within a few hours of casting, significant post-tensioning force could be applied to the slabs before anchorage zone cracking occurred. Ultimate concrete failure occurred in all Series I slabs but in only 3 of the 14 Series II slabs and 5 of the 14 Series III slabs. Of the remaining 11 slabs of Series II, 10 had ultimate failure by strand failure and one experienced a loading mechanism failure. Four of the Series II slabs never even experienced cracking. In Series III, of the nine slabs that did not fail ultimately, all experienced strand failure and two never cracked. The slab test data may be found in Table 5.2. The specimen designation is included and contains the time since casting. This time, however, is occasionally inaccurate due to the amount of time each test took. The reader should refer to the more detailed test description in Appendix B for more accurate testing times.

TABLE 5.1. SUMMARY OF THE CONCRETE STRENGTH DATA

Time Since Batch (Hrs)	Series I				Series II				Series III			
	Maturity	Compression	Tensile	Flexure	Maturity	Compression	Tensile	Flexure	Maturity	Compression	Tensile	Flexure
6.5	--	--	--	--	--	--	--	--	445	157	--	--
7.0	--	--	--	--	--	--	--	--	481	--	--	61
7.5	--	--	--	--	--	--	--	--	516	--	19	--
8.0	--	--	--	--	493	124	--	--	--	--	--	--
8.5	--	--	--	--	527	--	18	--	--	--	--	--
9.0	--	--	--	--	--	--	--	--	624	330	--	127
9.5	--	--	--	--	560	--	--	68	661	--	53	--
10.0	437	31	--	--	--	--	--	--	--	--	--	--
11.0	486	--	1	--	--	--	--	--	--	--	--	--
11.5	--	--	--	--	--	--	--	--	805	663	--	--
12.0	--	--	--	--	--	--	--	--	840	--	82	236
12.5	--	--	--	--	795	527	--	181	--	--	--	--
13.0	--	--	--	--	830	--	95	--	--	--	--	--
13.5	614	106	--	--	--	--	--	--	--	--	--	--
14.0	640	--	17	--	--	--	--	--	--	--	--	--
15.0	693	--	--	57	--	--	--	--	1041	1333	--	--
15.5	--	--	--	--	--	--	--	--	1073	--	192	373
18.5	--	--	--	--	1195	1680	--	--	--	--	--	--
19.5	930	260	--	93	--	--	--	--	--	--	--	--
20.0	--	--	--	--	1291	--	222	--	--	--	--	--
20.5	981	--	39	--	--	--	--	--	--	--	--	--
24.5	--	--	--	--	1576	2216	--	--	1612	--	288	478
25.0	--	--	--	--	1591	--	303	--	1642	2587	--	--
25.5	--	--	--	--	1607	--	--	504	--	--	--	--
26.5	1295	934	131	--	--	--	--	--	--	--	--	--
27.0	1320	--	--	175	--	--	--	--	--	--	--	--

TABLE 5.2. SUMMARY OF THE SLAB TEST DATA

Specimen	Compression Strength (psi)	Tensile Strength (psi)	Flexure Strength (psi)	Crack Load (kips)	Ultimate Load (kips)	Mode of Failure
I 606-16A1-1	40	1	--	1.75	2.62	Concrete Bearing
I 612-16A1-1	130	18	--	4.68	5.15	Concrete Bearing
I 612-16A1-2	130	18	--	4.68	5.15	Concrete Bearing
I 612-16A1-3	145	20	57	4.68	5.62	Concrete Bearing
I 618-16A1-1	260	35	93	12.97	14.83	Concrete Bearing
I 618-16A1-2	355	39	--	12.97	13.40	Concrete Bearing
I 618-16A1-3	405	41	--	13.84	15.56	Concrete Bearing
I 624-16A1-1	1030	147	--	31.72	34.13	Concrete Bursting
I 624-16A1-2	1080	154	--	29.53	33.69	Concrete Bursting
I 624-16A1-3	1180	170	--	28.44	33.69	Concrete Bursting
II 606-24A1	170	18	52	8.75	9.85	Concrete Bearing
II 606-24A2	215	29	68	10.94	13.13	Concrete Bearing
II 606-16A2	206	40	84	13.57	19.00	Concrete Bursting
II 612-16A2	527	84	181	37.20	--	Concrete Bursting
II 612-24A1	720	105	205	45.95	--	Concrete Bursting
II 612-24A2	800	125	218	46.44	--	Concrete Bursting
II 618-16A2	1680	192	330	--	--	Load Mechanism
II 618-24A1	1950	246	405	--	--	Strand
II 618-24A2	2000	254	417	--	--	Strand
II 618-16A1	2050	262	430	51.64	--	Crack/Strand
II 624-16A1	2090	270	442	50.76	--	Strand/Crack
II 624-16A2	2130	278	454	49.23	--	Crack/Strand
II 624-24A1	2180	287	467	--	--	Strand
II 624-24A2	2180	287	467	--	--	Strand
III 604-16A1	157	5	45	9.51	12.45	Concrete Bursting
III 804-16A1	192	11	61	18.16	29.66	Concrete Bursting
III 804-24A1	226	19	78	17.29	20.23	Concrete Bursting
III 804-12A1	261	28	94	26.80	37.87	Concrete Bursting

(continued)

TABLE 5.2. (CONTINUED)

Specimen	Compression Strength (psi)	Tensile Strength (psi)	Flexure Strength (psi)	Crack Load (kips)	Ultimate Load (kips)	Mode of Failure
III 608-16A1-2	330	53	127	--	--	Concrete Bursting
III 608-16A1	530	65	182	34.52	40.36	Concrete Bursting
III 808-16A1	596	70	200	43.79	--	Crack/Strand
III 808-12A1	759	82	236	48.95	--	Crack/Strand
III 808-24A1	854	98	256	51.52	--	Crack/Strand
III 612-16A1	1046	129	295	47.23	--	
III 812-16A1	1142	145	314	53.24	--	Strand/Crack
III 812-24A1	1237	161	334	--	--	Strand/Crack
III 816-24A1	1333	176	353	--	--	Strand
III 616-16A1	1333	176	353	45.08	--	Crack/Strand
III 816-16A1	1429	192	373	52.81	--	Strand/Crack

Two different modes of anchorage zone failure occurred in the test slabs. The first, a bearing or shearing failure, took place in the very early tests, 4 to 6 hours after casting; and the second, a bursting failure, took place in the later tests, 8 to 24 hours after casting.

Bearing Failure. A typical bearing type failure sequence is shown in Fig 5.1. First a crack forms above the anchor, angling off toward the sides of the slabs as shown in Fig 5.1(a). Often a short segment of this Y-shaped crack is parallel to the anchor plate immediately above it, and typically the intersection of the Y-shape is in this region directly above the anchor plate.

In the second stage of the failure increasing crack lengths and widths develop with increased load, as shown in Fig 5.1(b). As load is further increased, the anchor begins to lift and additional cracking occurs as a bulge forms (see Fig 5.1(c)).

Finally the anchor lifts up as a wedge of concrete directly in front of the anchor plate moves through the slab as shown in Fig 5.1(d). The angle of the large diagonal cracks is typically determined by the corner of the anchor plate and the corner of the closed reinforcing hoop.

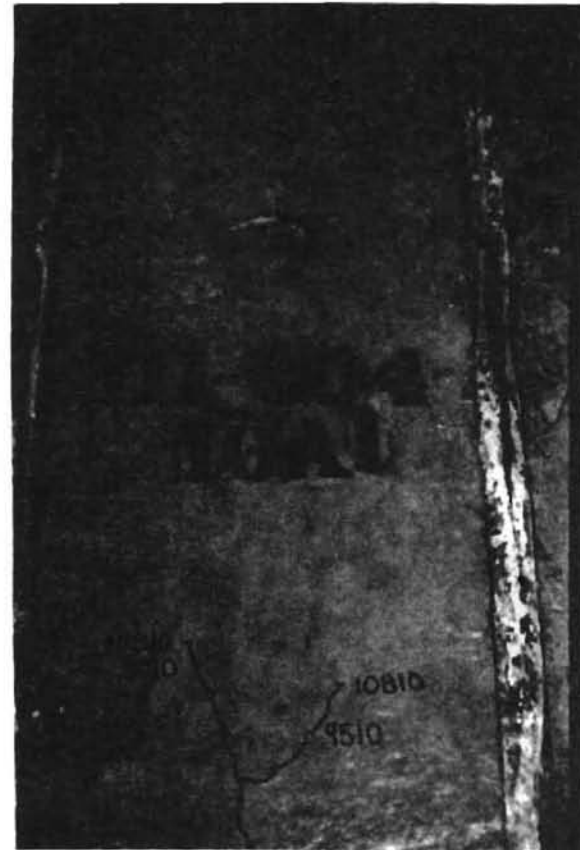
Figure 5.1(e) shows the slab after the loose cover was removed and Fig 5.1(f) shows the back edge of the slab after ultimate failure.

Bursting Failure. Bursting failures occur when the concrete has gained stiffness and strength and is able to absorb more energy. The additional stiffness leads to a quicker release of energy and a more violent explosive failure. The typical trend of a bursting stress failure is shown in Figs 5.2 and 5.3.

The first signs of failure show a crack along the tendon path beginning near the point of the anchor plate and extending into the slab some distance (Fig 5.3(a)). As the load increases the crack extends into the slab and back to the slab edge (Fig 5.3(b)). The crack continues to extend into the slab typically to a distance about equal to the slab width but occasionally farther (Fig 5.3(c)). Occasionally diagonal cracks form and an explosive bursting failure follows (Fig 5.2), but often these two stages occur simultaneously (Fig 5.3(d)).



(a) First crack at 9.51 kips.



(b) Extended cracks at 10.81 kips.

(continued)

Fig 5.1. Typical early test experiencing a bearing type failure.



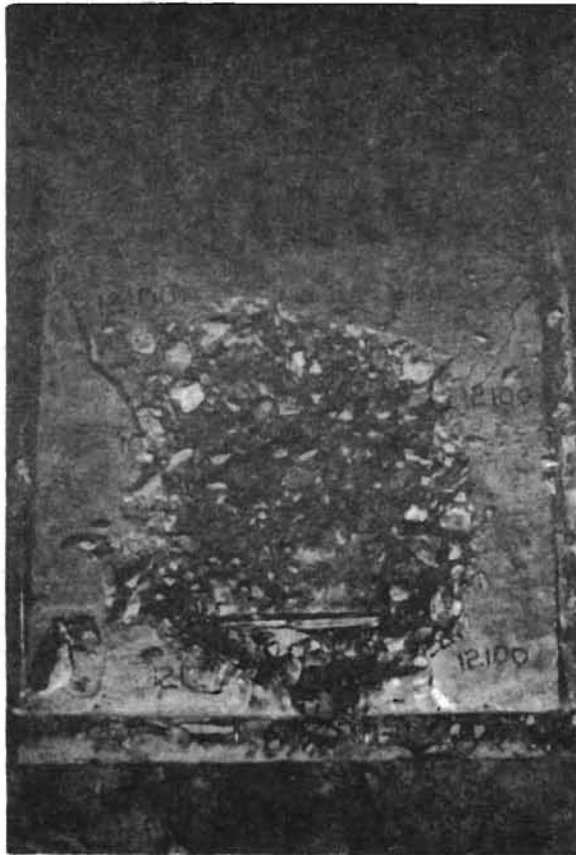
(c) Increased cracking at 12.10 kips.



(d) Ultimate failure at 12.45 kips.

(continued)

Fig 5.1. (continued).



(e) Anchorage zone after loose cover is removed after ultimate failure.



(f) Back edge of slab after ultimate failure.

Fig 5.1. (continued).

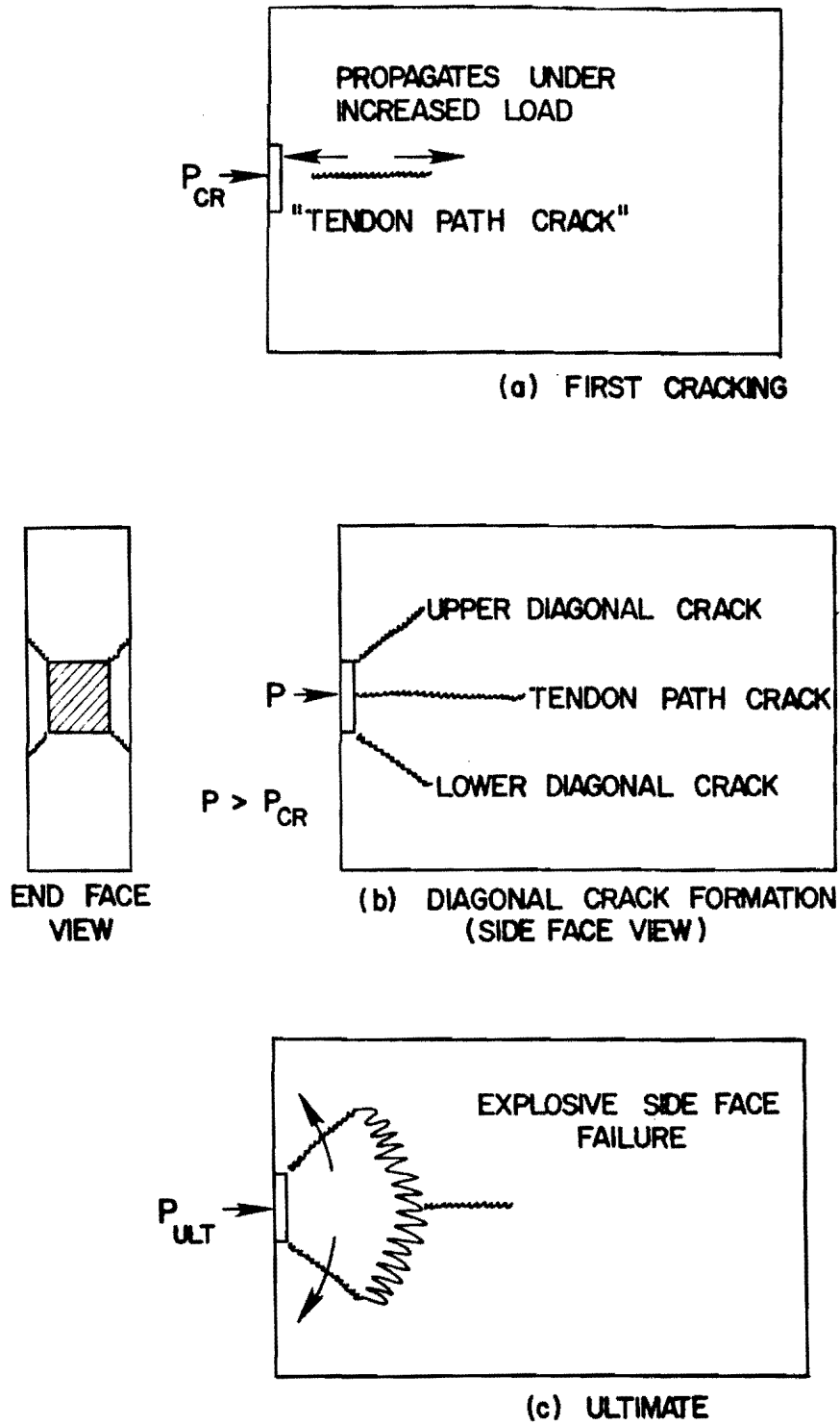


Fig 5.2. Bursting failure sequence (from Ref 23).



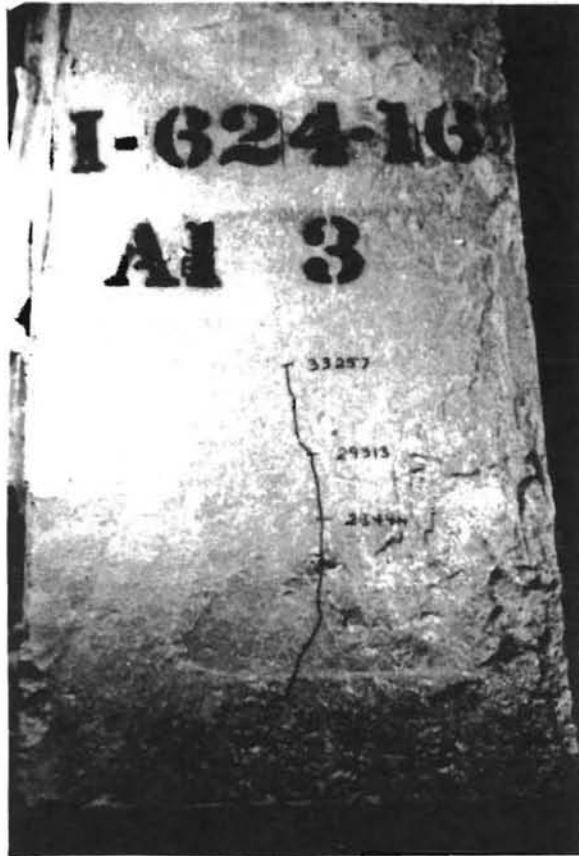
(a) First crack at 28.44 kips.



(b) Extended crack at 29.31 kips.

(continued)

Fig 5.3. Typical bursting type failure sequence of later tests.



(c) Extended crack at 33.26 kips.



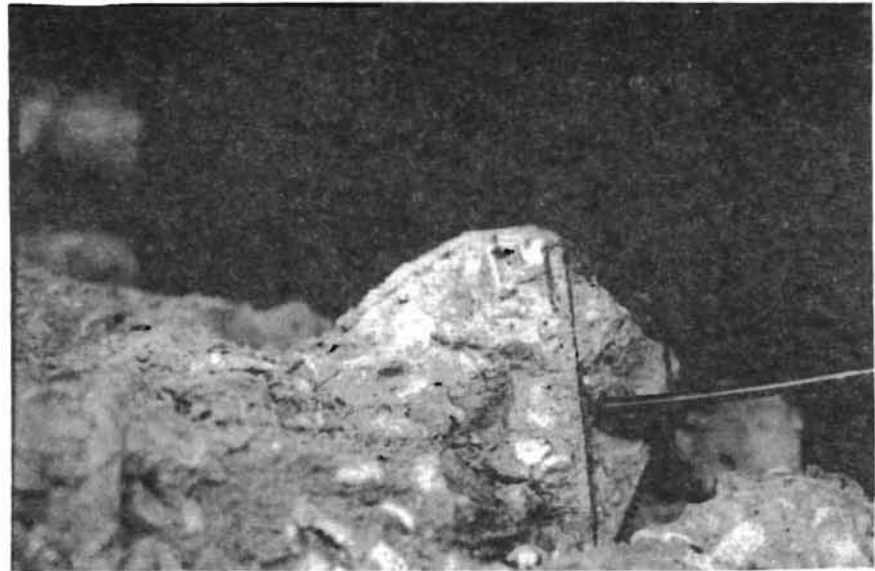
(d) Ultimate explosive failure at 33.69 kips.

(continued)

Fig 5.3. (continued).



(e) Destroyed anchorage zone  
after ultimate failure.



(f) Pyramid of concrete forming in front of  
the anchor plate.

Fig 5.3. (continued).

The destroyed anchorage zone is shown in Fig 5.3(e). A pyramid of concrete formed in front of all the anchorages in slabs that experienced ultimate failure as high localized compressive stresses were transferred from the plate to the concrete (see Fig 5.3(f)). This mechanism is important in the development of the bursting stresses and is covered in Chapter 6.

#### SUMMARY OF EACH SERIES

This section contains a brief summary of each of the three test series. The results that are presented pertain only to that series and not the testing program as a whole. A discussion of the results of the entire test program may be found in Chapter 6.

##### Series I

The concrete quality of the first series was very poor. The mix was very stiff at first (3/4 inch slump) so 15 gallons of water were added to 2-1/4 cubic yards of concrete. This made the mix very fluid. The slump was 4-1/2 inches but the concrete would not hold a cone shape very well. It was later discovered that the concrete appeared to be lacking fine aggregate.

The ambient temperature in the lab at the time of casting was 50°F. The low temperature was 49°F and the high was 57°F. The low ambient temperature yielded low concrete temperatures ranging from 50°F to 65°F and slow curing.

Test Slabs. Twelve identical slabs (6-inch thick and 16-inches wide) were cast and then were tested to failure. The remaining two were left over from the six hour test where only one slab was tested because of such low concrete strengths. Of the ten tests, the first seven slabs failed by the bearing mode previously described, and the remaining three experienced bursting failures.

Results. The purpose of casting identical slabs was to check the scatter of data. The test showed very little data scatter for this series as shown in Fig 5.4. Therefore, it was decided to do only one test, rather than three, for a given set of variables.

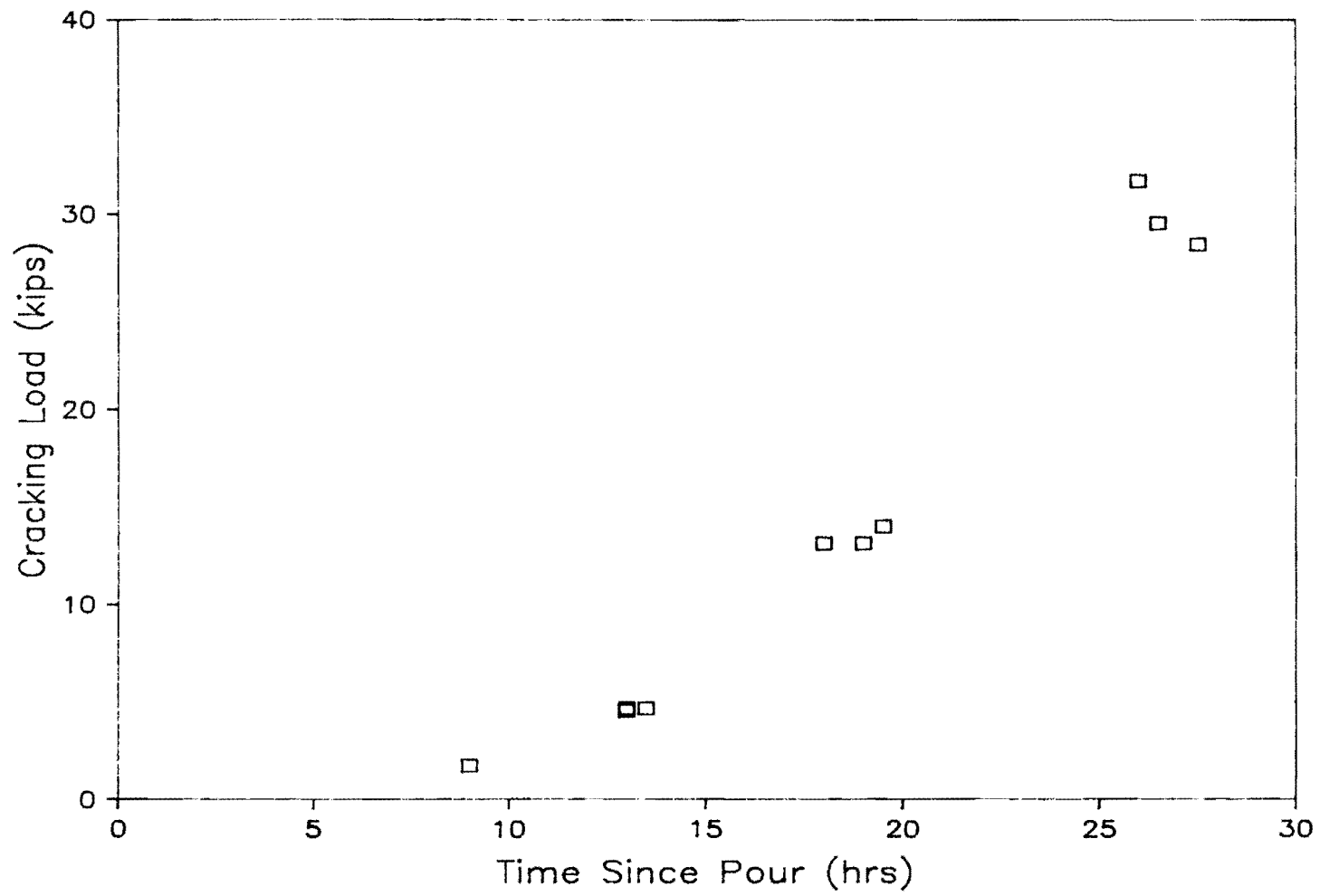


Fig 5.4. Degree of scatter for Series I Tests.

## Series II

Concrete quality was much better for this series, compared to Series I. A slump of one inch was measured and no water was added to the mix. Placement was more difficult for this series than for the first, but concrete was well vibrated and no honeycombing was noticed after forms were stripped and no voids were observed. Slabs were cured under wet burlap and plastic.

The ambient temperature was higher for this series than for the first, ranging from 64°F to 72°F. Ambient and concrete temperatures were both 69°F at the time of placement. The temperature range of the second group of slabs was 69°F to 79°F, and for the third the range was 69°F to 91°F. The difference was due to the fact that two groups of slabs had to be tested earlier than the third, and so the plastic and burlap had to be removed for the six-hour testing. The slabs were covered after tests were complete, but the two to three hours that they were exposed to cooler air prevented them from reaching the same temperature as the third group of slabs, which remained covered until the 12 hour test.

Test Slabs. Fourteen slabs were cast with varying anchor size and tendon spacing (slab width). One slab did not provide data because of a loading mechanism failure, which is described in greater detail in Appendix B. Of the remaining 13 slabs only the three 6-hour tests experienced a concrete ultimate failure. The failure of each of these three tests was the bearing type failure. Five of the remaining ten slabs produced the beginning cracks of the bursting type failure, but the strand failed before the concrete failed ultimately. Of the remaining five slabs, four never cracked, but experienced strand failures; the other was thought to be uncracked until the strand failed, and then a crack was noticed. This could be due to the dynamic effect with the breaking strand.

Results. The anchor size was varied in this series but no difference in slab performance or capacity between the two anchorages could be determined. As a result, anchor size was not varied in the third series, and only the smaller size anchorage was used.

### Series III

After Series II was completed and the data were studied, a few small changes were made in the testing program. The first change, which was previously mentioned was that the anchor size was no longer varied.

The second change came about because of the reduction in the number of tests due to the first change. The tests on 6-inch thick by 16-inch wide slabs with the small anchor were repeated because the poor quality concrete of Series I led to poor test data.

The third change, a result of the surprisingly high early strength of the concrete of the second series, was that testing times were changed to four hour intervals rather than six hour. This put the testing at 4, 8, 12, and 16 hours from casting.

Test Slabs. Fifteen slabs were cast in this series and 14 were tested successfully. One slab that had two strands was tested somewhat unsuccessfully for comparison to the single strand slabs. For a discussion of this test, see Appendix B.

Five slabs experienced ultimate concrete failures. Two of these five were bearing failures and three were bursting failures.

Five slabs experienced bursting stress cracks but had ultimate failure by strands breaking. Two slabs did not crack until after the strand broke and then slight cracks were noticed. Two slabs never cracked but experienced strand failures.

Results. Data were obtained to determine the effects of the variables listed in Chapter 4. The data reduction and conclusions on the effects of variables are covered in the next chapter.

This page replaces an intentionally blank page in the original.

-- CTR Library Digitization Team

## CHAPTER 6. DISCUSSION OF THE EFFECTS OF VARIABLES

### GENERAL

This chapter reviews the effects of the tested variables on concrete strength and slab cracking load. Also contained in this chapter is a comparison of test data to theory.

### CONCRETE STRENGTH

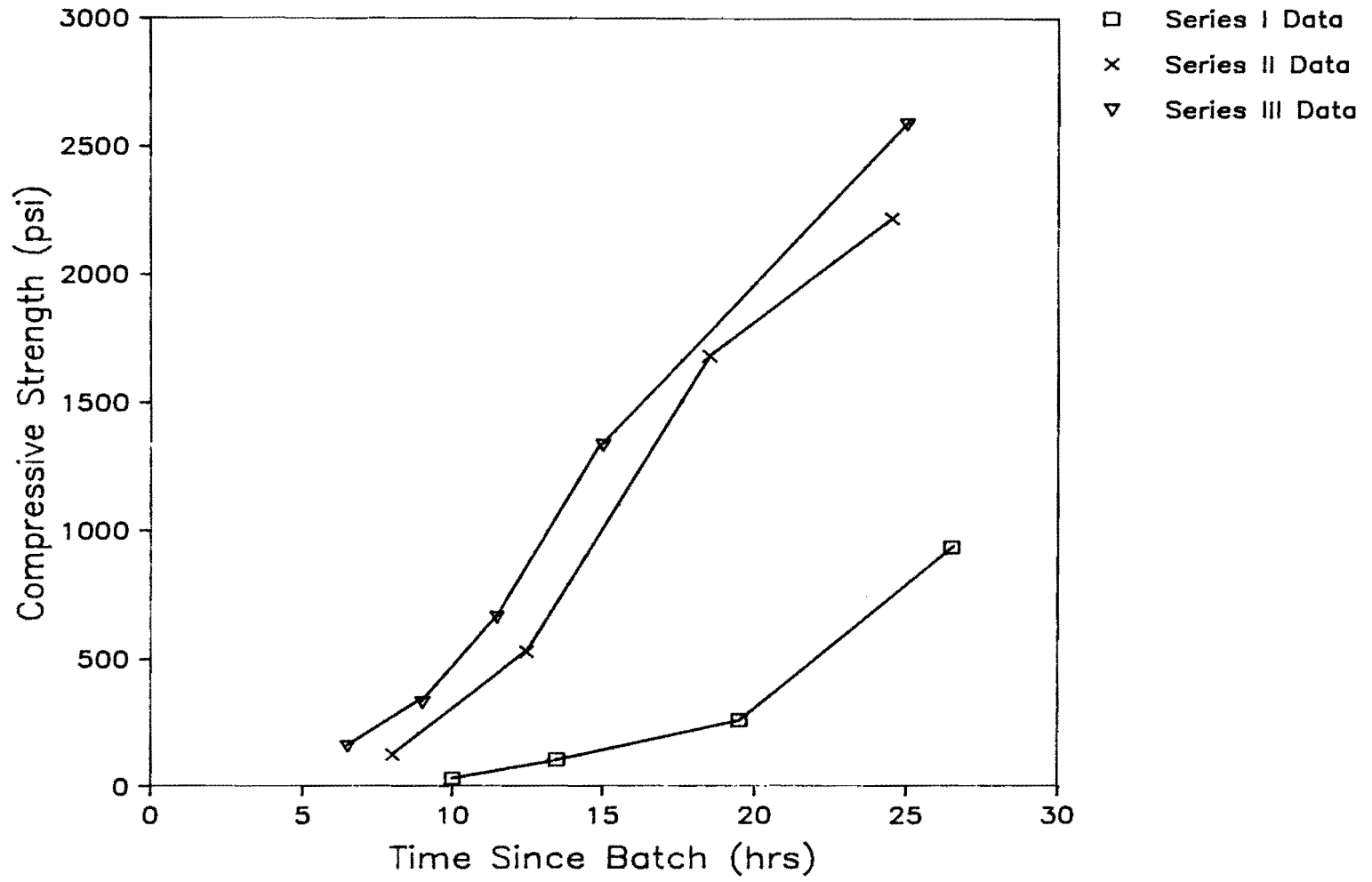
This section discusses the effects of time and temperature on the concrete strength. Temperature effects are incorporated into the maturity factor. This section also examines the difference in the concrete compressive strength gain and tensile strength gain.

#### Time Since Batch

Concrete strength was measured by three different methods. The first was compressive cylinders 6 inches in diameter. The second was a split tensile test using 6-inch-diameter cylinders. The third was a flexural test using a center point loaded 6 x 6 x 20-inch simply supported beam with an 18-inch span.

Each of these strength indicators is plotted against time since batching for the first 24 hours in Fig 6.1. Time since batching was chosen as the most practical indicator of time, since the concrete hydration process begins at this point. Placing began 30 minutes after batching for all three series and lasted one hour for Series I and II and 1-1/2 hours for Series III.

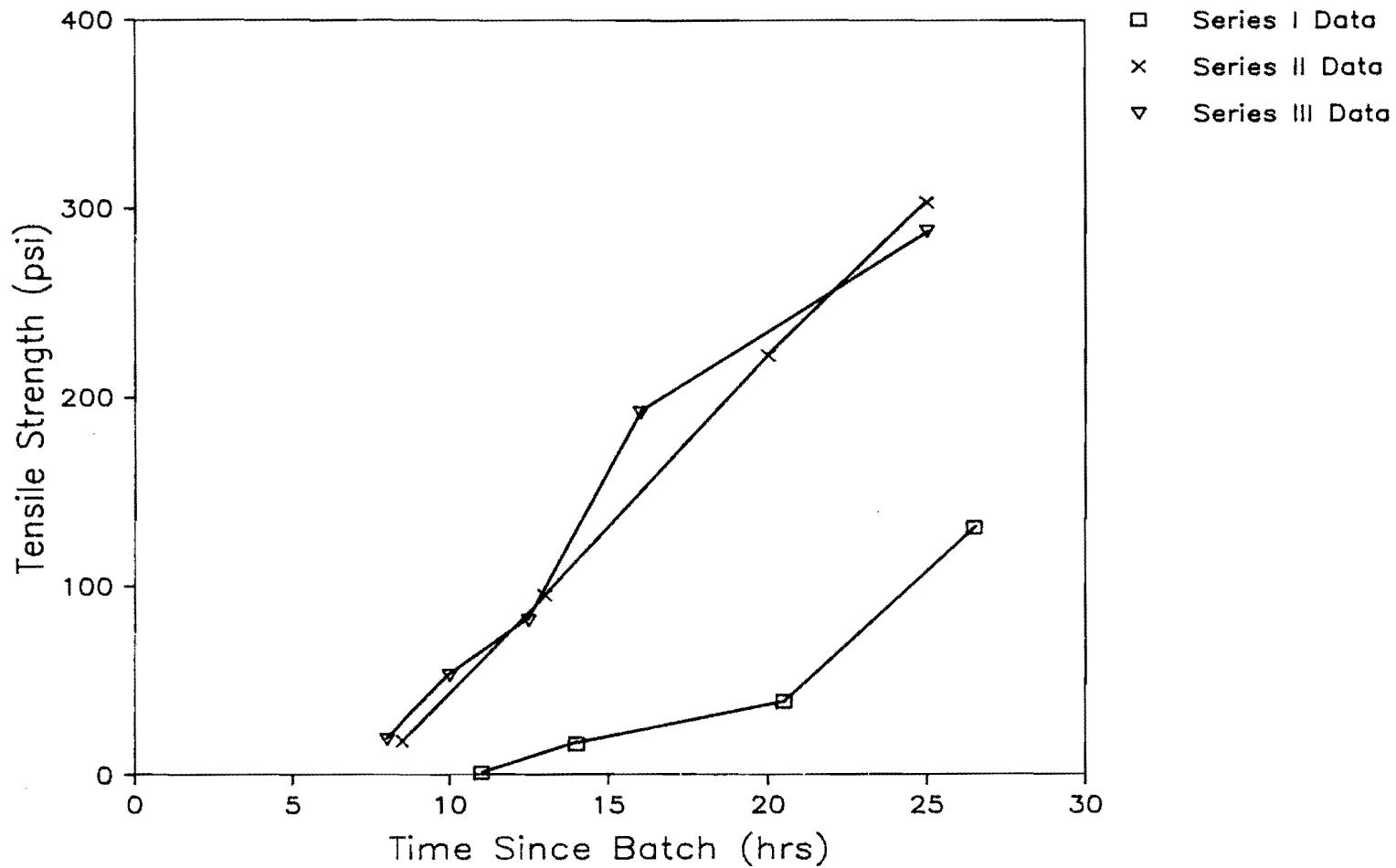
Strength gain to 28 days is also plotted against time and may be found in Fig 6.2.



(a) Compressive strength data

(continued)

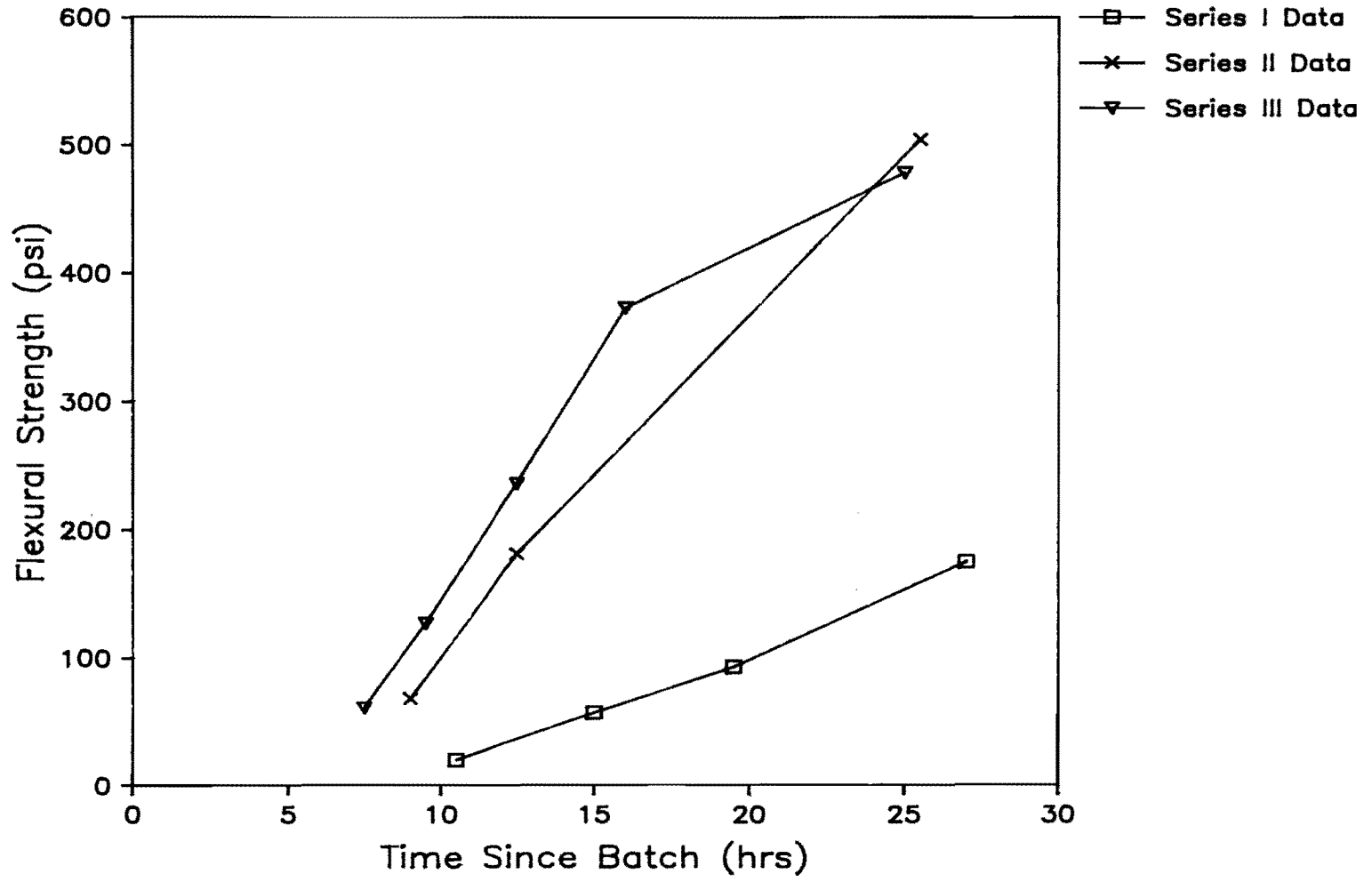
Fig 6.1. Early concrete strength data for each of the three test series.



(b) Tensile strength data.

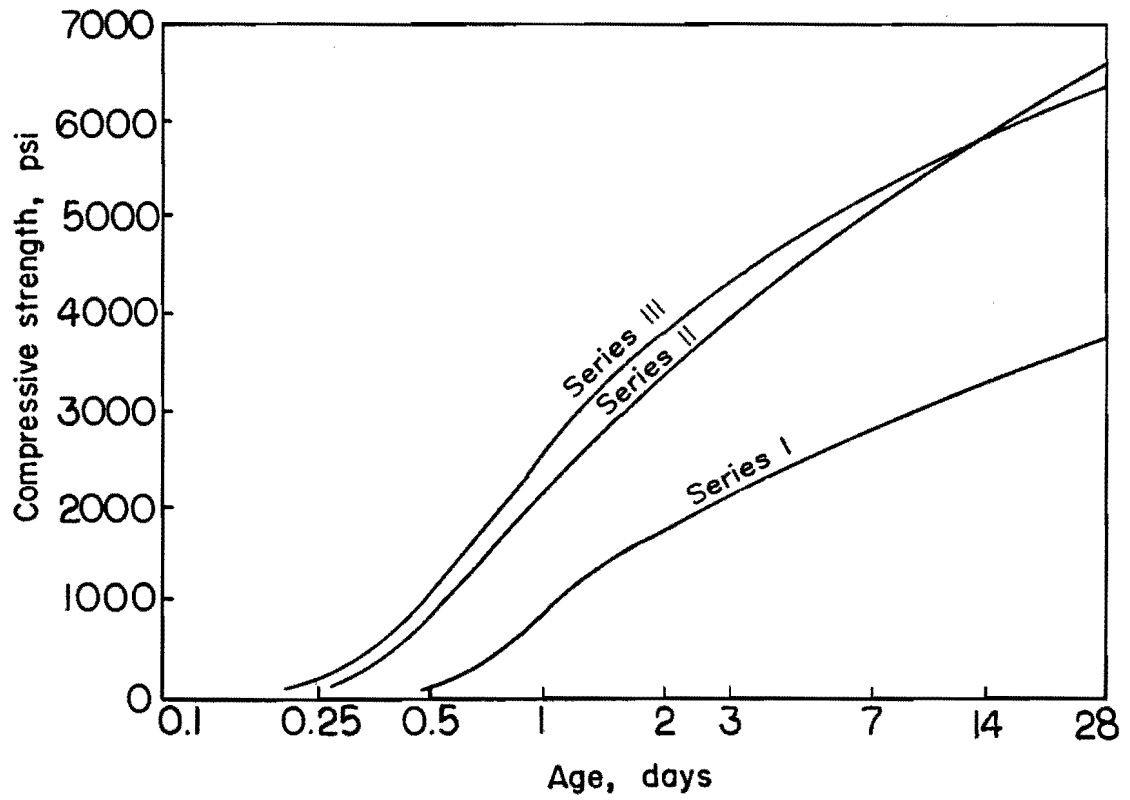
(continued)

Fig 6.1. (continued).



(c) Flexural strength data.

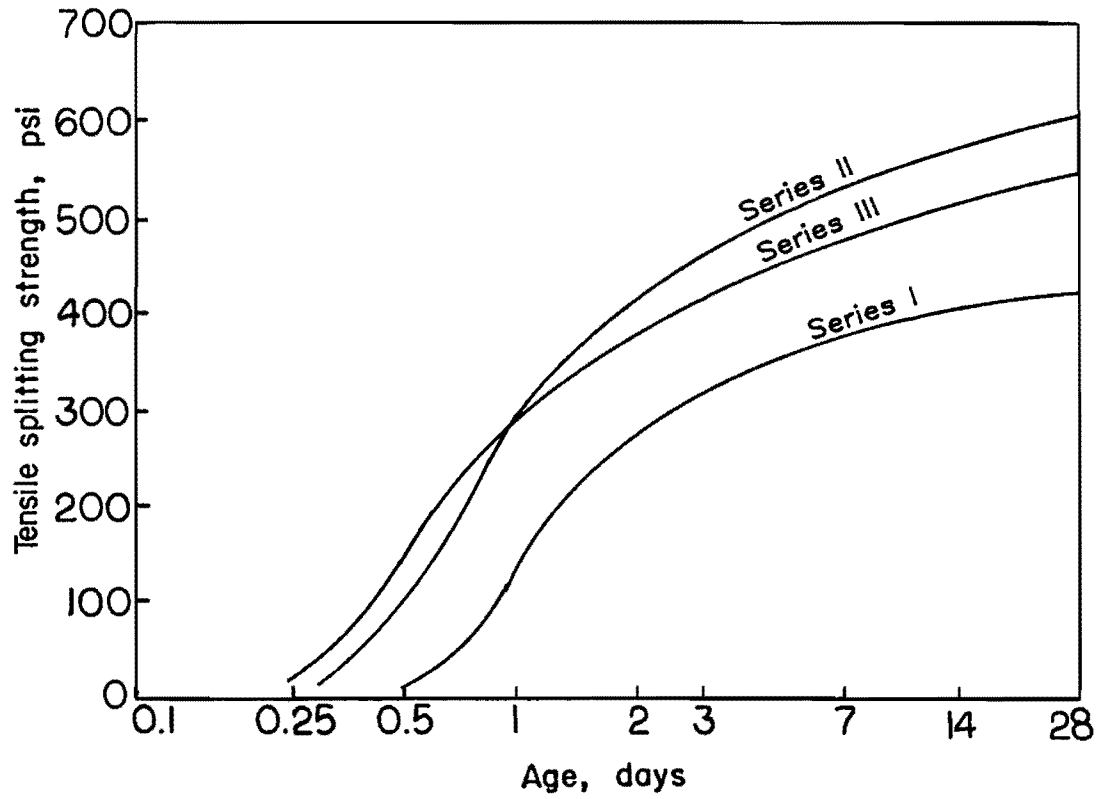
Fig 6.1. (continued).



(a) Compressive strength data.

(continued)

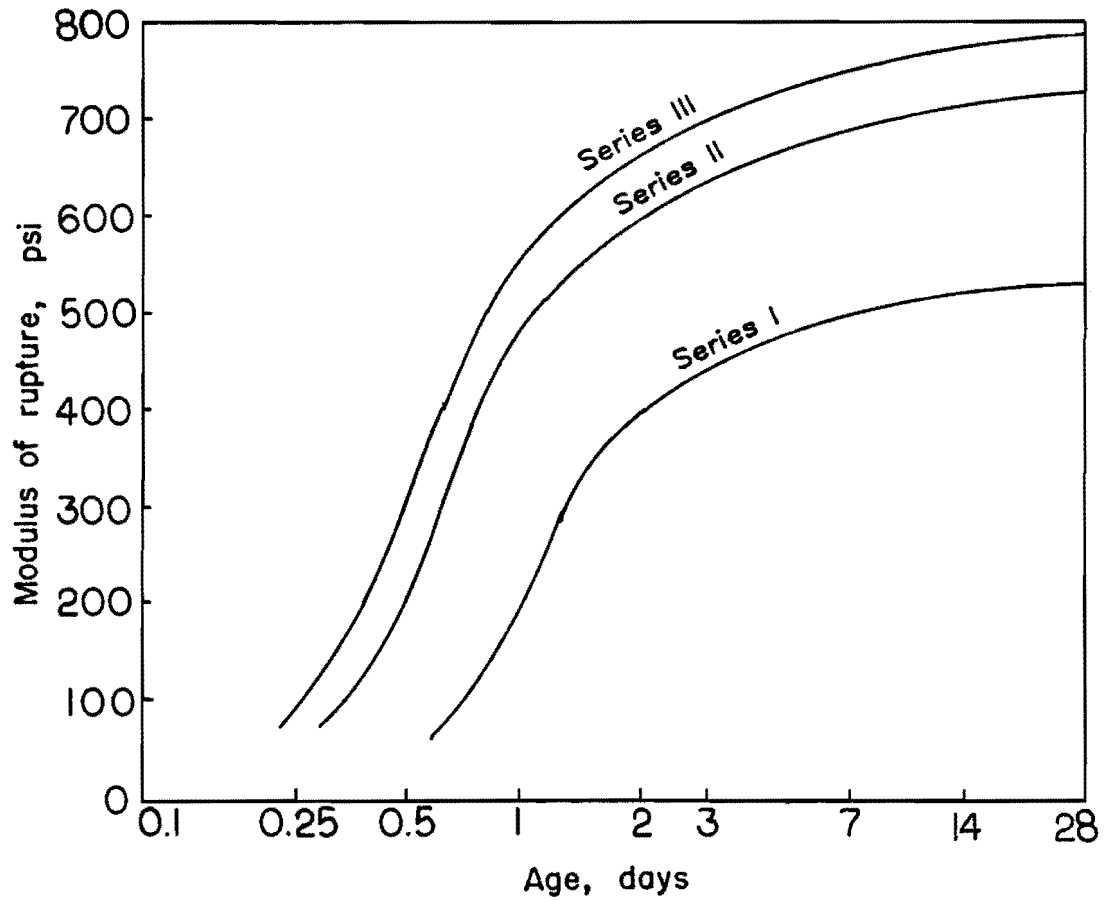
Fig 6.2. Concrete strength to 28 days for each of the three test series.



(b) Tensile strength data.

(continued)

Fig 6.2. (continued).



(c) Flexural strength data.

Fig 6.2. (continued).

### Maturity

Curing temperature is an extremely important factor in early concrete strength gain. Concrete maturity, which takes temperature into account, is a more accurate indicator of concrete strength gain than time alone.

The temperature was considerably lower for the first series than for the second and third series. Ambient temperature was recorded regularly from the time the concrete was placed until the testing of the slabs was complete. A plot of the lab ambient temperature versus time may be found in Fig 6.3(a).

The lower ambient temperature of Series I led to lower concrete temperature and, therefore, to a slower strength gain. The low temperature was not the only factor in the strength gain of Series I concrete; other factors previously mentioned also contributed to the lower strength. Concrete temperatures for all three series may be found in Fig 6.3(b).

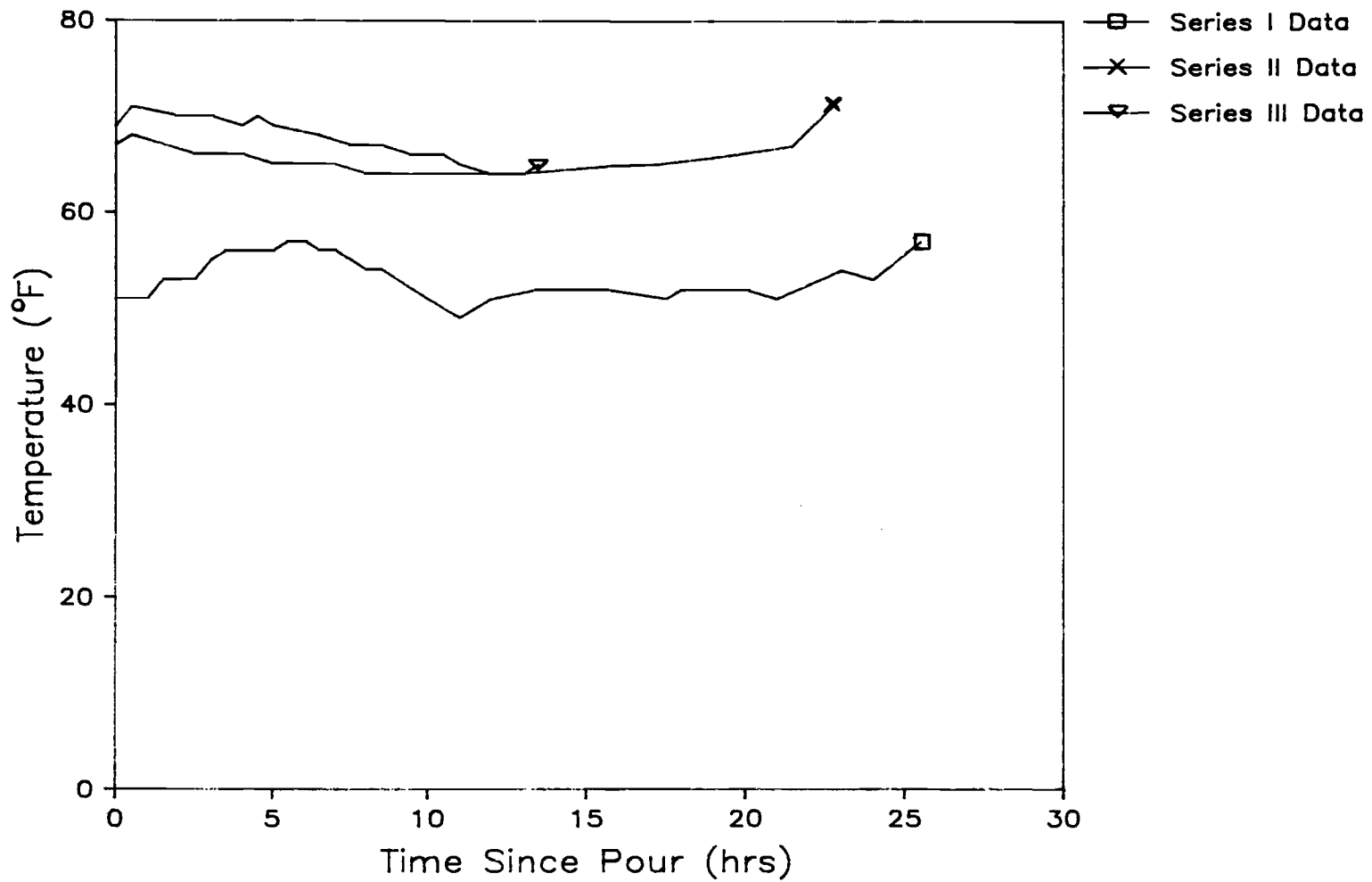
The effect of the curing temperatures becomes apparent when the concrete strength is plotted against maturity, as in Fig 6.4. In all three cases, the maturity factor is a better indicator of concrete strength than time.

### Comparison of Strength Gain

An interesting observation may be made about the early age concrete strength gain. Figure 6.5 shows concrete tensile strength plotted as a percentage of compressive strength versus time. At first the concrete gains some compressive strength with virtually no tensile strength. Then the tensile strength increases at a greater rate than compressive strength.

### SLAB TESTS

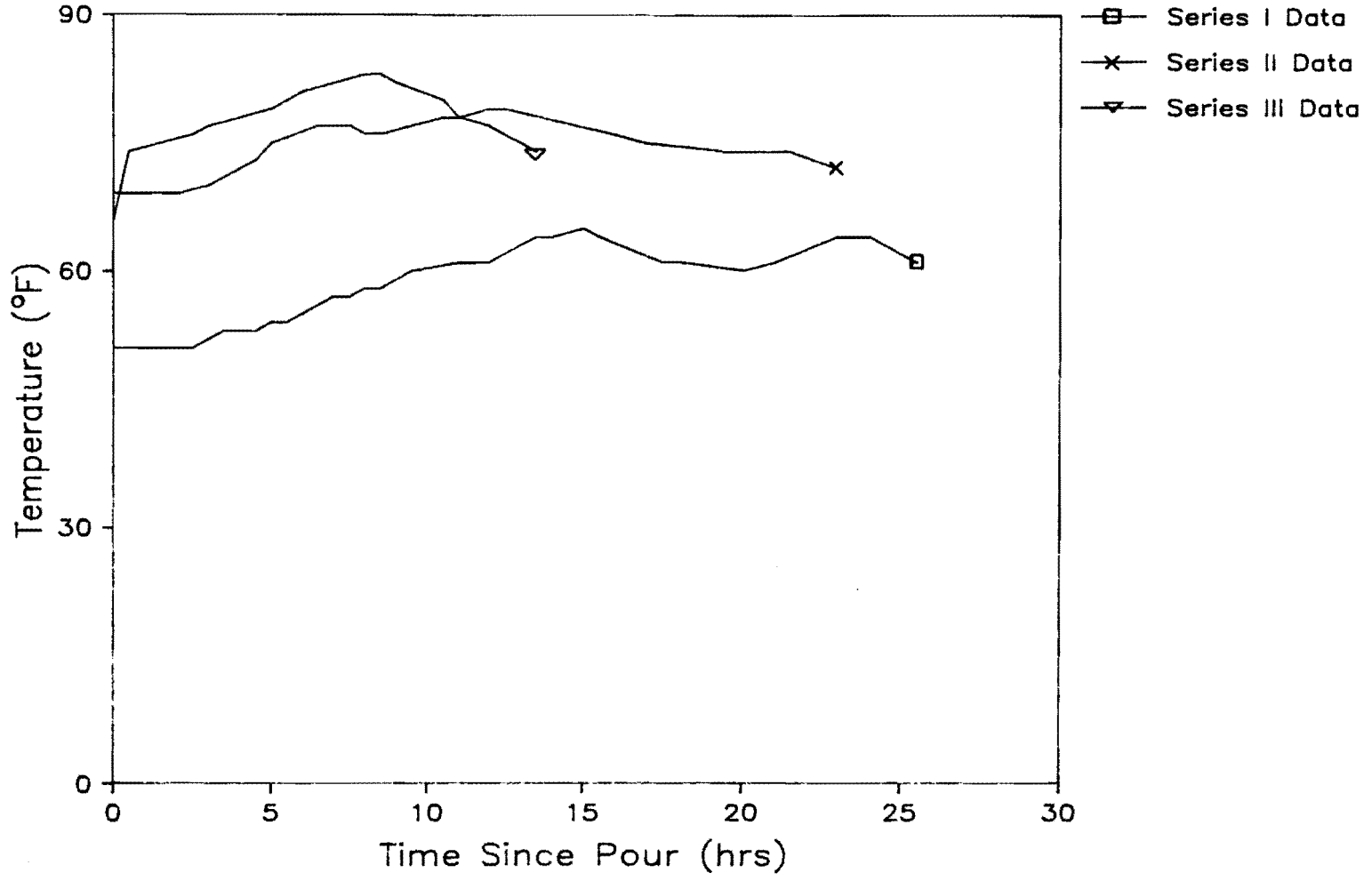
This section discusses the effects of the experimental parameters on the load which causes cracking in the anchorage zone and the load which causes ultimate failure.



(a) Ambient temperature.

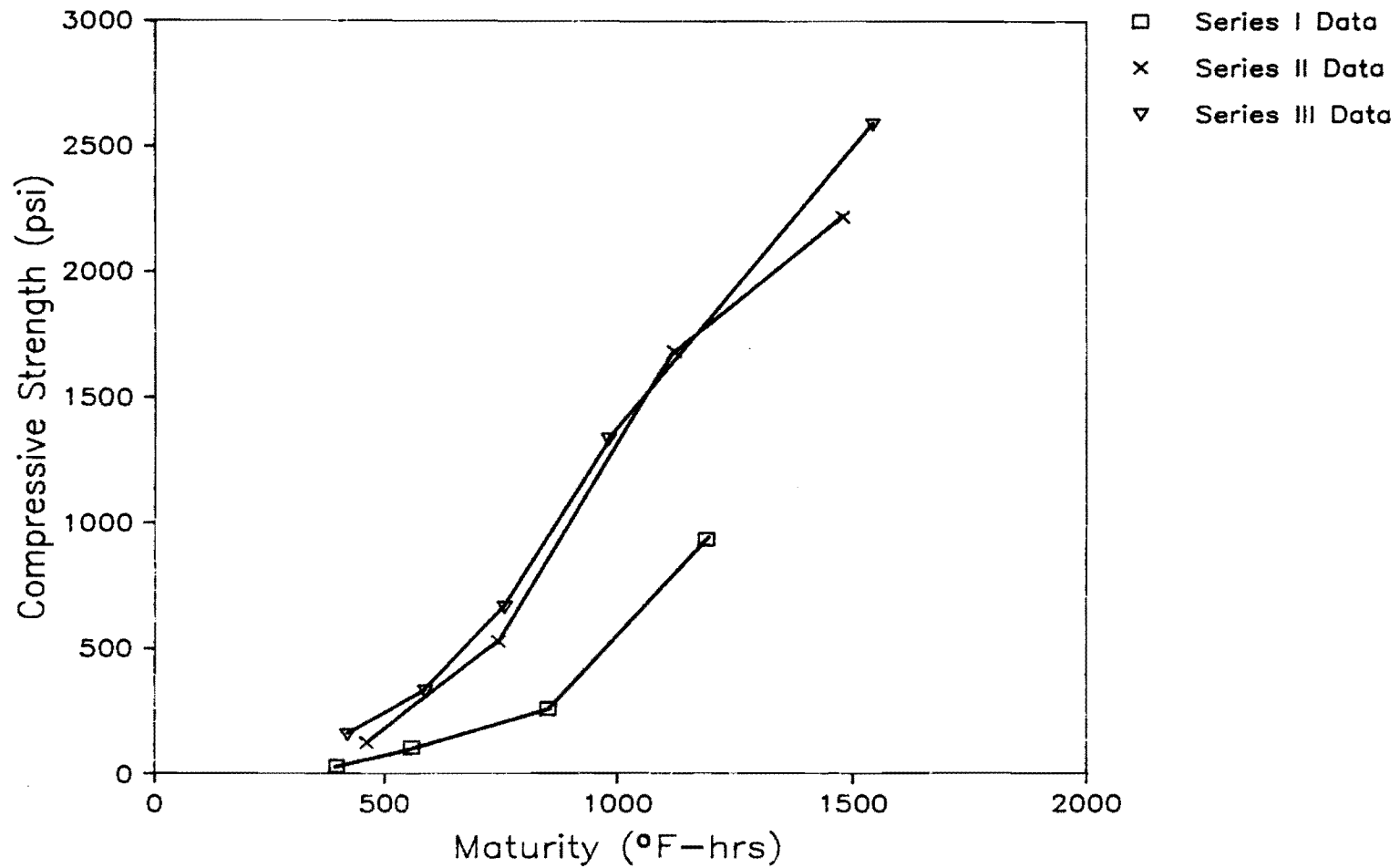
(continued)

Fig 6.3. Temperature variation for each of the three test series.



(b) Concrete temperature.

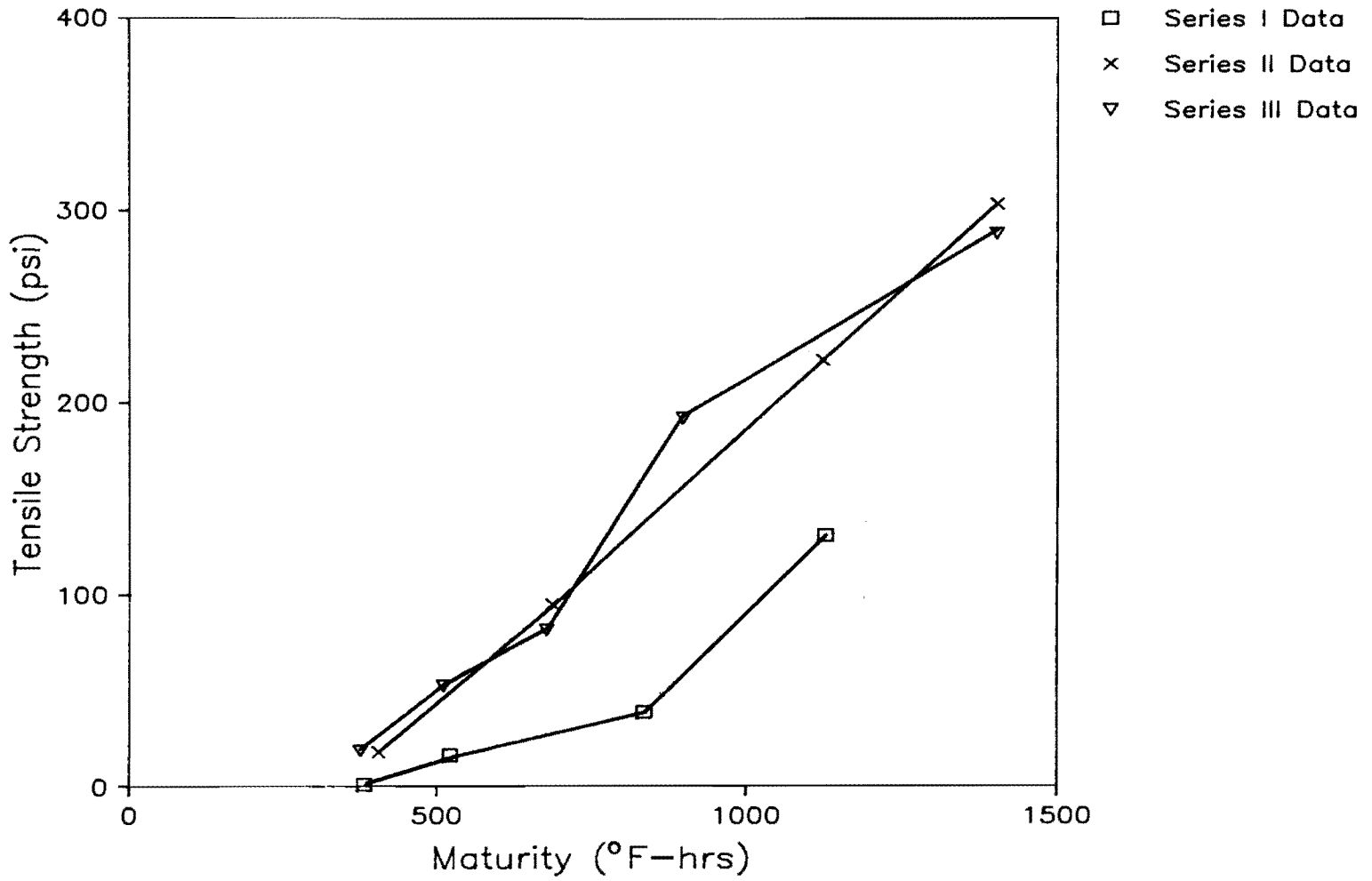
Fig 6.3. (continued).



(a) Compressive strength data.

(continued)

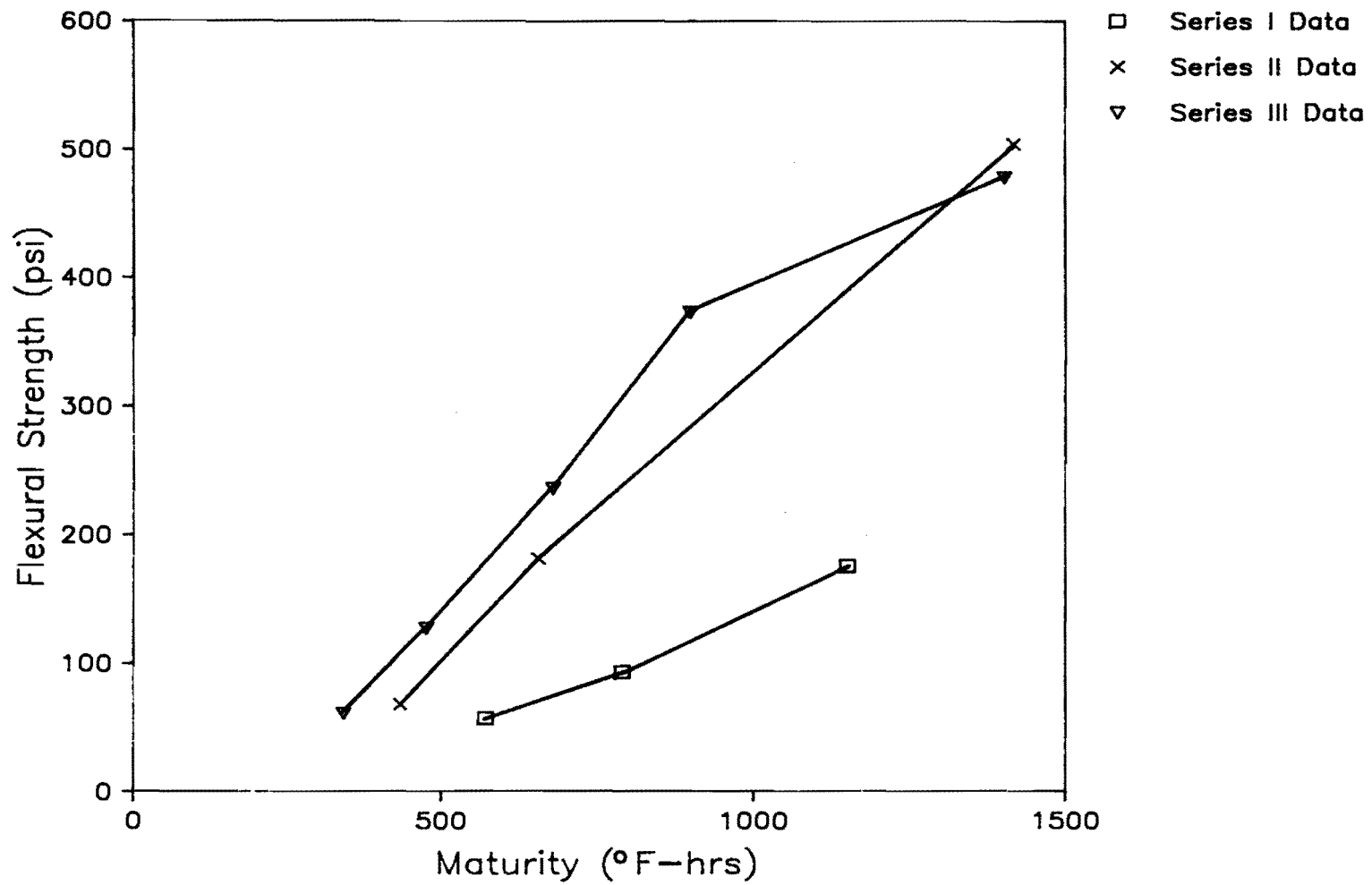
Fig 6.4. Early concrete strength versus maturity.



(b) Tensile strength data.

(continued)

Fig 6.4. (continued).



(c) Flexural strength data.

Fig 6.4. (continued).

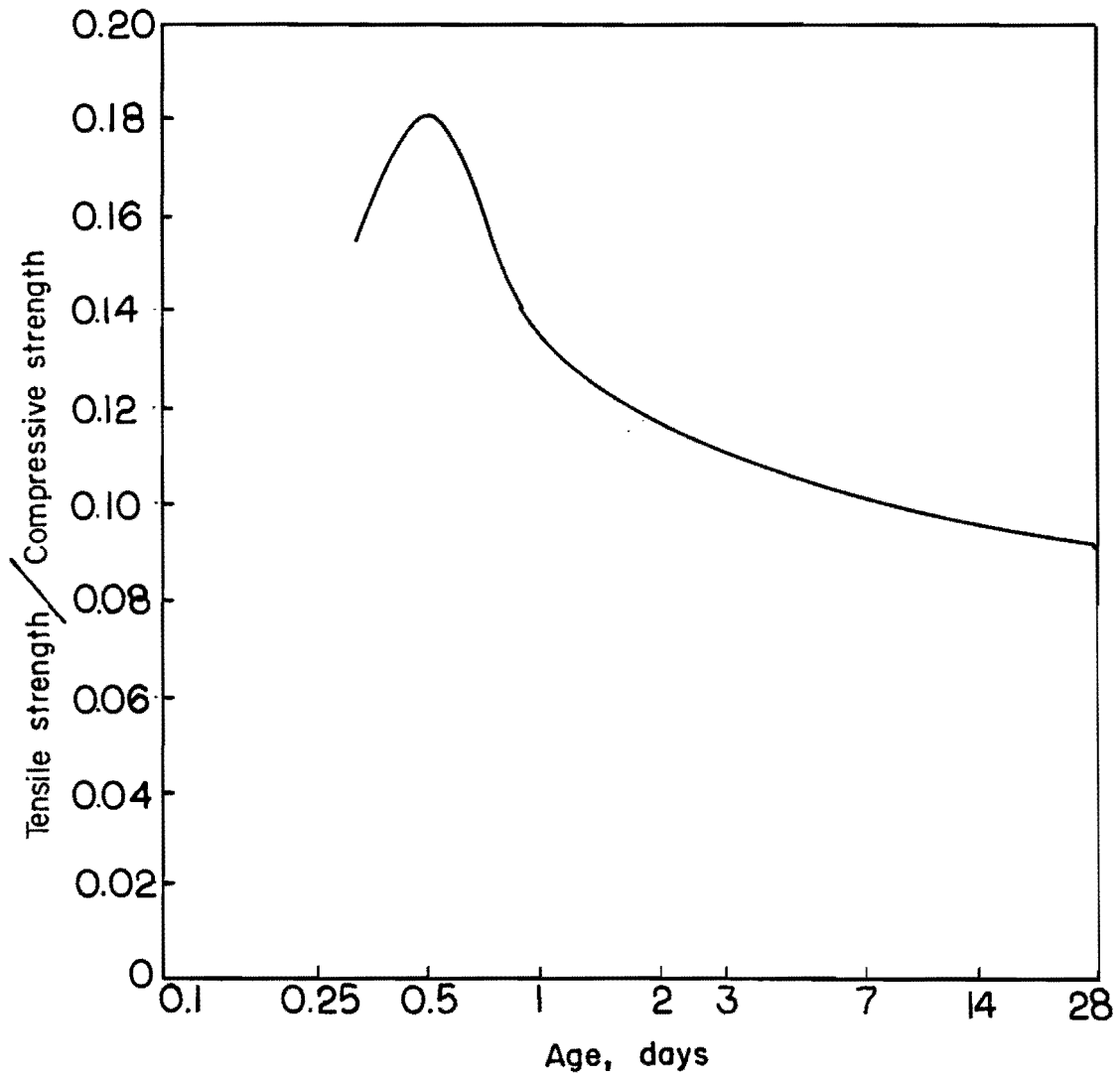


Fig 6.5. Comparison of the gain in concrete tensile strength to compressive strength.

### Effects of Variables on Cracking Load

Each variable considered had a degree of influence on the slab cracking load. In the following discussion the degree of influence of the variable will be determined so that predicting anchorage zone cracking loads may be possible.

Concrete Quality. Concrete quality was not intended to be a variable in the testing program but became one when a poor batch of concrete was delivered and placed. High slump, lack of fine aggregate, and low curing temperature all contributed to the poor concrete quality for Series I.

The poor quality concrete brought interesting results. It was assumed that for a given set of variables, a particular concrete strength would give a particular slab cracking load regardless of the concrete quality. Figure 6.6 shows that this assumption is false. With the same set of variables at 100 psi tensile strength, the cracking load ( $P_{cr}$ ) capacity for the Series III slab was 90 percent higher than that for the Series I slab. The same trend occurs when cracking load is compared to compressive and flexural strengths.

Anchor Size. The size of the anchor plate directly affects the magnitude of the bearing stress. If bearing stress is a factor in the cracking load then anchor size should have some effect. Two anchor sizes were tested in Series II, one anchor having 30 percent more bearing area than the other.

For the anchors tested, bearing area had no apparent effect on the cracking load. Figure 6.7 shows that in both 16-inch and 24-inch wide, 6-inch-thick slabs the increase in area did not affect cracking loads. In fact, the slabs with the smaller anchor (A1) experienced first cracking at a slightly higher load than those with the larger anchor. The difference, however, is small and can be attributed to scatter, as plotted in Fig 5.7.

Time. As the time after concrete batching increases, the concrete strength increases, as does the cracking load. Although concrete gains strength with time, maturity, a factor which combines time and temperature (see Chapters 3 and 6), provides a better indicator of concrete strength than

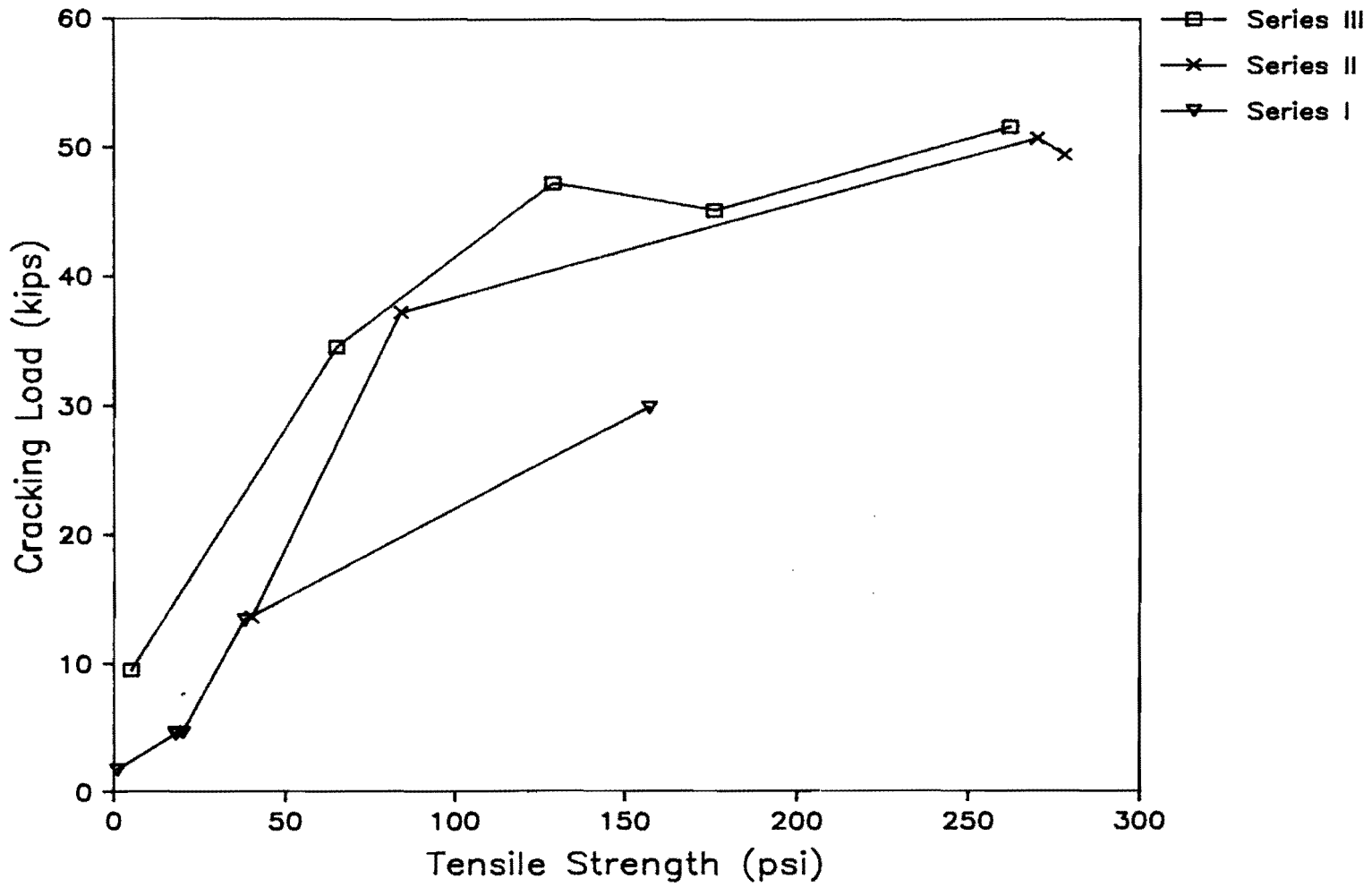


Fig 6.6. The effect of concrete quality on cracking load. Series I had poor quality concrete.

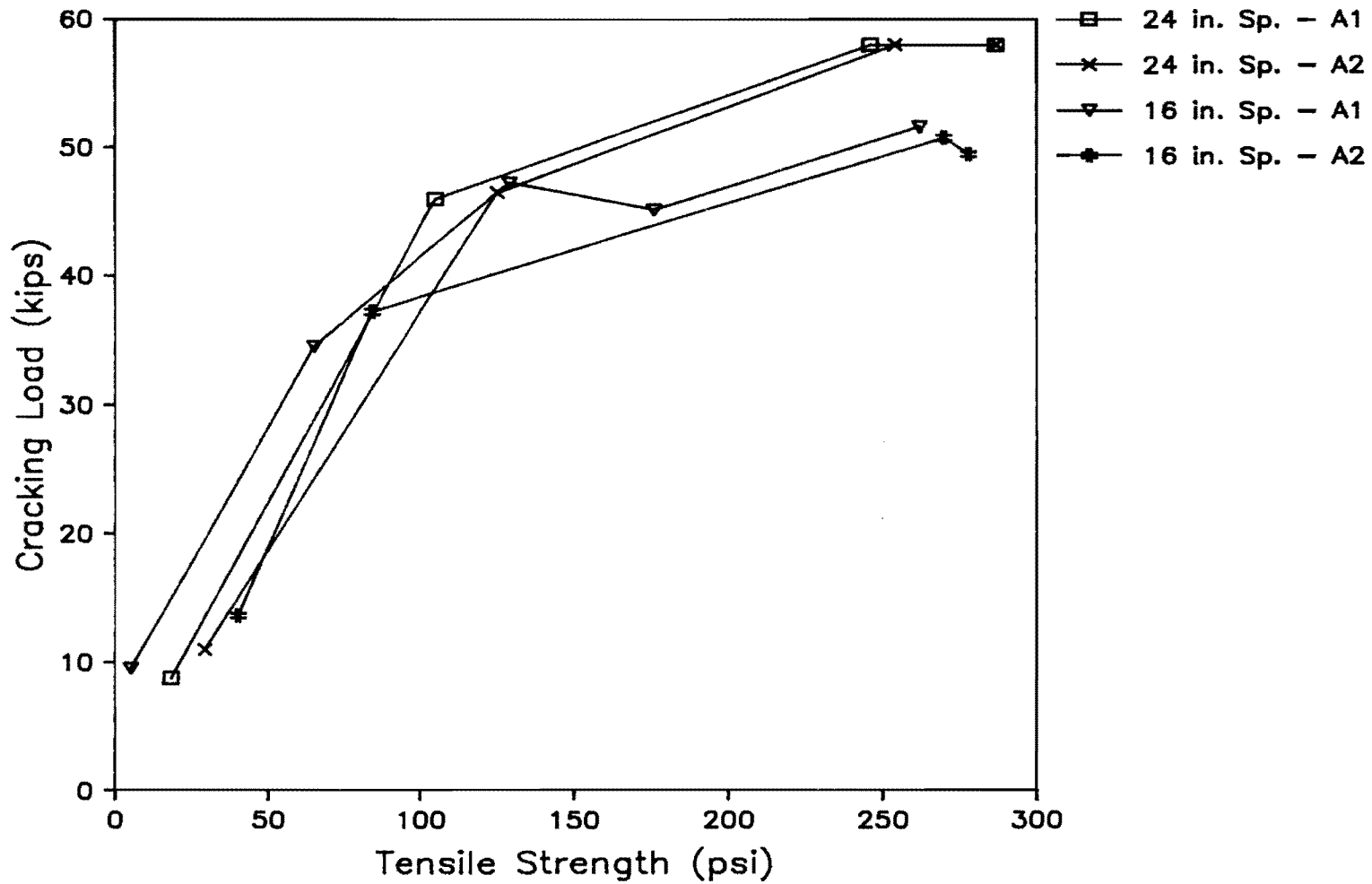


Fig 6.7. Effect of anchor size on cracking load in 6 inch slabs and for 16 and 24 inch strand spacings. Note: A1 is the smaller anchor and A2 the larger.

time alone. The high early rate of strength gain permits the application of substantial post-tension forces in the first several hours.

Strand Spacing. Strand spacing had little effect on the cracking load for the very early tests where the mode of failure was the bearing or shearing type. In fact, Fig 6.8 shows that the narrower slabs or closer strand spacings had slightly higher cracking loads. This is probably due to the slight confinement provided by the closed hoop reinforcement. The narrower slabs had a tighter hoop and provided a little more confinement than the wider slabs.

The actual slab design calls for continuous reinforcement, leading to the conclusion that the wider slabs better indicated the early failure load since they better simulated the actual field conditions.

At higher concrete strengths, when the mode of failure is bursting, strand spacing does have a slight effect on the cracking load.

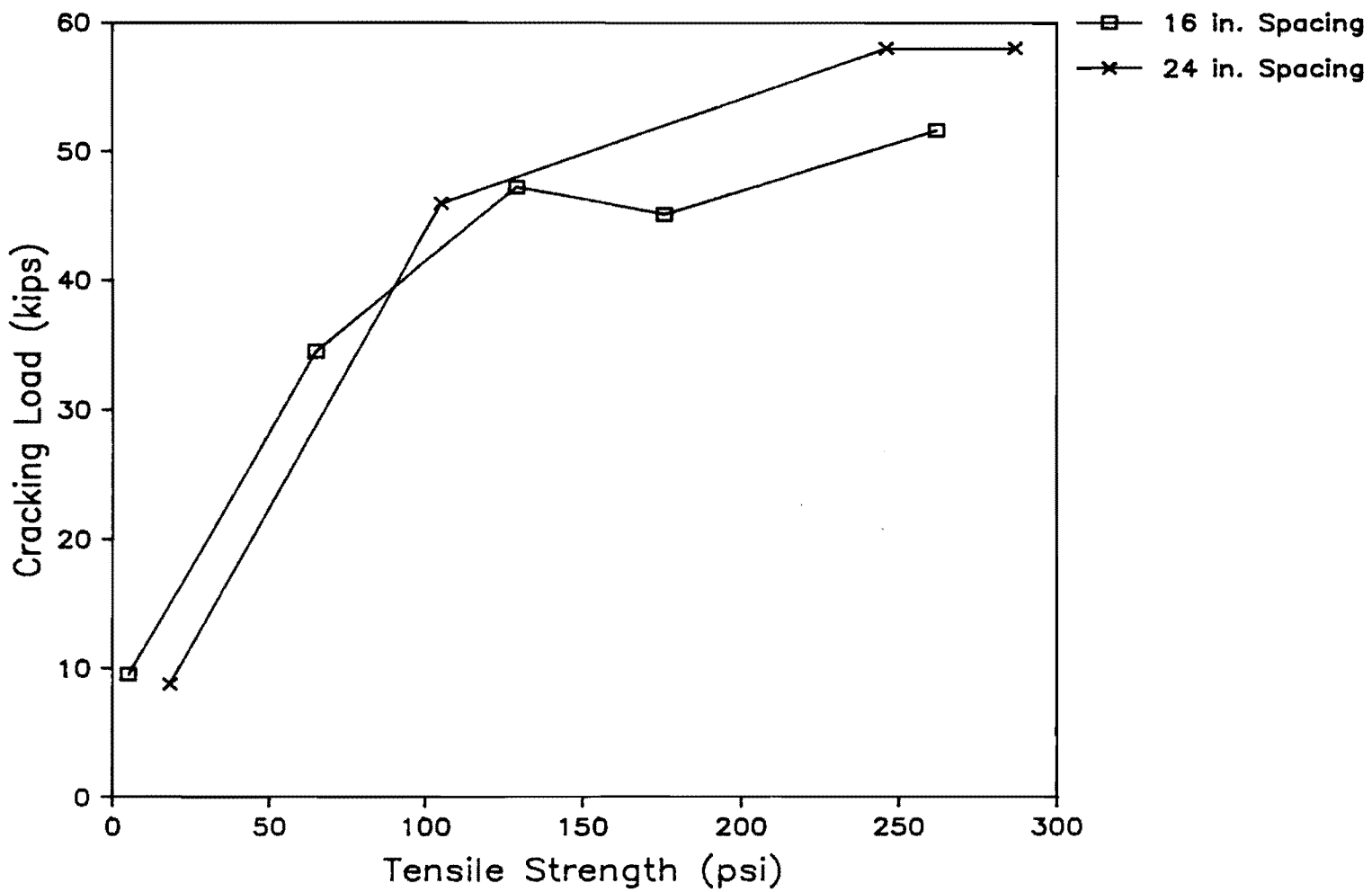
Slab Thickness. The most influential factor in cracking load for this testing program was slab thickness. Slab thickness affected the cracking load for both bearing and bursting failures (see Fig 6.9).

#### Ultimate Load

Ultimate load with concrete failure was attained in all 10 test cases of Series I but in only 8 of 27 tests of Series II and III. All other slabs encountered strand failure before ultimate concrete failure. Ultimate concrete failure could not be reached in the 6-inch slabs beyond a concrete tensile strength of about 85 psi, and in the 8-inch slabs beyond about 70 psi. In the tests where ultimate concrete failure was attained, the ultimate load was between 15 and 40 percent higher than the cracking load for the 6-inches slabs and 15 and 60 percent for the 8-inch slabs.

#### COMPARISON OF RESULTS TO EXPECTED VALUES

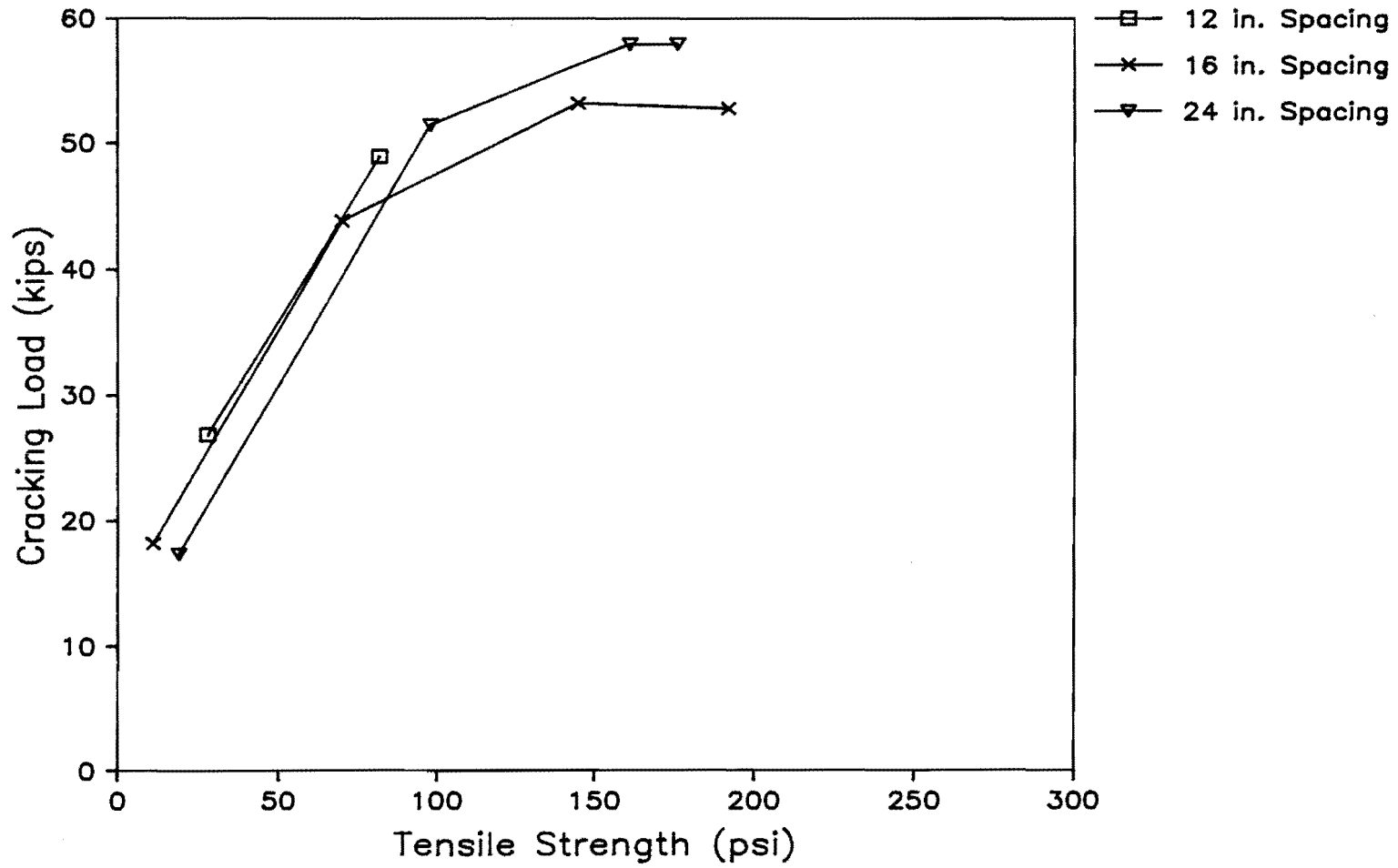
This section compares the test results to theoretical values for both concrete strength and anchorage zone cracking loads.



(a) 6-inch thick slab.

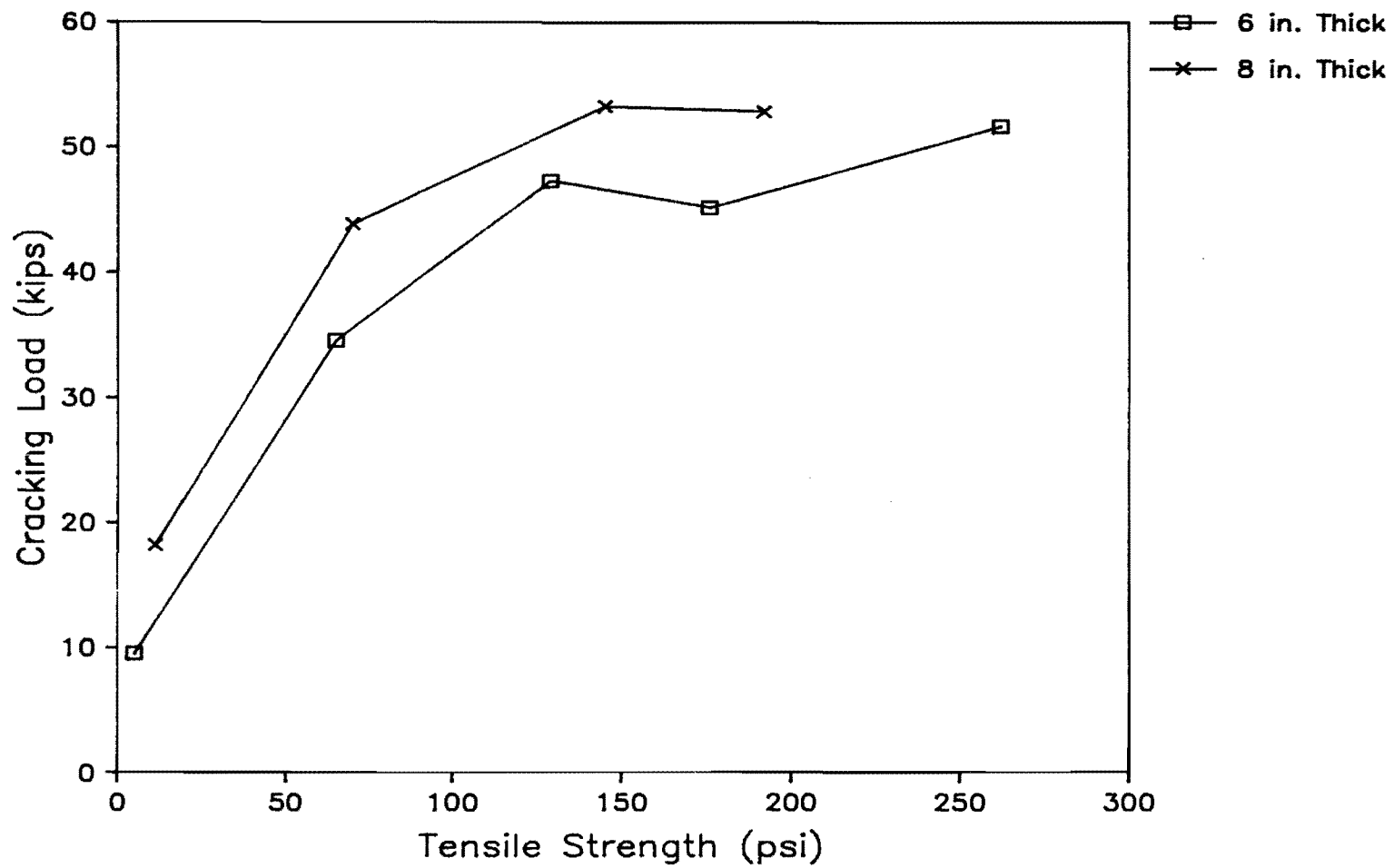
(continued)

Fig 6.8. Effect of strand spacing on the cracking load.



(b) 8-inch-thick slab

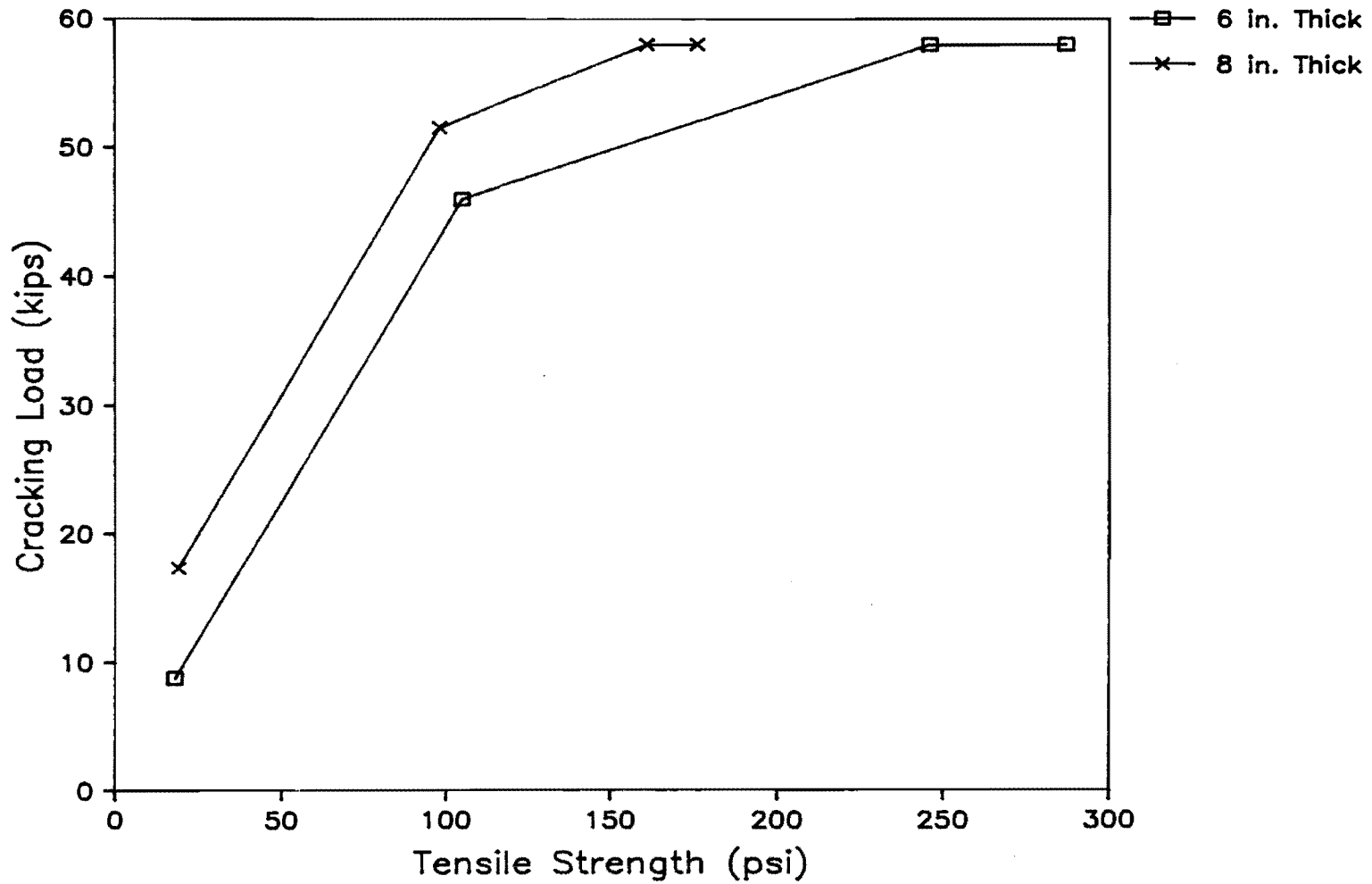
Fig 6.8. (continued)..



(a) 16 inch strand spacing.

(continued)

Fig 6.9. Effect of slab thickness on cracking load.



(b) 24 inch strand spacing.

Fig 6.9. (continued).

### Concrete Strength

Although the concrete strengths for this testing program were much higher than those of Friberg's tests (Ref 1), the general trends of strength gain are quite similar. Figure 6.2 shows the concrete strengths to 28 days for this series and Fig 3.11 shows that of Friberg's work.

### Cracking Load

This section compares the actual test cracking loads to Guyon's theoretical values, building code design values, other studies, and previous demonstration projects.

Guyon. Accurately predicting cracking load is one of the major interests of this study. Guyon developed the simple curves of maximum tensile bursting stress as a function of  $P$  and  $a'/a$ , where  $p = \frac{P}{2a}$  and  $a'$  and  $a$  are half the anchor width and slab width, respectively. This curve is shown in Chapter 3, Fig 3.6(b).

Guyon's curve may be used to predict cracking loads due to bursting stress by substituting the concrete tensile strength for bursting stress  $f_x$  and solving for  $P$ . A comparison of the cracking load calculated by this method ( $P_{cr}$  calculated) and the actual cracking load from test data ( $P_{cr}$  actual) is shown in Fig 6.10. Guyon's equation predicts cracking fairly well, especially for lower concrete strengths. Several points, however, lie below the line in the unconservative range. The reasons for this error are not certain, but a few possibilities exist.

One point (marked "a" in Fig 6.10) is from Series I data which is not representative of the other two series. Of the two pair of points lying beyond the 60-kip line, two of the tests (points "b" and "c") experienced strand failures before the points were noticed, and the other two (points "d" and "e") experienced strand yielding before the cracks were noticed.

There is a definite trend in the results shown in Fig 6.10 that the higher the concrete tensile strength becomes, the more unconservative Guyon's equation becomes. Stone and Breen made an interesting observation during their study of anchorage zone stresses in post-tensioned box girders (Ref 30). They noted that spalling stresses play a major roll in the

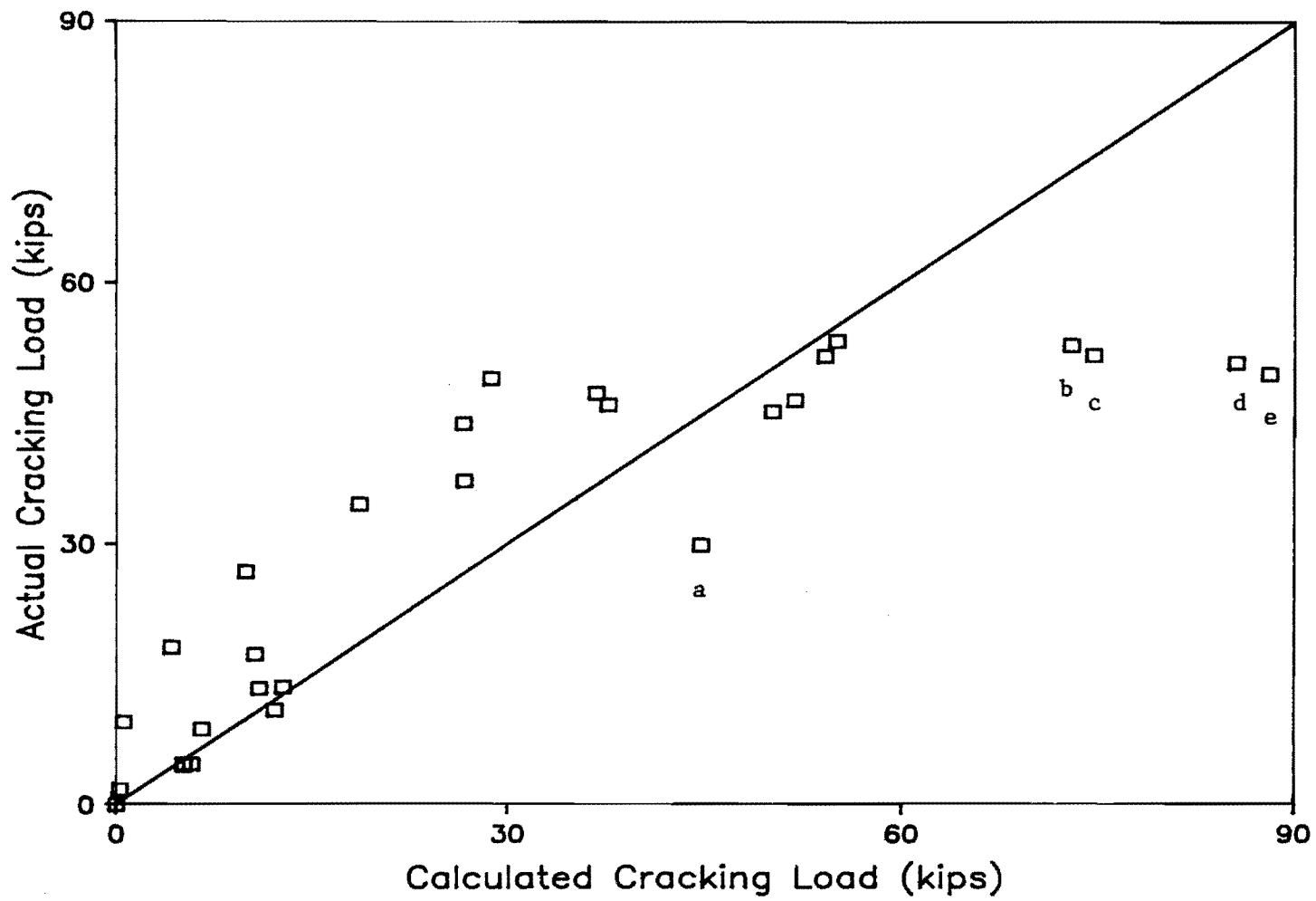
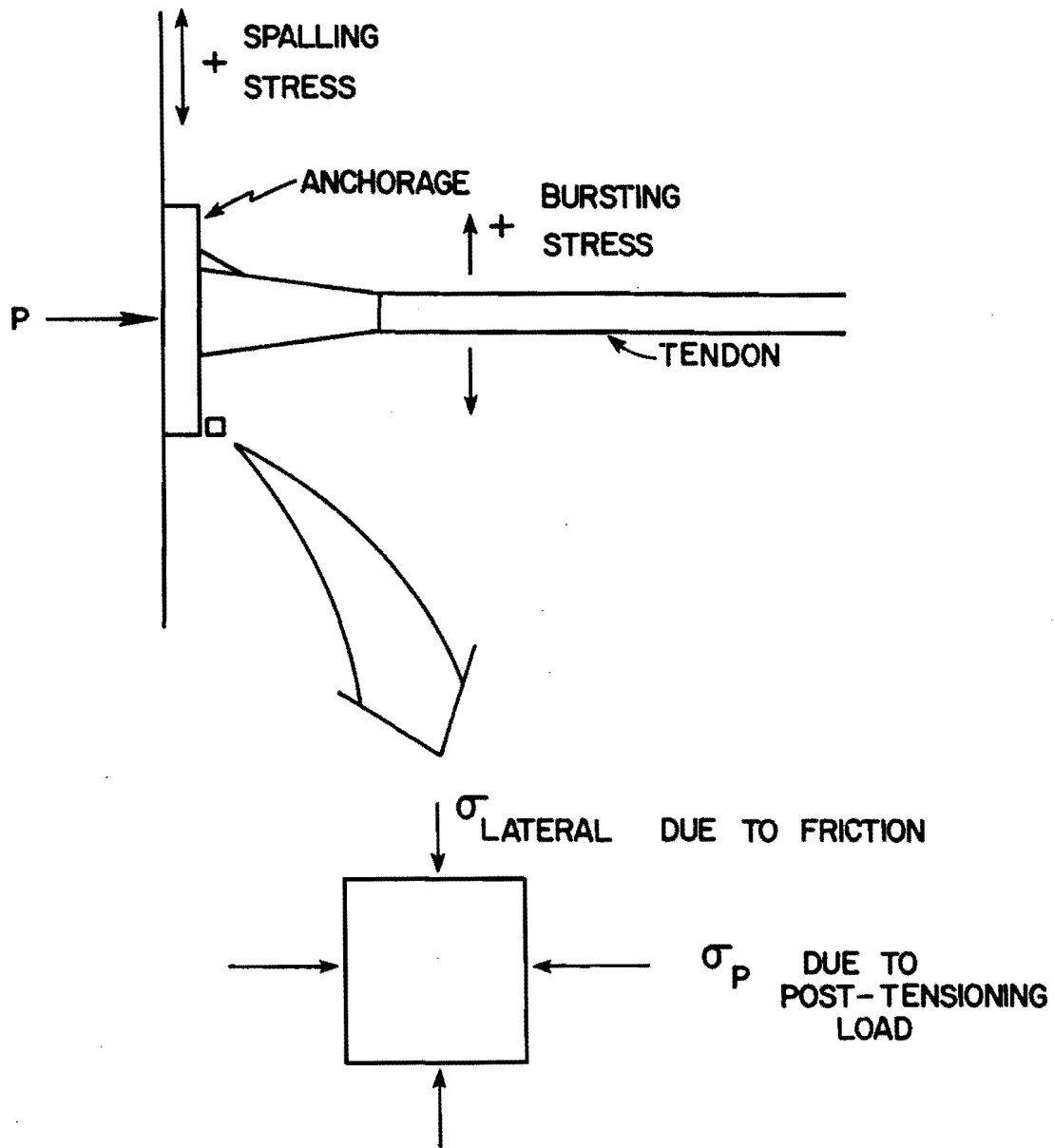


Fig 6.10. Comparison of calculated cracking load using Guyon's model to actual cracking load.

bursting stress failure even though no distress from spalling stresses is apparent.

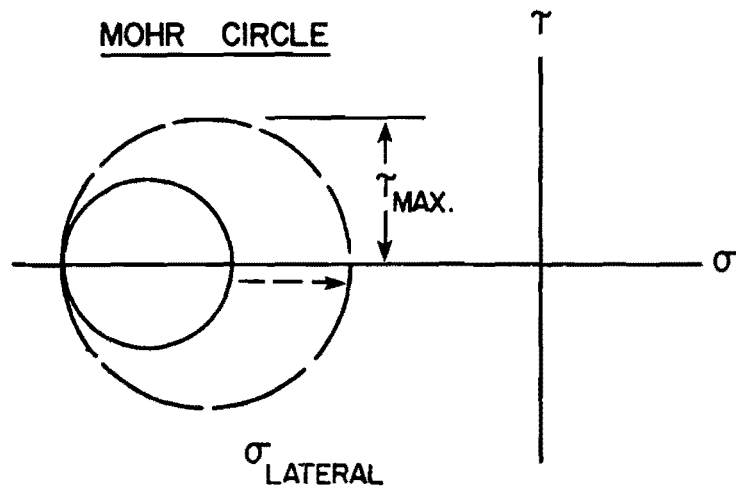
Stone and Breen describe a probable failure mechanism leading to anchorage zone failures for anchor plates as

- (1) Due to large friction forces developed directly beneath the anchor plate, Poisson ratio type lateral expansion of the concrete in this vicinity is restrained.
- (2) A complex, triaxial compressive stress state is thus set up which permits development of extremely high direct bearing stresses (up to 3 f'c) beneath the plate [see Fig 6.11(a)].
- (3) The confining lateral force at the edge of the plate is reduced by the presence of the spalling tensile stress (strain). As this reduction in lateral confining stress takes place the effect on the state of stress would be to increase the shearing stress, as can be seen from the increase in diameter of the Mohr's circle as illustrated in Fig 6.11(b).
- (4) At some level of applied load the confining stress is sufficiently reduced (though still in compression) that an internal shear failure occurs along the plane of maximum shear stress.
- (5) The maximum shearing stress plane occurs at an angle of 45° counterclockwise from the primary stress  $\sigma_p$  axis and thus propagates to form the 45° pyramidal "cone" seen for all anchor plate-type anchors [see Fig 6.11(c)].
- (6) Simultaneous with the formation of the cone, a tendon path crack propagates from the tip of the cone, as shown in Fig 6.11(c). (Phase 5 and 6 can be delayed by the presence of supplementary anchorage zone reinforcement. This delay can be substantial when spirals and lateral post-tensioning, which enhances confinement are used.)
- (7) The cone is forced into the anchorage zone, setting up large lateral forces which eventually produce the upper and lower diagonal cracks.

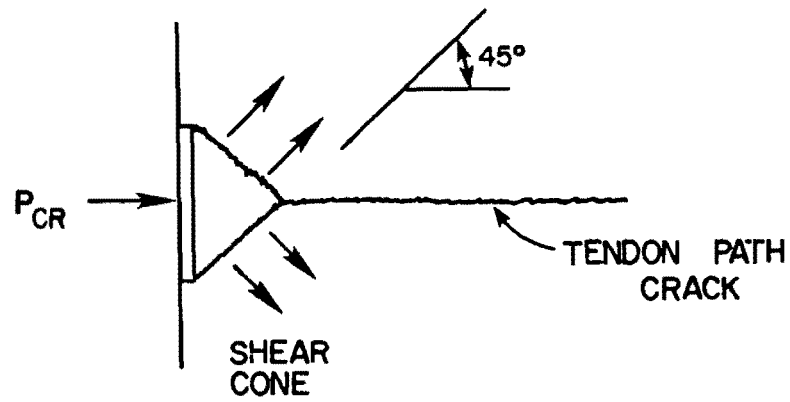


(continued)

Fig 6.11. Spalling initiated shear failure theory (from Ref 30).



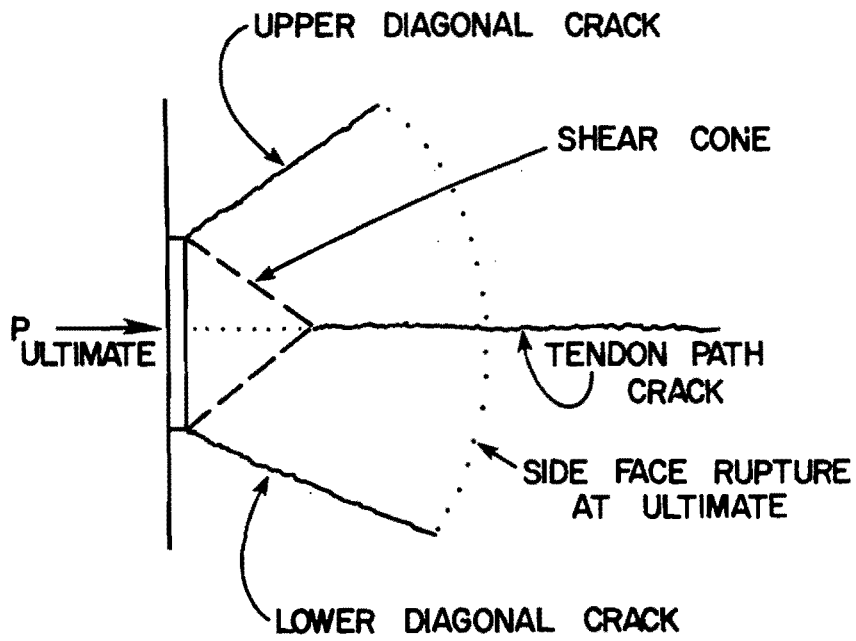
(b)



(c)

(continued)

Fig 6.11. (continued).



(d)

Fig 6.11. (continued).

- (8) Increases in load above that required for the formation of diagonal cracks lead to ultimate explosive failure of the side faces, bounded by the upper and lower diagonal cracks [see Fig 6.11(d)].

A very similar failure mechanism was apparent for the slabs for this testing program. Two types of failures have been described previously, in Chapter 5. The bursting-type failure follows the described failure mechanism very closely with the slight difference that often the diagonal cracks of step 7 and the explosive failure of step 8 happen simultaneously. This is due to the lack of reinforcement.

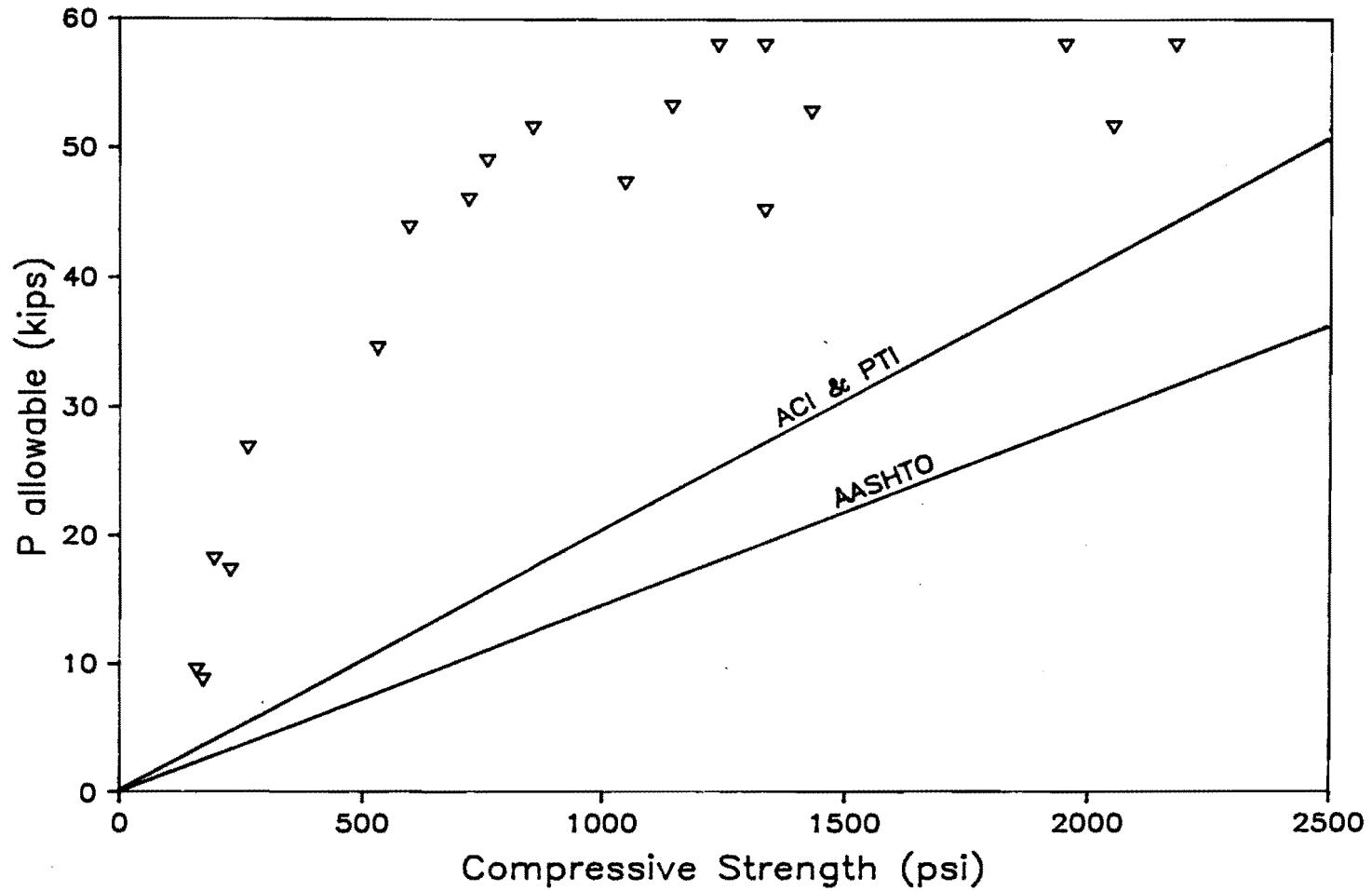
The bearing-type failure appears to follow steps 1 through 5 but the diagonal cracks form before the tendon path cracks. A possible reason for this is that the concrete lacks the stiffness to permit the high tensile stresses to form. The result is that the tendon path crack never forms, and the failure occurs along the diagonals in shear.

Design Codes and Manuals. The allowable bearing stress equations for ACI, PTI, and AASHTO, presented previously, in Chapter 3, were used to plot Fig 6.12 for anchors 1 and 2, respectively. Presented on the same plots are the actual data points. All cases for ACI-PTI were controlled by the maximum 1.25  $f'_c$  rule.

These figures show that both the ACI-PTI equation and the AASHTO equation are fairly conservative. For the range of prestress force of 10 to 20 kips for early post-tensioning, ACI and PTI are about 300 to 100 percent conservative and AASHTO is 450 to 300 percent conservative.

Other Studies. Due to the large differences in concrete strengths, comparing results to most other studies is not practical. However, a very similar study is currently underway in the United Kingdom, by VSL Systems, Ltd., and the available results compare exceedingly well to those of this study. At compressive strengths of 1,160 psi ( $8 \text{ N/mm}^2$ ) and 1,450 psi ( $10 \text{ N/mm}^2$ ) the cracking loads were 53 kips (235 kN) and 54 kips (240 kN), respectively. These are within 1 and 4 percent of the values of this study.

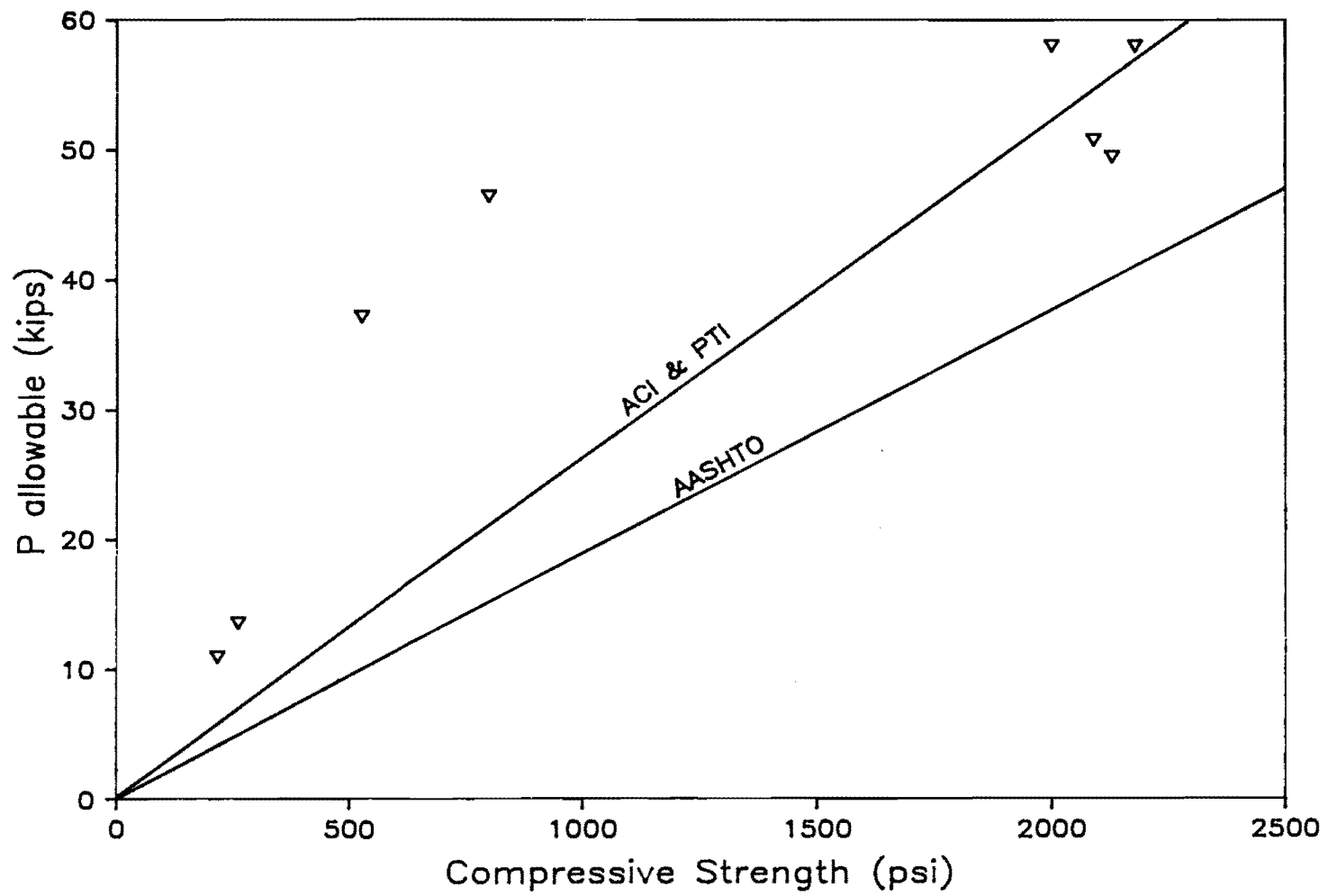
Previous Projects. The allowable bearing stresses for the four previous projects in the U.S., previously shown in Table 3.1, were extremely conservative. The earliest any slabs were post-tensioned was when the



(a) Small anchor.

(continued)

Fig 6.12. Comparison of actual cracking loads and allowable bearing loads according to ACI, PTI, and AASHTO.



(b) Larger anchor.

Fig 6.12 (continued).

concrete compressive strength had reached 1,000 psi. Often, cracks had already formed by this time. This study shows that post-tensioning could have been applied earlier and cracks avoided. The next chapter gives recommendations for safely post-tensioning before the cracks form.

## CHAPTER 7. RECOMMENDATIONS FOR FIELD USE

### GENERAL

One of the major purposes of this study was to obtain practical values for cracking loads for post-tensioned slabs and to make recommendations for field use. This chapter contains a reliability study, some design aids, and an outline for the procedure to follow in calculating a practical allowable post-tensioning force.

### DATA REGRESSION

A statistical computer program for stepwise multiple regression (STEP-01) was used to analyze the test data for the influence of the different variables on the cracking load. From the data, the program computes a sequence of multiple linear regression equations in a stepwise manner. Variables are added and removed from the regression equation depending on whether they improve the accuracy of the equation. The calculated cracking load is compared to the actual cracking load in Fig 7.1. The regression equation is presented in the next section.

### DESIGN AIDS

Three different methods for calculating the cracking load are presented below: a cracking load equation, tables of cracking loads for different variables, and graphs of cracking load versus concrete tensile strength for different variables.

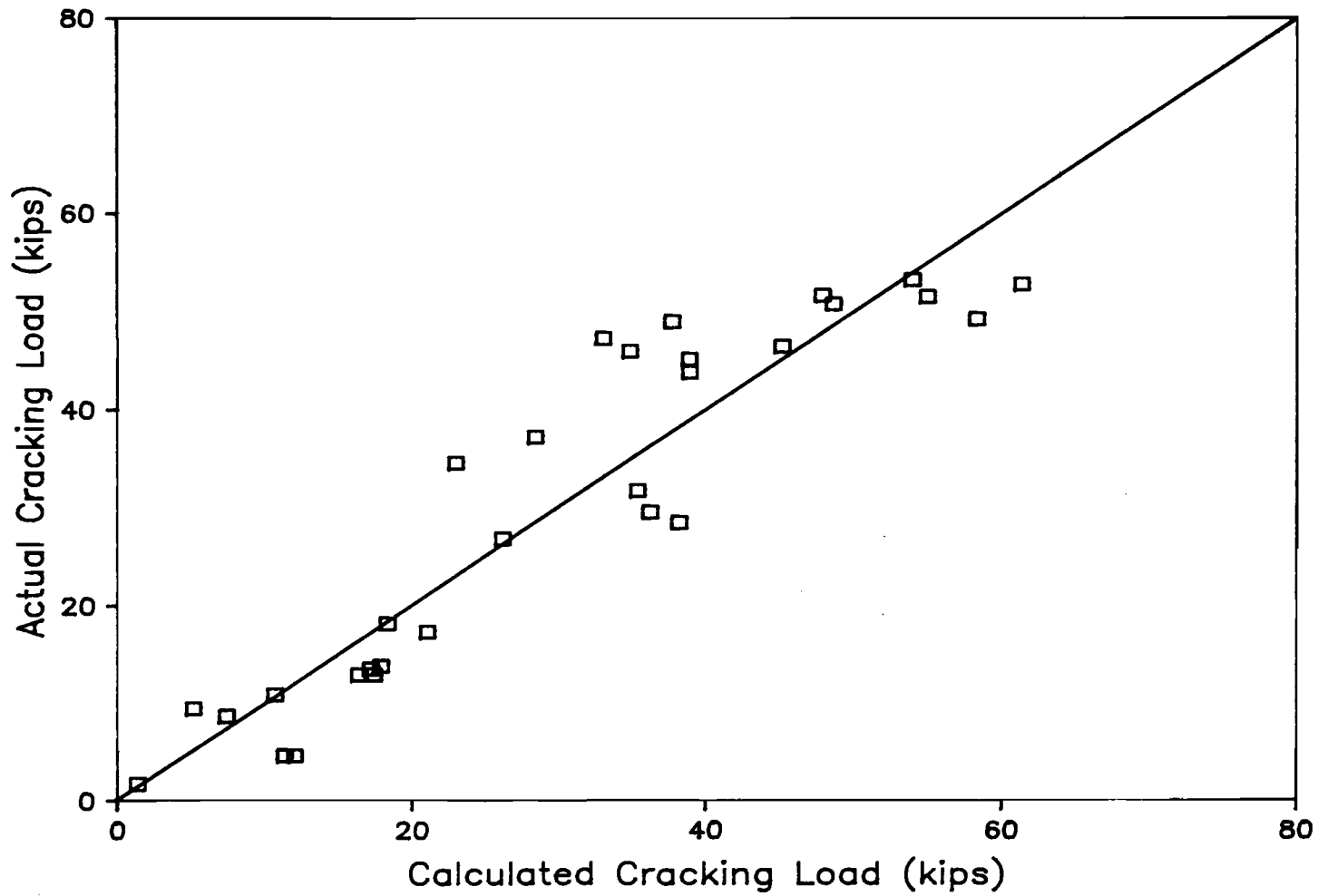


Fig 7.1. Comparison of cracking loads calculated by Eq. 1 to actual cracking loads.

### Limitations

Due to their empirical nature, each of the three methods for calculating cracking load is limited to applications similar to those of this study. The restrictions are:

- (1) Concrete tensile strengths were between 1 and 260 psi.
- (2) Slab thicknesses were 6 and 8 inches.
- (3) Strand spacings were between 12 and 24 inches.
- (4) Anchors were single 0.6-inch diameter strand flat plate anchors for slabs at 16.19 and 21.00 square inches in area.
- (5) Strands were placed 1/4 inch above mid-depth, but eccentricity was not varied.

### Equation

The data regression program yielded terms for an equation to estimate the cracking load. The equation in a slightly simplified form is

$$P_{cr} = 3.25t - 0.08 (2a)(a'') + 0.002 (f_{sp}^{\frac{1}{2}})t (2a)(a'') \quad (1)$$

where

- $P_{cr}$  = cracking load , kips,  
 $t$  = slab thickness, inches,  
 $2a$  = strand spacing, inches,  
 $f_{sp}$  = concrete tensile strength, psi, and  
 $a''$  = anchorage area, inches<sup>2</sup>.

The equation fits the test data well for most combinations of variables. Problems do arise when calculating cracking loads for very low concrete

strengths. For example, if a concrete tensile strength of zero psi is input, the cracking load does not come out to equal 0. For low values of thickness and high values of strand spacing and/or anchor size, the calculated cracking load is negative, which is conservative. For high values of thickness and low values of strand spacing and/or anchor size, the calculated cracking load is positive, which is unconservative.

This inconsistency is less severe as concrete strengths increase, and the problem does not exist above 20 psi tensile strength. The actual calculated values for low strengths may be seen in the table in the next section.

#### Table

Equation 1 was used to generate a table of cracking loads for the slab thicknesses and strand spacings to be used in the actual design of the prestressed concrete pavement (see Table 7.1). The smaller anchor (A1) used in the test was used in the calculations.

#### Graphs

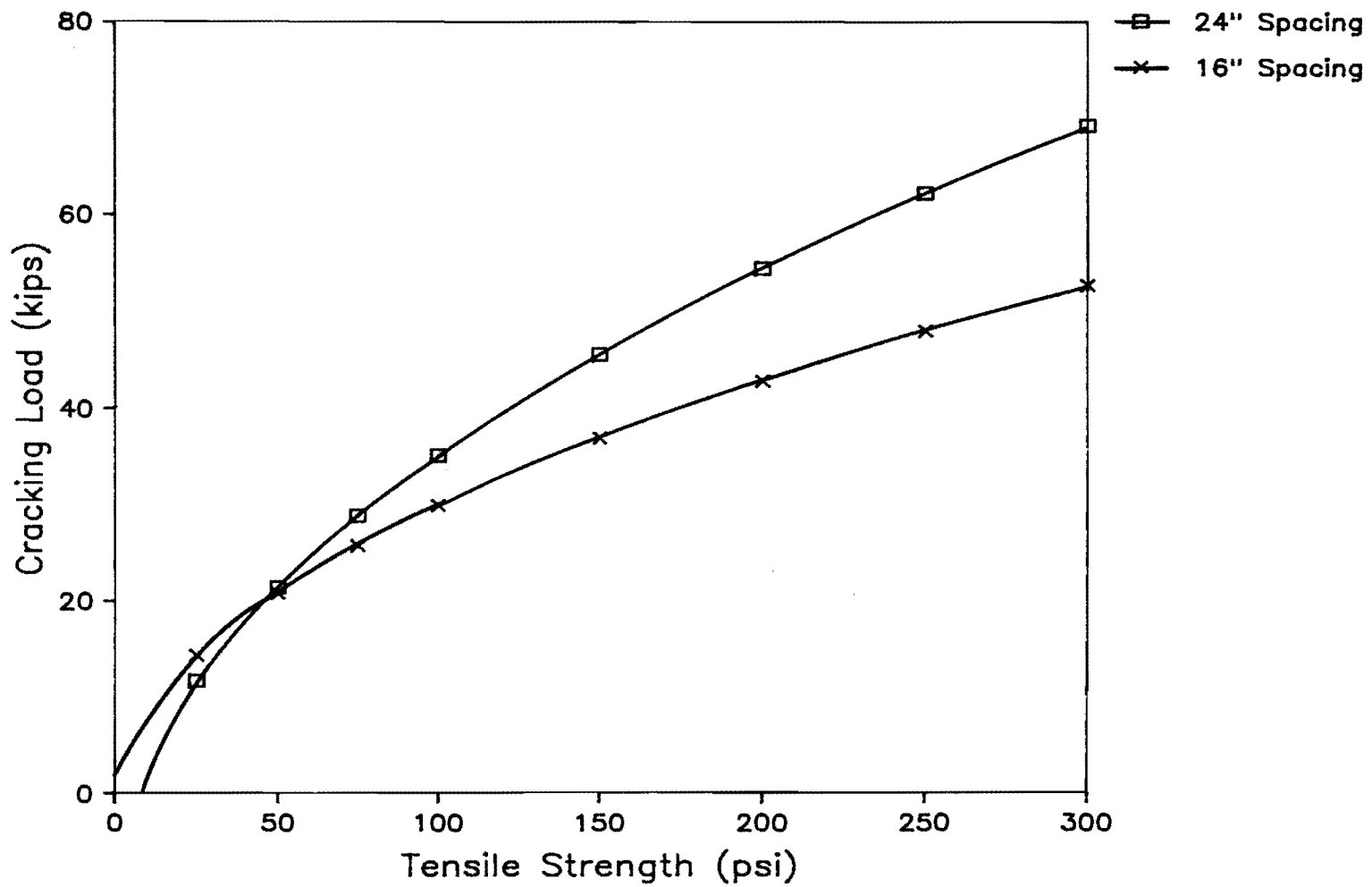
Equation 1 was used to generate Fig 7.2 for estimating cracking loads for different concrete strengths. Figure 7.2(a) is for a 6-inch-thick slab, and 16 and 24-inch strand spacing. Figure 7.2(b) is for an 8-inch-thick slab, and 12 and 18-inch strand spacing. Both figures are for the smaller anchor.

#### RELIABILITY STUDY

The safety factor applied to the cracking load depends on the desired reliability. Figure 7.3 shows the safety factor for different reliabilities as developed from the cracking load predictions and the actual cracking load values.

TABLE 7.1. PREDICTED CRACKING LOAD (KIPS) FOR DIFFERENT SLAB THICKNESSES, STRAND SPACINGS, AND CONCRETE STRENGTHS

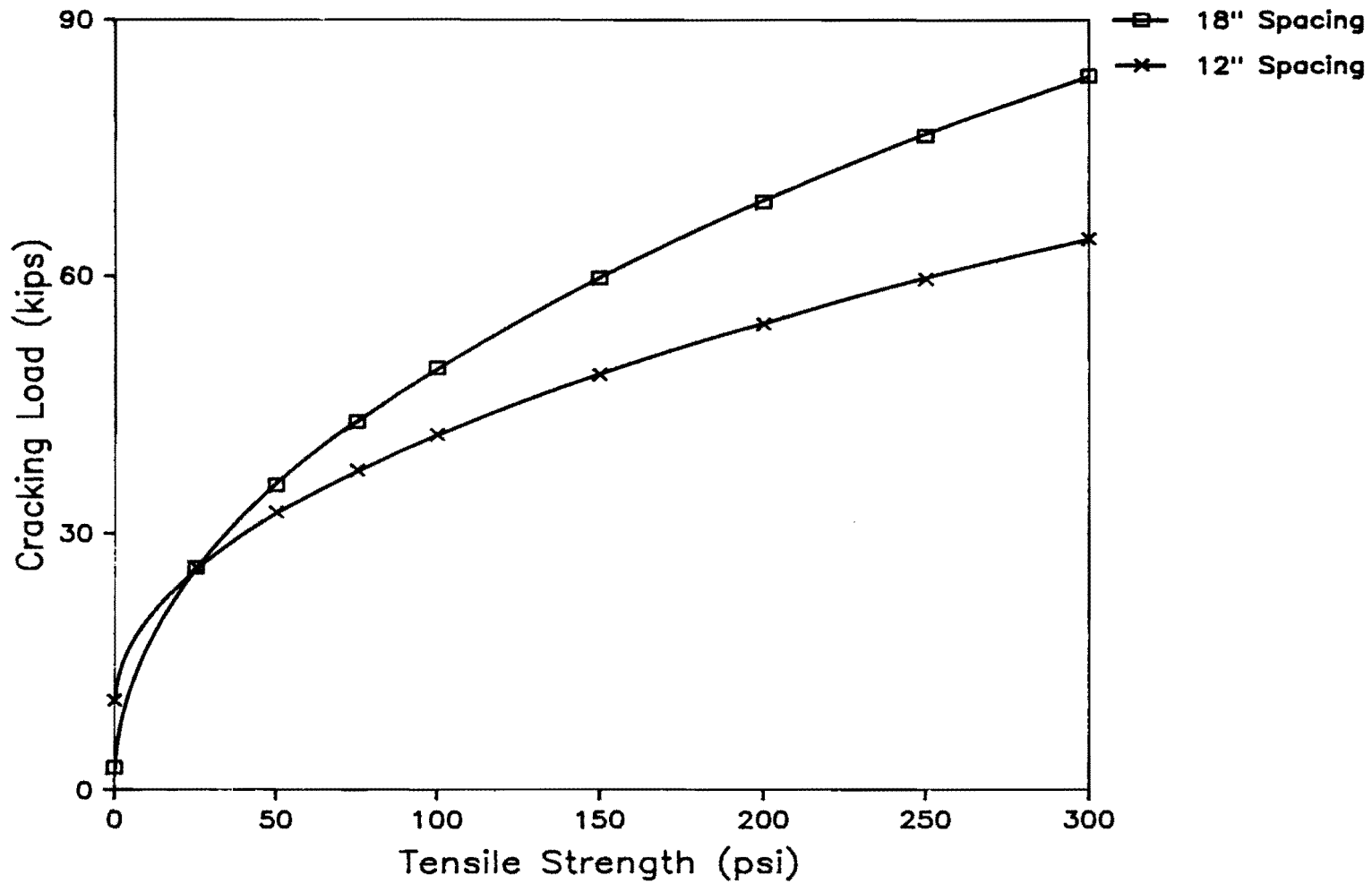
Thickness (6 in.)			Thickness (8 in.)		
Tensile Strength (psi)	Spacing (in.)		Tensile Strength (psi)	Spacing (in.)	
	16	24		12	18
0	-1.22	-11.58	0	10.46	2.69
10	8.61	3.16	10	20.29	17.43
20	12.68	9.27	20	24.36	23.54
30	15.80	13.95	30	27.48	28.23
40	18.44	17.90	40	30.12	32.18
50	20.76	21.39	50	32.44	35.66
60	22.85	24.53	60	34.54	38.80
70	24.78	27.43	70	36.47	41.70
80	26.58	30.12	80	38.26	44.39
90	28.27	32.65	90	39.95	46.92
100	29.86	35.04	100	41.54	49.31
110	31.38	37.32	110	43.06	51.59
120	32.83	39.49	120	44.51	53.76
130	34.22	41.58	130	45.90	55.85
140	35.56	43.59	140	47.24	57.86
150	36.85	45.52	150	48.53	59.79
160	38.10	47.39	160	49.78	61.67
170	39.31	49.21	170	50.99	63.48
180	40.48	50.97	180	52.16	65.24
190	41.62	52.69	190	53.31	66.96
200	42.74	54.36	200	54.42	68.63



(a) 6 inch thick slab with 16 and 24 inch strand spacings.

(continued)

Fig 7.2. Predicted cracking load using Eq. 1.



(b) 8 inch slab with 12 and 18 inch strand spacings.

Fig 7.2 (continued).

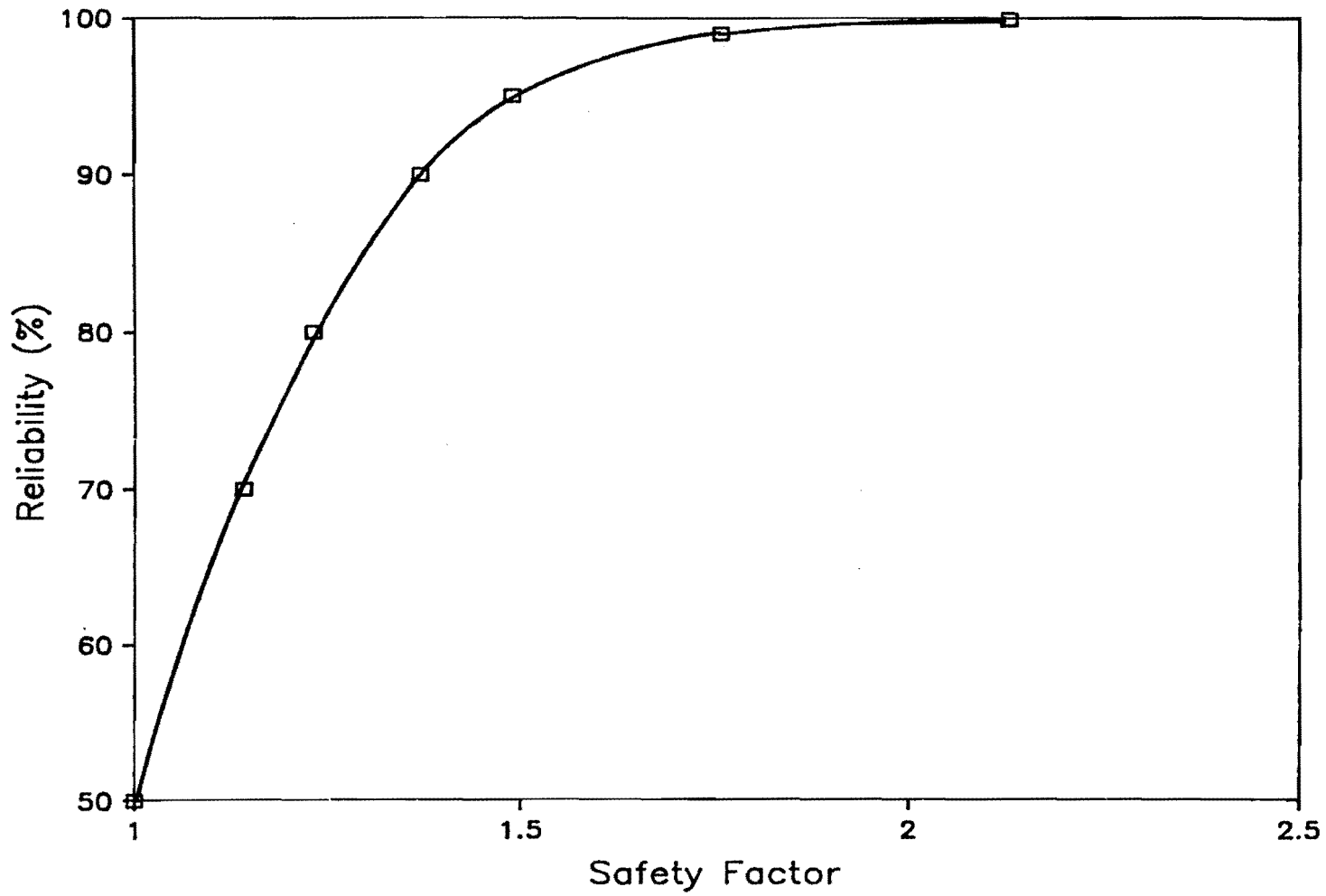


Fig 7.3. Safety factor to be applied to cracking load prediction for various reliabilities against cracking.

## CALCULATION PROCEDURE

The procedure for determining the allowable post-tensioning force is extremely simple. The following steps give the necessary force and allowable force required to prevent cracking.

- (1) Given slab length and drop in concrete temperature, determine the tensile stress in the slab using Fig 2.3.
- (2) Determine the concrete strength from the cylinder break or a previously established strength versus maturity curve.
- (3) Determine the required safety factor for the desired reliability against cracking from Fig 7.3 and calculate the allowable post-tensioning force ( $P_{allow}$ ). Note:  $P_{allow} \leq 0.8 f_y \times A_s$ , where  $f_x =$  STRAND YIELD, and  $A_s =$  area of steel.
- (4) Check the slab compressive stress due to  $P_{allow}$ , minus the tensile strength of the concrete to see if it exceeds the tensile stress due to temperature drop. (Note: It is not necessary to overcome 100 percent of the tensile stress because the concrete has some tensile strength.)

This procedure is illustrated in the following example. The cracking load equation, table, and graphs for concrete compressive strength rather than tensile strength are provided in Appendix C.

### EXAMPLE

The slab is 440 feet long x 6 inches thick with strand spacing at 16 inches on center. At 12 hours from concrete batching the concrete temperature has dropped 10°F. A split cylinder tensile test shows the concrete tensile strength to be 100 psi.

## SOLUTION

Given  $L = 440$  ft,  $t = 6$  in.,  $a = 16$  in., and  $f_{sp} = 100$  psi.

(1) Determine the Tensile Stress

From Fig 2.3 for  $L = 440$  feet,  $T = 10^\circ\text{F}$

$$\sigma_t = 200 \text{ psi}$$

(2) Determine  $P_{cr}$

From Eq 1, Table 7.1, or Fig 7.2

$P_{cr} = 29.86$  kips for a concrete tensile strength of 100 psi.

(3) Determine  $P_{allowable}$

For 95 percent reliability the safety factor equals 1.5 (Fig 7.3)

$$P_{allow} = \frac{P_{cr}}{SF} = \frac{29.86 \text{ kips}}{1.5}$$

$$= 19.91 \text{ kips}$$

(3) Check

The compressive stress in the slab equals

$$\sigma_c = \frac{P_{\text{allow}}}{\text{at}} = \frac{19.91 \text{ kips}}{(16 \text{ in.}) (6 \text{ in.})} = 0.207 \text{ ksi} = 207 \text{ psi}$$

$$\sigma_t - f_{sp} = 200 - 100 = 100 \text{ psi}$$

$$\sigma_c > (\sigma_t - f_{sp})$$

therefore,  $P_{\text{allow}}$  is acceptable.

This page replaces an intentionally blank page in the original.

-- CTR Library Digitization Team

## CHAPTER 8. CONCLUSIONS AND RECOMMENDATIONS

### GENERAL

Although prestressed concrete pavement is not a new concept in highway design, it is not currently widely accepted as an alternate solution to conventional highway pavements. Material savings, low maintenance and long life are all factors that make prestressed pavement an attractive research topic and a possibly viable alternative to conventional concrete pavements.

Design and construction problems of previous prestressed pavements continue to be studied and solved. Early temperature and shrinkage cracking is the problem that this study has addressed. Early post-tensioning is a feasible solution to this problem, but caution must be taken during early post-tensioning to avoid anchorage zone failures.

### CONCLUSIONS

#### Concrete Strength Conclusions

Based on this study and the analysis of data from the tests, the following conclusions about concrete strength have been reached:

- (1) Fairly high concrete strengths can be reached in the first 24 hours for 5 sack mix, Type I cement with low water/cement ratios.
- (2) Concrete gains tensile strength more rapidly than compressive strength.
- (3) Maturity method is an accurate indicator of concrete strength for a given mix.

#### Slab Cracking Load Conclusions

For the general range of variables studied, these are the major conclusions about post-tensioning loads.

- (1) Post-tensioning forces can be safely applied within the first 12 or 24 hours after casting for low slump concrete.
- (2) Slab thickness has a large influence on the post-tensioning cracking load. The thicker the slab, the higher the load.
- (3) Concrete strength has a large influence on the post-tensioning cracking load. The stronger the concrete, the higher the load.
- (4) Concrete quality has a large influence on the post-tensioning load. At the same strength, slabs with poor quality concrete crack at lower loads.
- (5) Bearing stress has little influence on the post-tensioning cracking load.
- (6) Strand spacing has little influence on the post-tensioning cracking load at very low concrete strengths but moderate influence at higher strengths.
- (7) Allowable post-tensioning design loads for ACI, PTI, AASHTO and previous prestressed concrete pavement projects are very conservative for early post-tensioning at fairly low concrete strengths.

#### RECOMMENDATIONS FOR FURTHER RESEARCH

Because this investigation was empirical, further study of some areas would be helpful. Some possible additional studies are:

- (1) Use two and three dimensional finite element analysis study to model the anchorage zone and compare to experimental results.
- (2) Vary the type of reinforcement in the anchorage zone by using more reinforcement, spirals and lateral post-tensioning.
- (3) Vary the concrete slump or design strength to see the effects on the cracking load.

## REFERENCES

1. Friberg, Bengt F., "Investigation of Prestressed Concrete for Pavements," Highway Research Board Bulletin 332, National Academy of Sciences, National Research Council, Washington, D.C., 1962, pp 40-94.
2. Hanna, A. N., et al, "Technological Review of Prestressed Pavements," Report No. FHWA-RD-77-8, Federal Highway Administration, December 1976.
3. "Prestressed Highway Pavement in Service," Roads and Streets, Vol 114, No. 10, October 1971, pp 56.
4. Pasko, T. J., "Prestressed Highway Pavement at Dulles Airport for Transpo 72," Journal of the Prestressed Concrete Institute, Vol 17, No. 2, March/April 1972, pp 46 - 54.
5. Rivero-Vallejo, F., and B. F. McCullough, "Drying Shrinkage and Temperature Drop Stresses in Jointed Reinforced Concrete Pavement," Research Report 177-1, Center for Highway Research, The University of Texas at Austin, August 1975.
6. Albritton, Gayle E., "Prestrssed Concrete Highway Pavement: Construction - As-Built Performance," Report No. FHWA-DP-17-2-1, Federal Highway Administration, August 1978.
7. Morris, G. R., and H. C. Emery, "The Design and Construction of Arizona[s Prestressed Concrete Pavement," Arizona Department of Transportation, January 1978.
8. Brunner, R. J., "Prestressed Pavement Demonstration Project," Research Project No. 72-22(2), Pennsylvania Department of Transportation, February 1974.
9. Stone, W. C., and J. E. Breen, "Analysis of Post-tensioning Girder Anchorage Zones," Research Report 208-1, Center for Transportation Research, The University of Texas at Austin, June 1981.

10. Burns, N. H., and W. N. Berezovytch, "A Study of the Behavior of the CCL S9 Single-Strand Post-Tensioning Anchor in Concrete Slabs," prepared for the Prescon Corporation, The University of Texas at Austin, May 1970.
11. Guyon, Yves, Prestressed Concrete, John Wiley and Sons, Inc., New York, 1953.
12. Tesar, M., International Association for Bridge and Structural Engineering, 1932.
13. Douglas, D. J., and N. S. Trahair, "An Examination of the Stresses in the Anchorage Zone of a Post-tensioned Prestressed Concrete Beam," Magazine of Concrete Research, Vol 12, No. 34, March 1960, pp 9-18.
14. Iyengar, K. T. S. R., "Two-Dimensional Theories of Anchorage Zone Stresses in Post-Tensioned Prestressed Beams," Journal of the American Concrete Institute, Vol 59, No. 10, October 1962, pp 1443 - 1446.
15. Gergely, P., M. A. Sozen, and C. P. Siess, "The Effects of Reinforcement on Anchorage Zone Cracks in Prestressed Concrete Members," Civil Engineering Structural Research Series, University of Illinois, No. 271, July 1963.
16. Christodoulides, S. P., "Three-Dimensional Investigation of the Stresses in the End Anchorage Bioces of a Prestressed Concrete Gantry Beam," The Structural Engineer, Vol 35, No. 9, September 1957.
17. Sargious, M., "Beitrag zur Ermittlung der Hauptzugspannungen am Endauflager Vorgespannter Betonbalken," Ph. D. Dissertation, Technische Hochschule, Stuttgart, July 1970.
18. Vaughn, S. D., "An Exploratory Photoelastic Investigation of Post-tensioned Concrete Anchorage Zone Bursting Stresses," unpublished
19. Zielinski, T., and R. E. Rowe, "The Stress Distribution Associated with Grouts of Anchorages in Post-Tensioned Concrete Members," Research Report 13, Cement and Concrete Association, London, October 1969.  
Distribution in the Anchorage Zones of Post-Tensioned Concrete Membon, September 1960.

21. Taylor, S. J., "Anchorage Bearing Stresses," Conference on PCPV, Group H, Paper 49, March 13-17, 1967 (London), The Institute of Civil Engineers, London, 1968.
22. Breen, J. E., R. L. Cooper, and T. M. Gallaway, "Minimizing Construction Problems in Segmentally Precast Box Girder Bridges," Research Report 121-6F, Center for Highway Reserach, The University of Texas at Austin, August 1975.
23. Stone, W. C., W. Paes-Filho, and J. E. Breen, "Behavior of Post-Tensioned Girder Anchorage Zones," Research Report 208-2, Center for Transportation Research, The University of Texas at Austin, April 1981.
24. Saul, A.G.A., "Principles Underlying the Stream Curing of Concrete at Atmospheric Pressure," Magazine of Concrete Research, (London), Vol 2, No.6, March 1951, pp 127-140.
25. Carino, N. J., H. S. Lew, and C. K. Volz, "Early Age Temperature Effects on Concrete Strength Predictions by the Maturity Method," Journal of the American Concrete Institute, March-April 1983, pp 93-101.
26. Parsons, T. J., and T. R. Naik, "Early Age Concrete Strength Determined by Maturity," Concrete International, February 1985, pp 37-43.
27. American Concrete Institute, Building Code Requirements for Reinforced Concrete and Commentary (ACI-318-83), Detroit, Michigan, 1983.
28. Post-Tensioning Institute, Post-Tensioning Manual, Pheonix, Arizona, 1976.
29. American Association of State Highway and Transportation Officials, Standard Specifications for Highway Bridges, 12th Edition, 1977.
30. Stone, W. C., and J. E. Breen, "Design of Post-Tensioned Girder Anchorage Zones," Research Report 208-3F, Center for Transportation Research, The University of Texas at Austin, June 1981.

This page replaces an intentionally blank page in the original.

-- CTR Library Digitization Team

**APPENDIX A**  
**CONCRETE BATCH MIX**

This page replaces an intentionally blank page in the original.

-- CTR Library Digitization Team

TABLE A.1 CONCRETE BATCH DESIGN USED IN TEST SERIES

READYMIX BATCH DESIGN  
 FOR USE ON EXPERIMENTAL CONCRETE  
 CONTRACTOR: U. T. FERGUSON LABORATORY

		CMT:	470	F.A.:	1365	C.A.:	1825	WATER:	28	SPEC	494	15	SOLAIR:	2.5
		DESIGNED SLUMP : 2 "												
CU YDS	CEMENT	TYPE A	SOLAIR	< 2% MOIST. >			< 4% MOIST. >			< 6% MOIST. >				
				SAND	TOT AG	WATER	SAND	TOT AG	WATER	SAND	TOT AG	WATER		
0.25	118	4	1	348	804	6	355	811	5	362	818	5		
0.5	235	8	1	696	1609	12	710	1622	11	723	1636	9		
0.75	353	11	2	1044	2413	19	1065	2433	16	1085	2454	14		
1	470	15	3	1392	3217	25	1420	3245	21	1447	3272	18		
1.25	588	19	3	1740	4022	31	1775	4056	27	1809	4090	23		
1.5	705	23	4	2088	4826	37	2129	4867	32	2170	4908	27		
1.75	823	26	4	2437	5630	43	2484	5678	38	2532	5726	32		
2	940	30	5	2785	6435	49	2839	6489	43	2894	6544	36		
2.25	1058	34	6	3133	7239	56	3194	7300	48	3256	7362	41		
2.5	1175	38	6	3481	8043	62	3549	8112	54	3617	8190	45		
2.75	1293	41	7	3829	8848	68	3904	8923	59	3979	8998	50		
3	1410	45	8	4177	9652	74	4259	9734	64	4341	9816	55		
3.25	1528	49	8	4525	10456	80	4614	10545	70	4702	10634	59		
3.5	1645	53	9	4873	11261	87	4969	11356	75	5064	11452	64		
3.75	1763	56	9	5221	12065	93	5324	12167	80	5426	12270	68		
4	1880	60	10	5569	12869	99	5678	12978	86	5788	13088	73		
4.25	1998	64	11	5917	13674	105	6033	13790	91	6149	13906	77		
4.5	2115	68	11	6265	14478	111	6388	14601	97	6511	14724	82		
-----														
4.75	2233	71	12	6613	15282	117	6743	15412	102	6873	15542	86		
5	2350	75	13	6962	16087	124	7098	16223	107	7235	16360	91		
5.25	2468	79	13	7310	16891	130	7453	17034	113	7596	17177	95		
5.5	2585	83	14	7658	17695	136	7808	17845	118	7958	17995	100		
5.75	2703	86	14	8006	18499	142	8163	18656	123	8320	18813	104		
6	2820	90	15	8354	19304	148	8518	19468	129	8681	19631	109		
6.25	2938	94	16	8702	20108	155	8873	20279	134	9043	20449	114		
6.5	3055	98	16	9050	20912	161	9227	21090	139	9405	21267	118		
6.75	3173	101	17	9398	21717	167	9582	21901	145	9767	22085	123		
7	3290	105	18	9746	22521	173	9937	22712	150	10128	22903	127		
7.25	3408	109	18	10094	23325	179	10292	23523	155	10490	23721	132		
7.5	3525	113	19	10442	24130	185	10647	24335	161	10852	24539	136		
7.75	3643	116	19	10790	24934	192	11002	25146	166	11213	25357	141		
8	3760	120	20	11138	25738	198	11357	25957	172	11575	26175	145		
8.25	3878	124	21	11486	26543	204	11712	26768	177	11937	26993	150		
8.5	3995	128	21	11835	27347	210	12067	27579	182	12299	27811	154		
8.75	4113	131	22	12183	28151	216	12422	28390	188	12660	28629	159		
9	4230	135	23	12531	28956	223	12776	29201	193	13022	29447	164		

DESIGNED SLUMP : 2 INCH



**APPENDIX B**  
**DETAILED TEST RESULTS**



## APPENDIX B. DETAILED TEST RESULTS

### SERIES I

#### Six Hour Tests

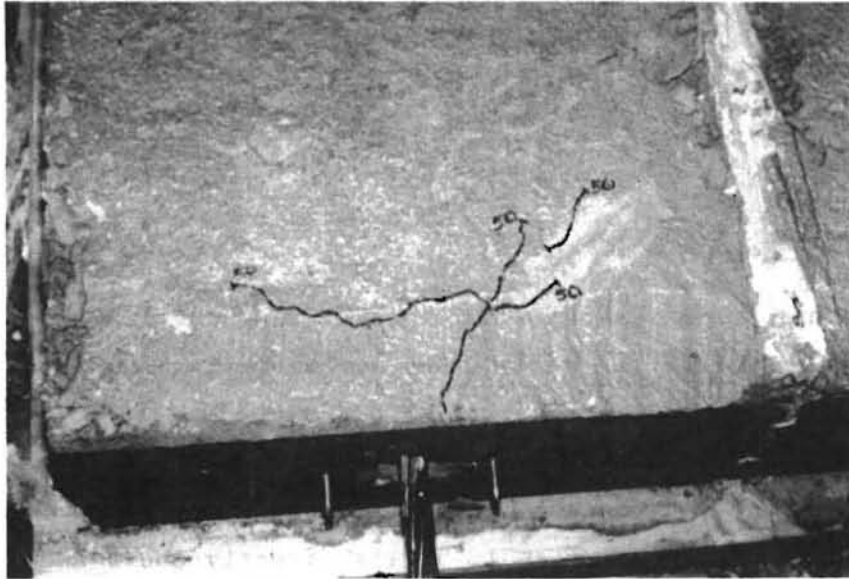
At six hours after casting the forms could not be stripped without damaging the concrete so the first test was delayed three hours, giving a testing time of nine hours after casting. Compressive strength was 31 psi and tensile strength was about 1 psi.

Due to the very low concrete strength, only one slab was tested at this time. First cracking occurred at 1.75 kips directly above and in the same plane as the anchor plate [see Fig B.1(a)]. As the load increased the cracks grew into the slab and toward the sides as a wedge of concrete in front of the anchorage moved through the slab. Ultimate failure occurred at 2.62 kips [see Fig B.1(b)].

#### Twelve Hour-Test

The 12 hour-test was delayed one hour, and so it actually occurred at 13 hours. Concrete strength was 130 psi in compression, 20 psi in tension and 55 psi in flexure. Three slabs were tested but failures were very similar so only one set of photographs is presented.

First cracking occurred at 4.68 kips for all three slabs [see Fig B.2(a)]. Diagonal cracks extended into the slab as load increased. The angle at which the cracks formed was defined by the position of the anchor and the reinforcement. Diagonal cracks began at the corner of the anchor and extended past the corner of the closed stirrup, and out to the slab edge. Each of the three slabs experienced a bearing typed ultimate failure at loads of 5.15, 5.15, and 5.62 kips, respectively [see Fig B.2(b)].

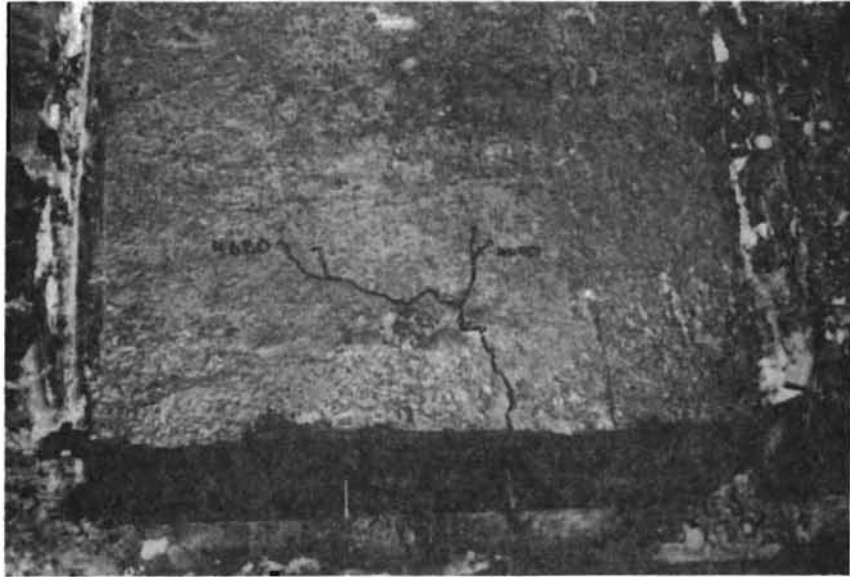


(a) First cracking at 1.75 kips.



(b) Ultimate failure at 2.62 kips.

Fig B.1. Failure of Specimen I 606-16A1-1.



(a) First crack at 4.68 kips .



(b) Ultimate failure at 5.15 kips .

Fig B.2. Failure of Specimen I 612-16A1-1.

### Eighteen Hour Tests

By 18 hours, the concrete had gained a compressive strength of 260 psi, tensile strength of 35 psi, and flexural strength of 95 psi.

Because the concrete was stiffer, the first cracking patterns began to change and become more like the patterns described in previous tests. A longitudinal crack in front of the anchor along the tendon path appeared along with the diagonal cracks. First cracking occurred at 12.97, 12.97, and 13.84 kips, respectively for the three tests [see Fig B.3(a)].

As the load increased, both the longitudinal cracks and the diagonal cracks extended into the slab until a bursting failure occurred [see Fig .3(b)]. Ultimate loads were 14.83, 13.40, and 15.56 kips.

### Twenty-Four Hour Test

The 24-hour tests were actually conducted at 26 hours. Concrete strength had increased to about 1,030 psi in compression, 150 psi in tension, and 180 psi in flexure.

Longitudinal cracks along the tendon path occurred first at 31.72, 29.53, and 28.44 kips respectively [see Fig B.4(a)]. Diagonal cracks formed at higher loads [see Fig B.4(b)] followed by a violent explosive failure.

## SERIES II

### Six Hour Tests

At six hours after casting, forms were stripped and slabs were ready to be tested. At about seven hours the first slab was tested.

II 606-24A1. Concrete strength was about 170 psi in compression, 18 psi in tension, and 52 psi in flexure. First cracking occurred at 8.75 kips and resembled the pattern of the Series I, 12-hour tests (see Fig B.5(a)).

As load was increased the cracks enlarged until the anchor lifted out the top of the slabs at an ultimate load of 9.85 kips [see Fig B.5(b)]. The ultimate failure was more brittle than for the 12 hour test of Series I. This was probably due to the stronger, stiffer concrete.



(a) First cracking at 13.84 kips.

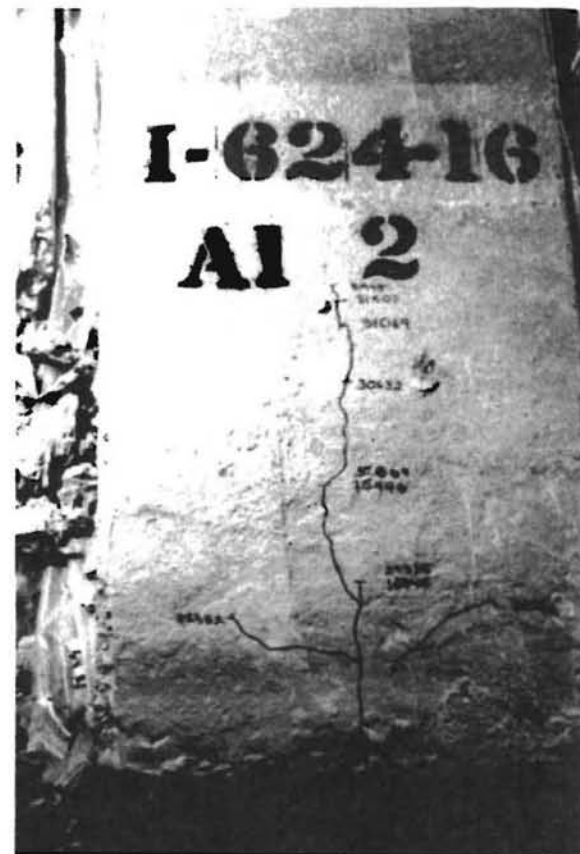


(b) Ultimate failure at 15.56 kips.

Fig B.3. Failure of Specimen I 618-16A1-3.

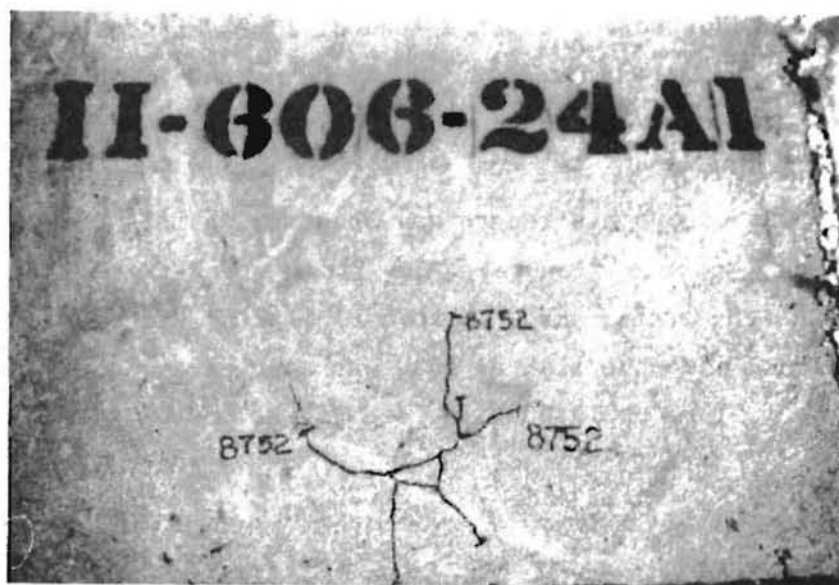


(a) First crack at 29.53 kips .



(b) Extended cracks just before explosive failure at 33.69 kips.

Fig B.4. Failure of Specimen I 624-16A1-2.



(a) First crack at 8.75 kips.



(b) Ultimate failure at 9.85 kips.

Fig B.5. Failure of Specimen II 606-24A1.

II 606-24A2. Concrete strengths had increased to about 215 psi in compression, 29 psi in tension, and 68 psi in flexure. First cracks formed in front of the anchor at angles at a load of 10.94 kips [see Fig B.6(a)].

Again, as load was increased cracks grew and ultimately the anchor popped up and lifted the concrete on top of the slab at a load of 13.13 kips [see Fig B.6(b)].

II 606-16A2. Concrete strength was about 260 psi in compression, 40 psi in tension and 84 psi in flexure. The first crack formed in front of and perpendicular to the anchor at a load of 13.57 kips, as shown in Fig A.7(a). The crack extended into the slab as load was applied and ultimate failure was a bursting type failure at 19.00 kips [see Fig B.7(b)].

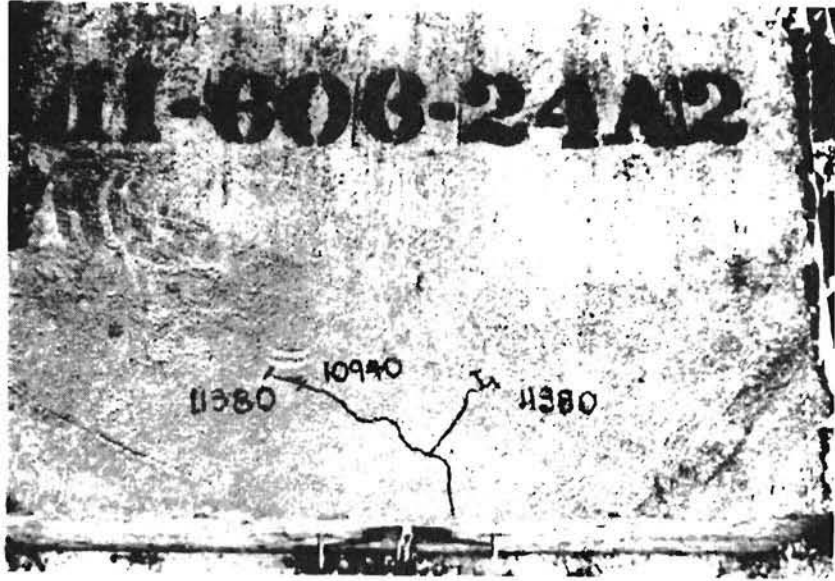
#### Twelve-Hour Tests

At twelve hours, three more slabs were tested varying spacing and anchor size. It was interesting to find that at even this extremely early age it was impossible to completely fail the slabs. Each slab cracked, but none of the slabs had ultimate failures.

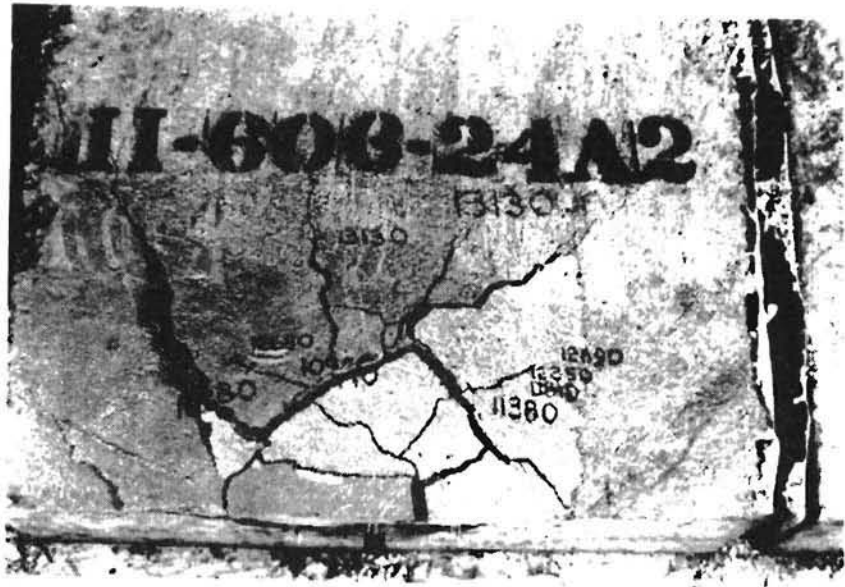
II 612-16A2. Eleven hours after casting, Specimen II 6-12-16A2 was tested. Concrete compressive strength was about 530 psi, tensile strength was about 85 psi, and flexural strength was about 180 psi.

At a load of 37.20 kips, the first crack occurred, perpendicular to the anchor plate and extending from the slab edge to a distance 6 inches into the slab, about 3 inches beyond the location of the anchor itself [see Fig B.8(a)]. As load increased the crack extended into the slab. Loading was stopped at about 44 kips (76 percent of ultimate load for the strand) and the crack had extended into the slab a distance of 15 inches from the slab edge, 12 inches (2a) from the anchor [see Fig B.8(b)]. Twelve inches is about equal to the width of the slab, dimensions 2a according to Guyon, where tensile stresses become negligible.

II 612-24A1. At 12 hours since casting, when specimen II 612-24A1 was tested, concrete strength had increased to 720 psi in compression, 105 psi in tension, and 205 psi in flexure.



(a) First crack at 10.94 kips and extended at 11.38 kips.



(b) Ultimate failure at 13.13 kips.

Fig B.6. Failure of Specimen II 606-24A2.

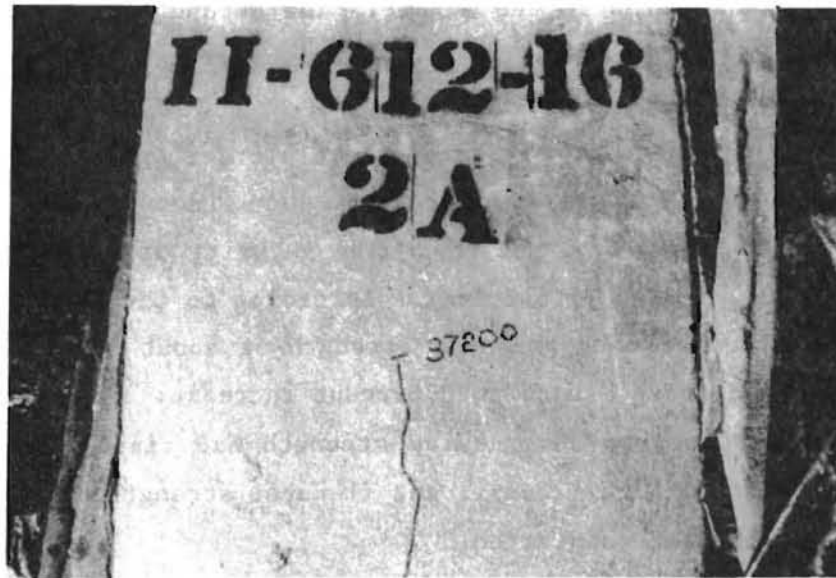


(a) First crack at 13.57 kips.

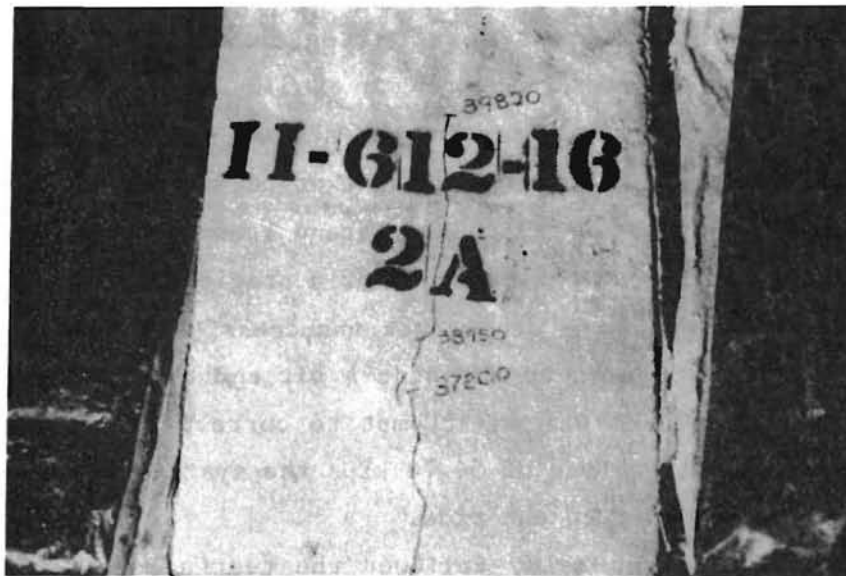


(b) Extended crack before ultimate failure at 19.00 kips.

Fig B.7. Failure of Specimen II 606-16A2.



(a) First crack at 37.20 kips.



(b) Extended crack at 39.82 kips.

Fig B.8. Failure of Specimen II 612-16A2.

Two small cracks formed at a load of 45.95 kips (79 percent of ultimate). The first began directly above the anchor and extended 3 inches into the slab perpendicular to the anchor. The second began 4-1/2 inches in front of the anchor and extended one inch, again perpendicular to the anchor (see Fig B.9).

The concrete in this slab may have been a bit stronger than that of Slab II 612-16A2 because the temperature rose higher since it was left covered longer (see Chapter 5 for explanation). The maturity of II 612-24A1 was 834 compared to the 706 of Slab II 612-16A2. According to the theory of concrete maturity this would give a compressive strength of about 870 psi rather than 720 psi as indicated above, about a 20 percent increase.

II 612-24A2. Concrete compressive strength had risen to approximately 800 psi, tensile strength to 125 psi, and flexural strength to 220 psi by the time Specimen II 612-24A2 was tested.

Cracking did not occur in this slab until a load of 46.44 kips (80 percent of strand ultimate strength), when a crack formed along the tendon path into the slab about 35 inches, and a Y-shaped crack formed, as shown in Fig B.10. The tops of the Y extended about 4 inches past the anchor plate.

II 618-16A2. With a compressive strength of 1,680 psi, a tensile strength of 190 psi and a flexural strength of 330 psi, Specimen II 618-16A2 was loaded with a double strand system as shown in Fig B.11. The actual loading device was a stiff beam with a nose that pushed against the back side of the anchor. The purpose of the double strand loading device was to enable the slabs to be loaded beyond the capacity of a single strand.

Unfortunately this loading scheme was unsuccessful. As load increased, the loading beam began to tilt to the side a bit and the load was then being applied at an angle. There was an attempt to correct the problem but this too was unsuccessful. At a load of 54.70 kips the system became unstable and the loading beam buckled out to the side.

II 618-24A1. A slight delay followed the testing of Specimen II 618-16A2 because a remedy to the unstable loading device problem was attempted, which was unsuccessful. By 20 hours after casting, Specimen II 618-24A1 was tested. Concrete strength was about 1,950 psi in compression, 246 psi in tension and 405 psi in flexure.

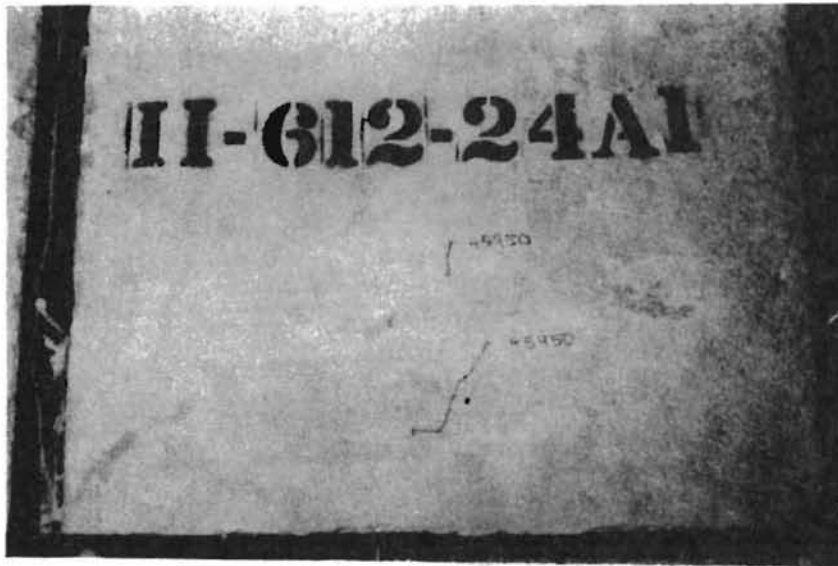


Fig B.9. First crack at 45.45 kips for Specimen II 612-24A1.



Fig B.10. First crack at 46.44 kips for Specimen II 612-24A2.

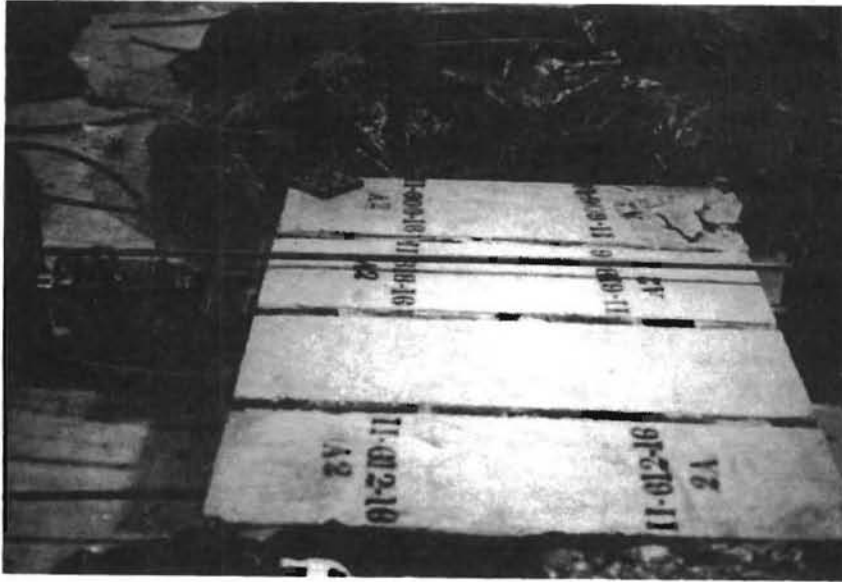


Fig B.11. Double strain loading scheme for Specimen II 618-16A2.



Fig B.12. First crack at 51.64 kips for Specimen II 618-16A1.  
This crack occurred as the strand began to yield.

At a load of 52.5 kips (91 percent of ultimate) the strand began to yield and at 52.64 kips one of the seven wires broke. No cracks occurred.

II 618-24A2. With concrete strength about 2,000 psi in compression, 254 psi in tension, and 417 psi in flexure, Specimen II 618-24A2 was loaded until the strand yielded at 52.0 kips. No cracking could be detected.

II 618-16A1. The final 18-hour test specimen tested was II 618-16A1. Concrete compressive strength was about 2,050 psi. Tensile strength was about 260 psi, and flexural strength was about 430 psi.

The slab was loaded and checked for cracks regularly. No cracks were detected until the strand yielded at 51.64 kips. At this time a single crack extended from the edge of the slab along the tendon path 8-1/2 inches into the slab (5-1/2 inches past the anchor), as shown in Fig B.12.

#### Twenty-Four Hour Tests

After the 18-hour series slabs performed so well, it was feared that at 24 hours even the 16-inch slab would not crack, so the 24 hour series immediately followed the 18 hour series.

II 624-16A1. by the time the 24-hour testing series began, with Specimen II 624-16A1, compressive strength had reached about 2,090 psi, tensile stress about 270 psi, and flexural strength about 440 psi.

Again, the slab was loaded and checked regularly for cracks. No cracks were detected until after the strand failed at 50.76 kips. At this point a crack along the tendon path beginning 1-3/4 inches from the edge and extending 4 inches was seen. It is shown in Fig B.13.

II 624-16A2. For the next test concrete strengths had increased slightly, to about 2,130 psi in compression, 280 psi in tension, and 455 psi in flexure.

The slab was loaded and checked for cracks. At 49.23 kips the first crack was noticed. The crack began one inch in from the edge and extended 6-1/4 inches along the tendon path (see Fig B.14). At 51.64 kips the strand failed and the crack extended another 1-3/4 inches.

II 624-24A1. Concrete strength was about 2,180 psi in compression, 290 psi in tension, and 470 psi in flexure. The strand was loaded up to 44.64



Fig B.13. First crack detected after strand failure at 50.76 kips for Specimen II 624-16A1.



Fig. B.14. First crack at 49.23 kips for Specimen II 624-16A2. Strand failed at 51.64 kips.

kips and had to be unloaded to adjust the loading device. The strand was reloaded and failed at 45.07 kips. No cracks were detected.

II 624-24A2. Concrete strengths were the same as for Specimen II 624-24A1. At a load of 48.14 kips the strand failed and no cracks were detected.

### SERIES III

#### Four-Hour Tests

Due to the time needed to strip the forms and prepare for testing, the four hour tests were slightly delayed and actually began five hours after casting.

II 604-16A1 With concrete strength about 157 psi in compression, 5 psi in tension, and 45 psi in flexure, Specimen III 604-16A1 was tested. First cracking occurred at 9.51 kips in a pattern characteristic of the early type bearing failures. Figure B.15(a) shows the first cracks, which extended into the slab 7 inches. The intersection of the cracks occurs directly above the anchor plate.

As load was increased to 10.81 kips the cracks extended into the slab. At 12.10 kips the cracks grew more and new cracks formed as the anchor began to lift up, as in previous tests.

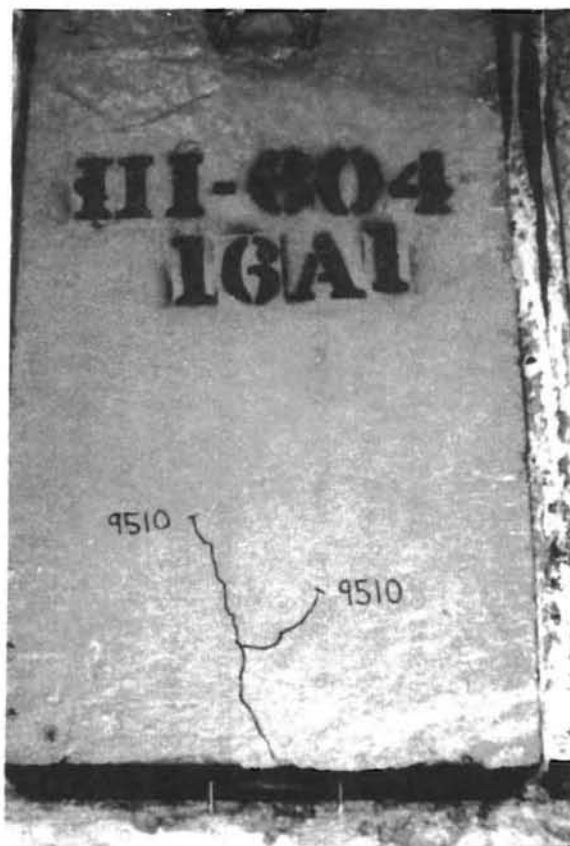
Finally at 12.45 kips the slab reached ultimate load and the anchor lifted breaking the cover off the top of the slab [see Fig B.15(b)].

III 804-16A1. Concrete strength was about 190 psi in compression, 11 psi in tension, and 61 psi in flexure. The first crack occurred along the tendon path at a load of 18.16 kips [see Fig B.16(a)].

The crack began directly above the anchor extending into the slab 5 inches.

As loading continued, the crack extended along the tendon path, as shown in Fig B.16(b), until an explosive failure occurred at 29.66 kips. The condition of the slab following ultimate failure may be seen in Fig B.16(c).

III 804-24A1. At 6 hours Specimen III 804-24A1 was tested. Concrete strengths had reached about 225 psi in compression, 19 psi in tension, and 78



(a) First crack at 9.51 kips,



(b) Ultimate failure at 12.45 kips.

Fig B.15. Failure of Specimen III 604-16A-1.



(a) First crack at 18.16 kips.



(b) Extended crack at 23.34 kips.

Fig B.16. Failure of Specimen III 804-16A1.

(continued)



(c) Ultimate failure at 29.66 kips.

Fig B.16 (continued).

psi in flexure. The first crack, at 17.29 kips, extended far into the slab along the tendon path and also out at angles beginning above the anchor plate [see Fig B.17(a)]. Ultimate failure occurred at 20.23 kips [see Fig B.17(b)].

III 804-12A1. At 6-1/2 hours, with concrete strength about 260 psi in compression, 28 psi in tension, and 94 psi in flexure, specimen III 804-12A1 was tested. The first crack occurred along the tendon path beginning slightly behind the anchor, extending into the slab 5 inches, as shown in Fig B.18(a). As the load increased the crack extended [see (Fig B.18(b))] until an explosive failure occurred at 37.87 kips. Figure B.18(c) shows the slab immediately after the ultimate failure.

#### Eight-Hour Tests

III 608-16A1-2. This test was different from the others in that the slab contained two strands spaced at 16 inches and loaded simultaneously. The purpose was to compare its cracking load with the single strand slabs.

In Fig B.19(a) the loading scheme is shown and it may be observed that the load distributing beam absent. This was because they would not fit properly. This was unfortunate because the failure occurred at the bearing surface of the loading mechanism. This portion of the slab was unreinforced so once a crack formed, the slab split open.

Cracking occurred at 19.45 kips on one strand and 18.54 kips on the other [see Fig B.19(b)]. Slight cracking occurred in the anchorage zone, as shown in Fig B.19(c), but the ultimate failure was in bearing at the load cell at 23.85 kips.

III 608-16A1. The next slab was tested at nine hours. Concrete strength had increased to about 530 psi in compression, 65 in tension, and 180 psi in flexure.

At 34.52 kips first cracking occurred along the tendon path, beginning slightly behind the anchor and extending about 5 inches, as shown in Fig B.20(a). At 37.11 kips a second crack formed, diagonally intersecting the first crack directly above the anchor, as shown in Fig B.20(b).



(a) First crack at 17.29 kips .



(b) Ultimate failure at 20.23 kips,

Fig B.17. Failure of Specimen III 804-24A1.



(a) First crack at 26.88 kips.



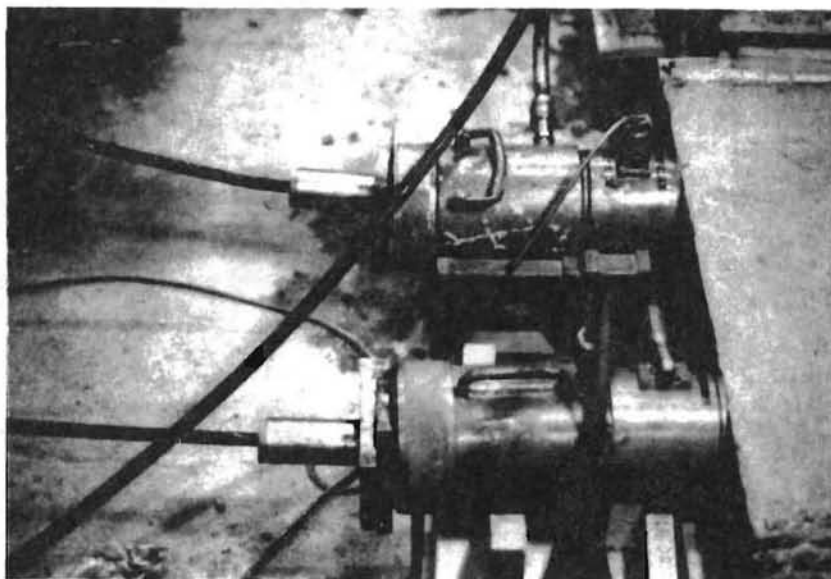
(b) Extended crack at 34.58 kips.

Fig B.18. Failure of Specimen III 804-12A1. (Note: Slab designation is wrong in photo.)  
(continued)

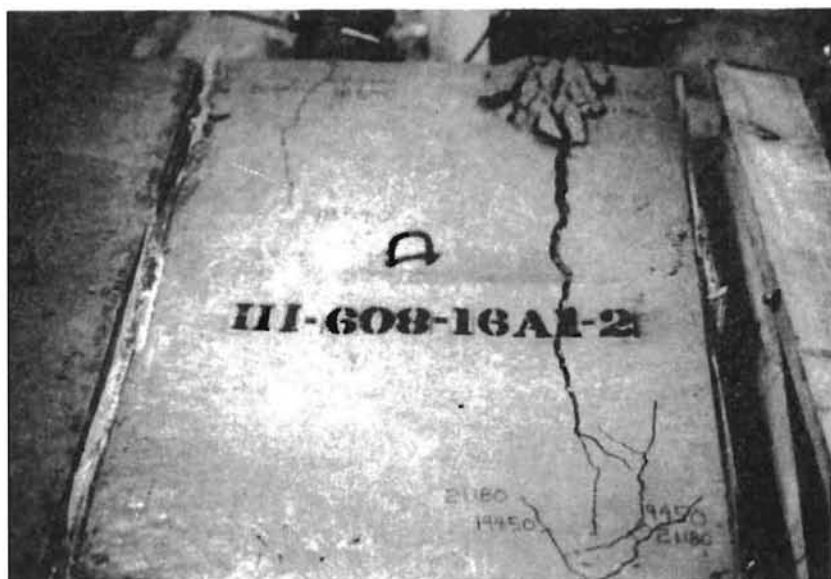


(c) Ultimate failure at 37.87 kips .

Fig B.18 (continued).



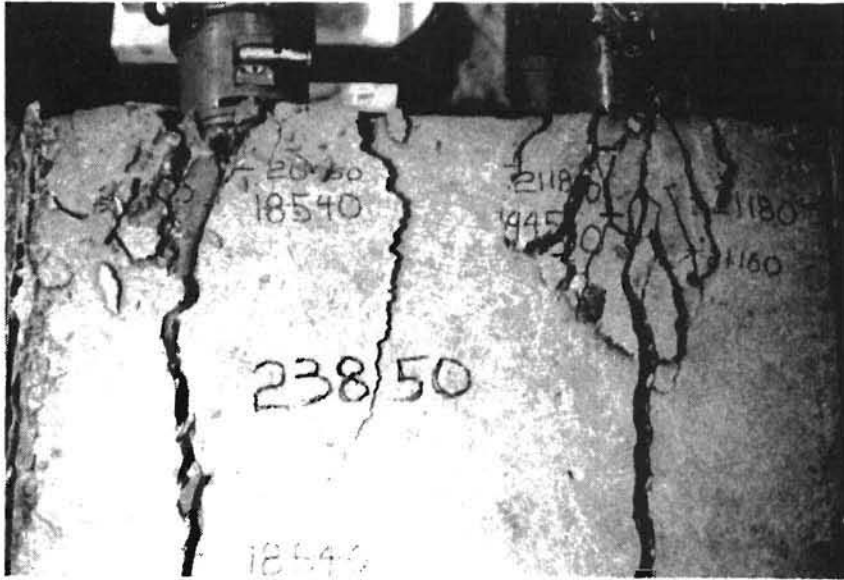
(a) Loading scheme of double strand slab.



(b) Ultimate failure at slab loading edge with some anchorage zone cracking.

(continued)

Fig B.19. Loading and failure of Specimen III 608-16A1-2.



(c) Ultimate failure at slab loading edge at 23.85 kips.

Fig B.19. (continued).



(a) First crack at 34.52 kips.



(b) Extended cracks at 37.11 kips.

(continued)

Fig B.20. Failure of Specimen III 608-16A1.

At 40.36 kips an explosive failure blew concrete cover completely away from the slab. Figure B.20(c) shows the slab after the failure.

III 808-16A1. At 9-1/2 hours the concrete strength was about 595 psi in compression, 70 psi in tension, and 200 psi in flexure. First cracking occurred at 43.79 kips along the tendon path, beginning slightly in front of the anchor and extending about 2 inches [see Fig B.21(a)]. As the load was increased the crack extended until the strand failed at 52.81 kips [see Fig B.21(b)].

III 808-12A1. Slab III 808-12A1 was tested at 10-1/2 hours. Concrete strength had increased to 760 psi in compression, 82 psi in tension, and 235 psi in flexure. At 48.95 first cracking occurred along the tendon path from the slab edge to a distance of 8-1/2 inches [see Fig B.22(a)]. The single crack extended as the load was increased until the tendon failed at 51.52 kips [see Fig B.22(b)].

III 808-24A1. Specimen III 808-24A1 was tested 11 hours after casting with concrete strength about 855 psi in compression, 100 psi in tension, and 255 psi in flexure. At a load of 51.52 kips a single crack along the tendon path, beginning 5-1/2 inches from the edge and extending 3 inches, was detected [see Fig B.23(a)]. The crack extended with increased load. Loading was complete when the strand broke at 54.10 kips [see Fig B.23(b)].

#### Twelve Hour Tests

III 612-16A1. Specimen III 612-16A1 was tested at 12 hours after casting. Concrete strength was about 1,050 psi in compression, 130 psi in tension, and 295 psi in flexure.

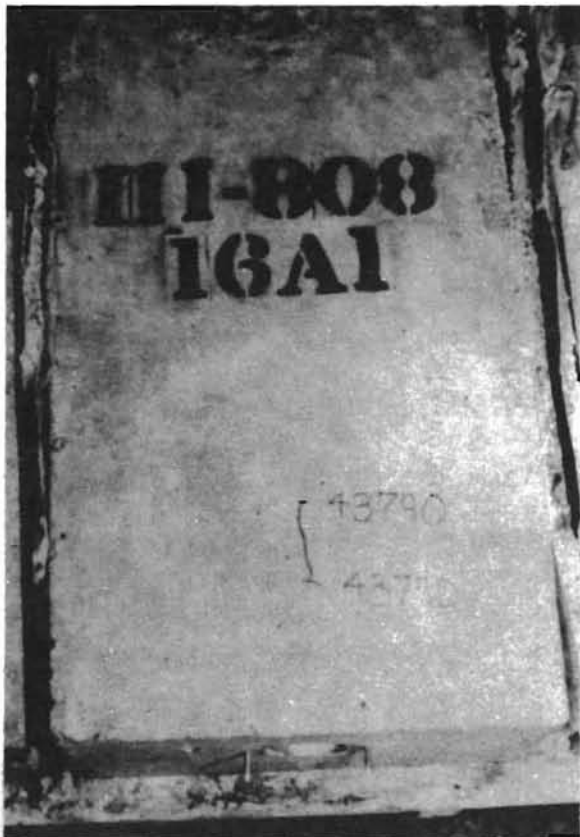
A single crack along the tendon path, beginning 1-inch from the edge and extending 7 inches into the slab, occurred at a load of 47.23 kips, as shown in Fig A.46. The crack grew 3 more inches with increased load until the strand failed at 50.23 kips (see Fig B.24).

III 812-16A1. Specimen III 812-16A1 was tested next, 12-1/2 hours after casting. Concrete strength was about 1,140 in compression, 145 in tension, and 315 in flexure.



(c) Ultimate failure at 40.36 kips.

Fig B.20. (continued).



(a) First crack at 43.79 kips.

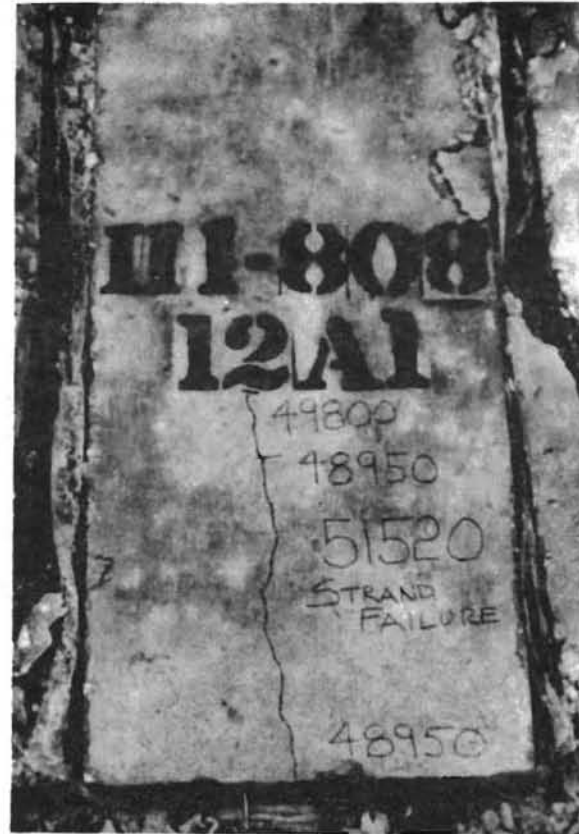


(b) Strand failure at 52.81 kips.

Fig B.21. Failure of Specimen III 808-16A1.

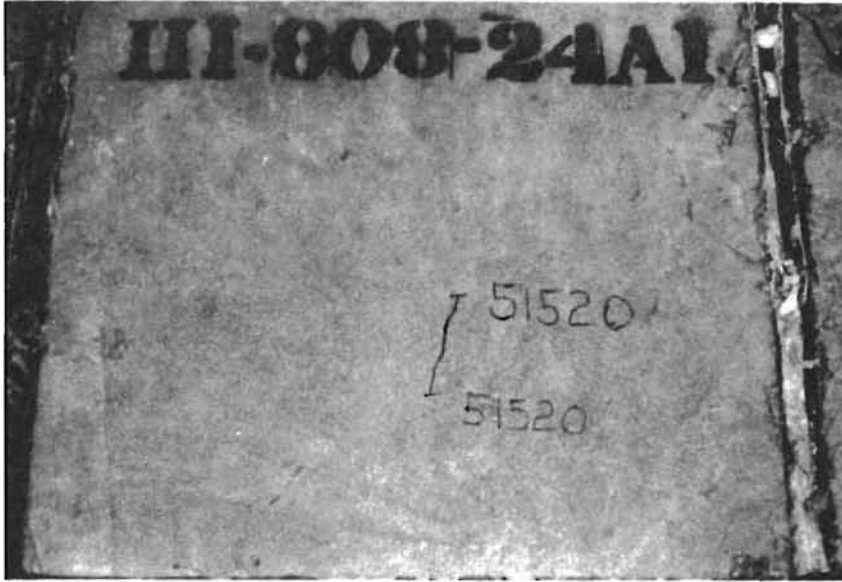


(a) First crack at 48.95 kips .



(b) Strand failure at 51.52 kips .

Fig B.22. Failure of Specimen III 808-12A1.



(a) First crack at 51.52 kips .



(b) Strand failure at 54.10 kips .

Fig B.23. Failure of Specimen III 808-24A1.



Fig B.24. First crack at 47.23 kips followed by strand failure at 50.23 kips for Specimen III 612-16A1.

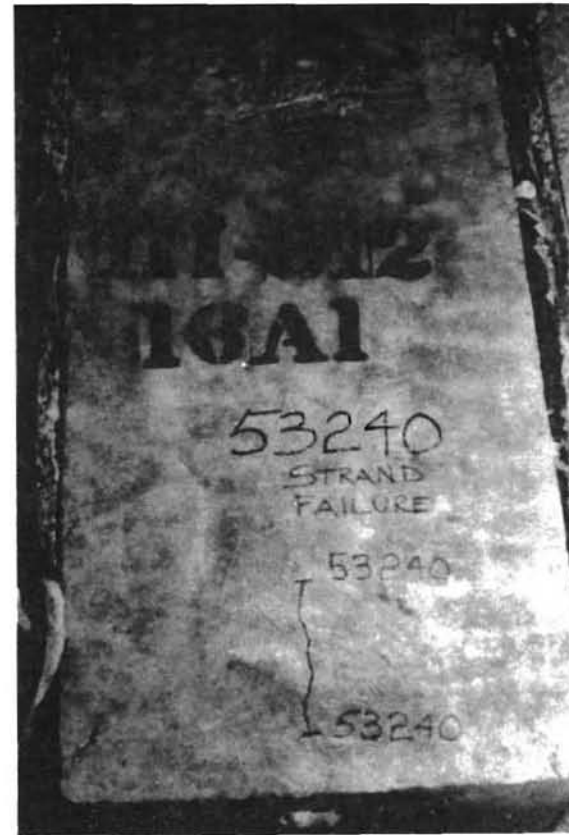


Fig B.25. First crack detected after strand failure at 53.24 kips for Specimen III 812-16A1.

The slab was stressed and checked for cracks but no cracks were noticed. At 53.24 kips the strand failed and the slab was checked for cracks one more. A slight crack formed, beginning 1-1/2 inches from the slab edge and extending 4-1/2 inches along the tendon path, as shown in Fig B.25.

III 812-24A1. Specimen III 812-24A1 was tested at 13 hours with concrete strength about 1,240 in compression, 160 in tension, and 334 in flexure.

The slab was stressed until the strand failed at 54.53 kips, but no cracks could be detected (see Fig B.26).

#### Sixteen-Hour Tests

With high concrete strengths and ultimate loads governed by strand failure, the sixteen-hour tests were performed beginning immediately after the twelve hour tests in order to obtain the most meaningful information. The objective was to obtain data for concrete cracking loads rather than strand ultimate loads.

III 816-24A1. At 13-1/2 hours after casting, specimen III 816-24A1 was tested. Concrete strength had increased to about 1,330 psi in compression, 175 psi in tension, and 350 psi in flexure.

The results were very similar to III 812-24A1. No cracks were detected after the strand failed at 54.10 kips. This specimen is shown in Fig B.27.

III 616-16A1. Specimen III 616-16A1 was tested at about 13-1/2 hours, also, so the concrete strength is the same as for Specimen III 816-24A1.

The first crack occurred along the tendon path beginning one inch from the slab edge and extending 5-1/4 inches at a load of 45.08 kips. At 51.09 kips the strand failed and the crack had extended out to the slab edge and in 1-3/4 inches. Photographs of the slab at first cracking and after the strand failures may be found in Fig B.28.

III 816-16A1. The final test was done 14 hours after casting. Concrete Strength was about 1,430 psi in compression, 190 psi in tension, and 370 psi in flexure.

The slab was loaded but no cracks were detected before the strand failed at 52.81 kips. After the strand failed, however, a crack was noticed along

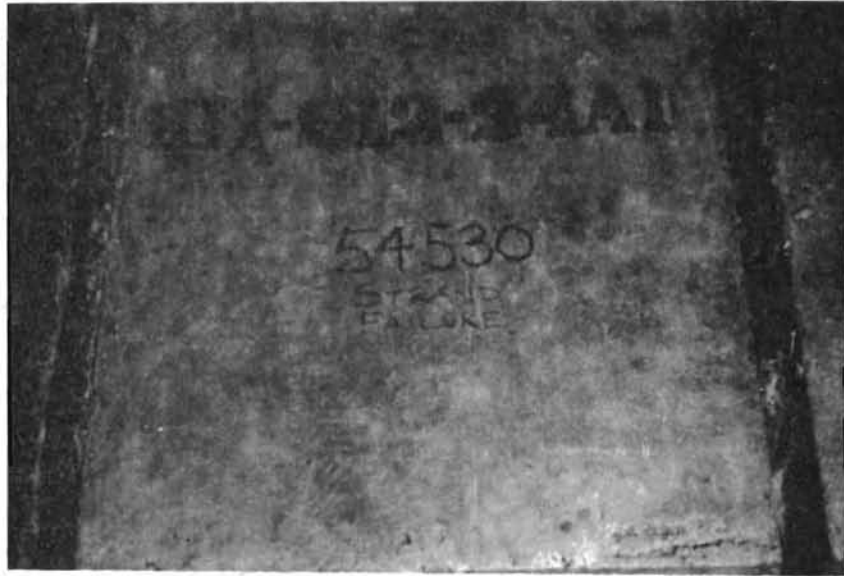


Fig B.26. Strand failure at 54.53 kips for Specimen III 812-24A1. No cracks detected.

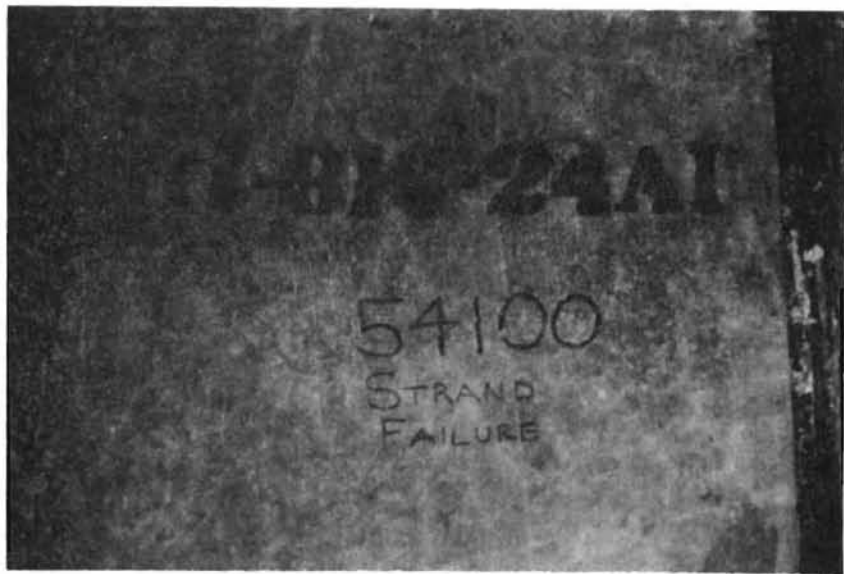


Fig B.27. Strand failure at 54.10 kips for Specimen III 816-24A1. No cracks detected.



(a) First crack at 45.08 kips.



(b) Strand failure at 51.09 kips.

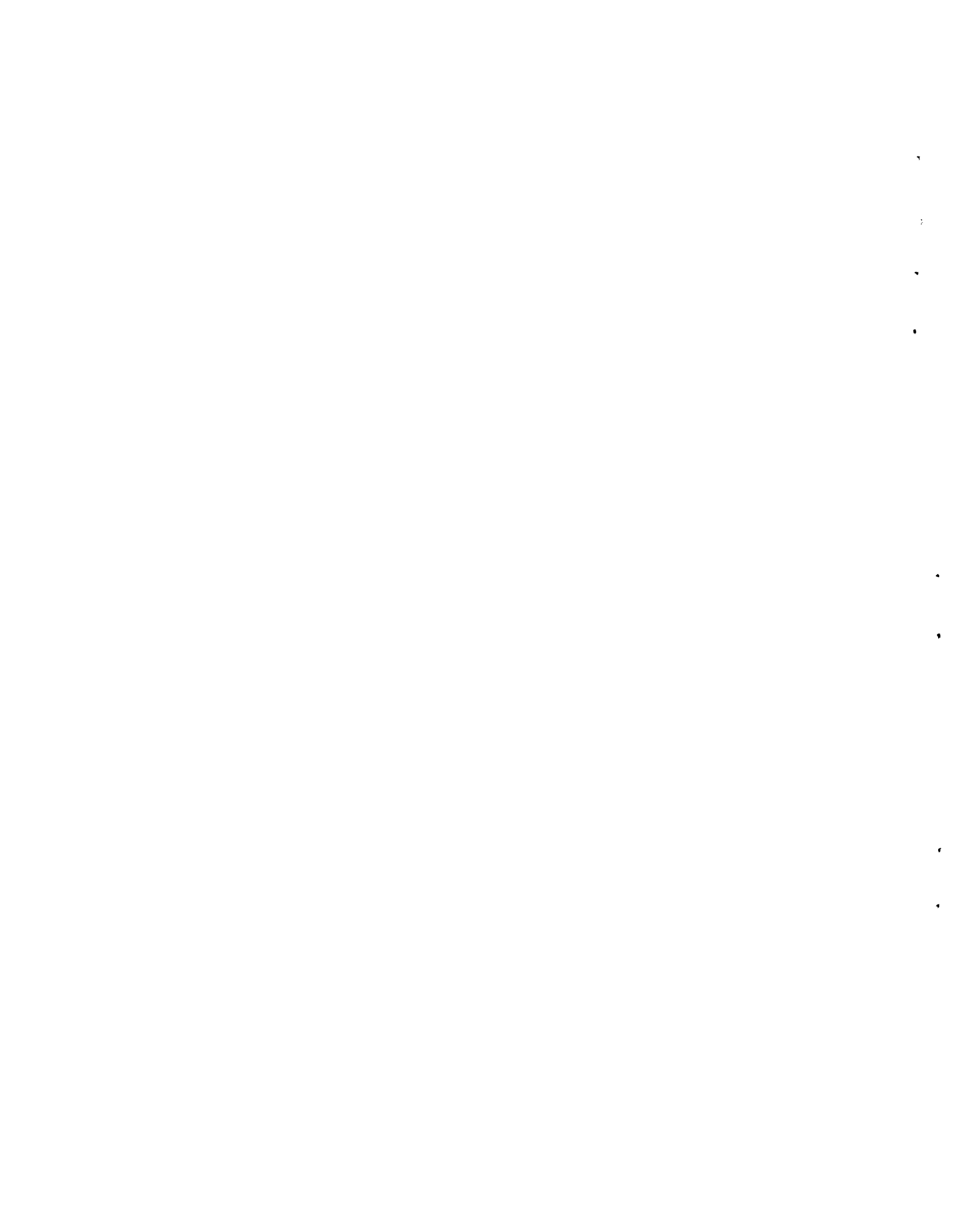
Fig B.28. Failure of Specimen III 616-16A1.

the tendon path beginning 2 inches from the edge and extending 4 inches (see Fig B.29).



Fig B.29. First crack detected after strand failure at 52.81 kips for Specimen III 816-16A1.

**APPENDIX C**  
**DESIGN AIDS USING CONCRETE COMPRESSION STRENGTH**



## APPENDIX C. DESIGN AIDS USING CONCRETE COMPRESSION STRENGTH

The following equation and figures are intended to be used as design aids for concrete compression strength rather than tensile strength, as used in Chapter 7.

$$\begin{aligned} P_{cr} = & 19.45 f'_{ci} + 19.27t + 0.295 (2a)(a'') - 105 \\ & - 0.064(t)(2a)(a'') - 0.294(f'_{ci})(t)(a'') \\ & + 0.037 (f'_{ci})^{1/2}(t)(2a)(a'') \end{aligned} \quad (C.1)$$

where

- $P_{cr}$  = estimated cracking load (kips),
- $f'_{ci}$  = concrete compression strength (ksi),
- $t$  = slab thickness (inches),
- $2a$  = strand spacing (inches), and
- $a''$  = anchor plate bearing area (inches<sup>2</sup>).

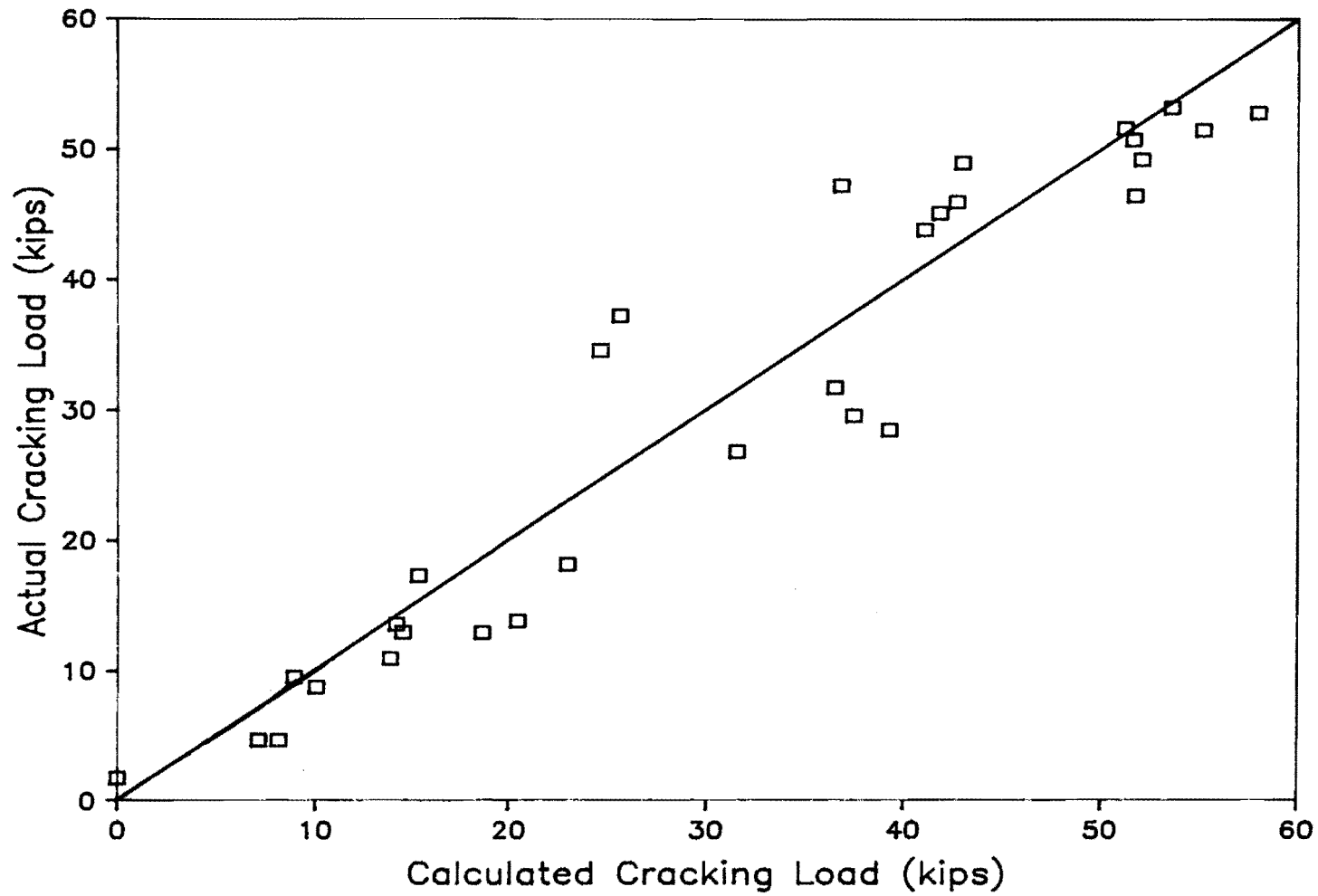


Fig C.1. Comparison of cracking load calculated using Eq. C.1 to actual cracking loads.

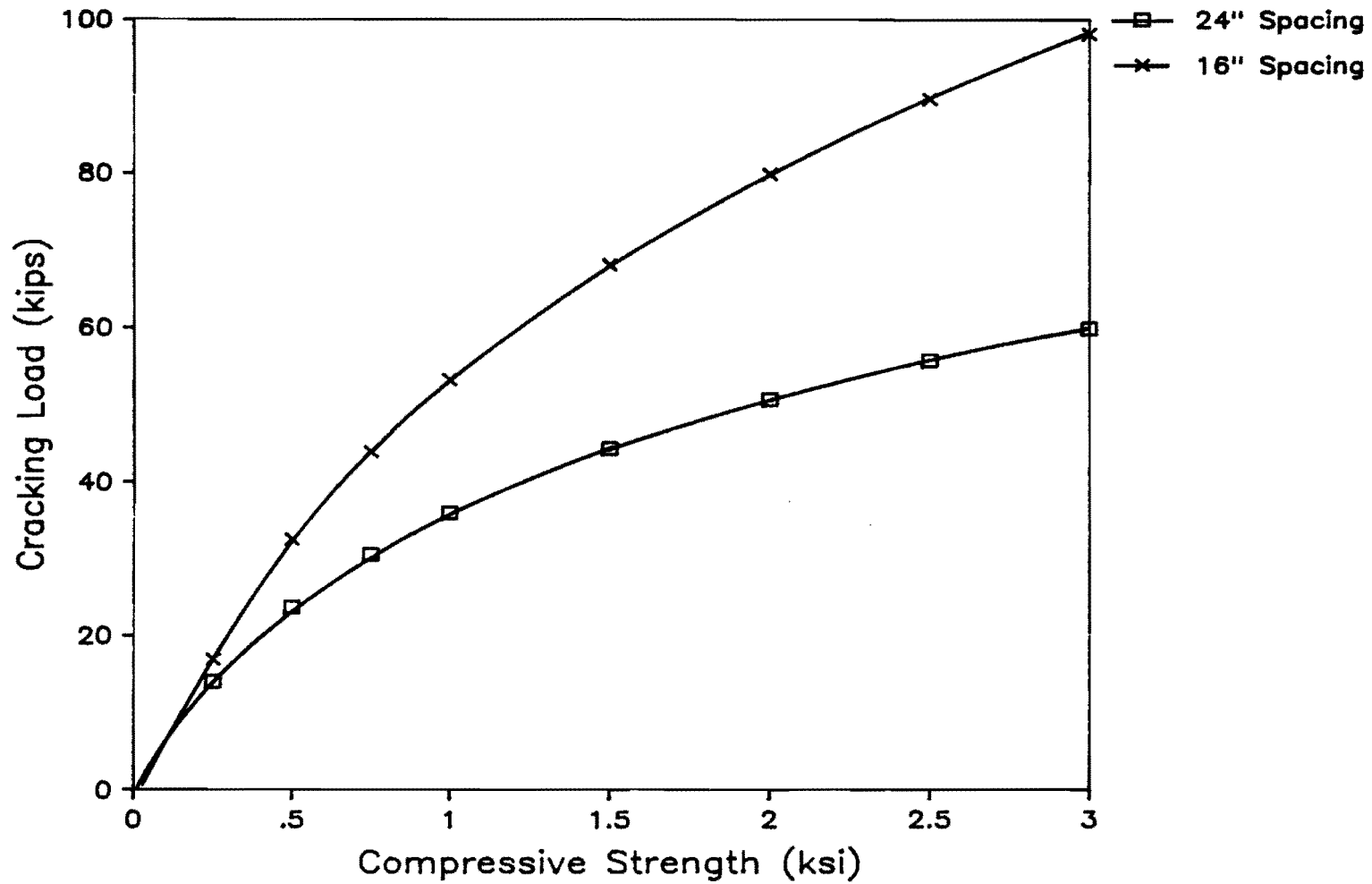


Fig C.2. Predicted cracking loads using Eq. C.1 for a 6 inch slab with 16 and 24 inch strands.

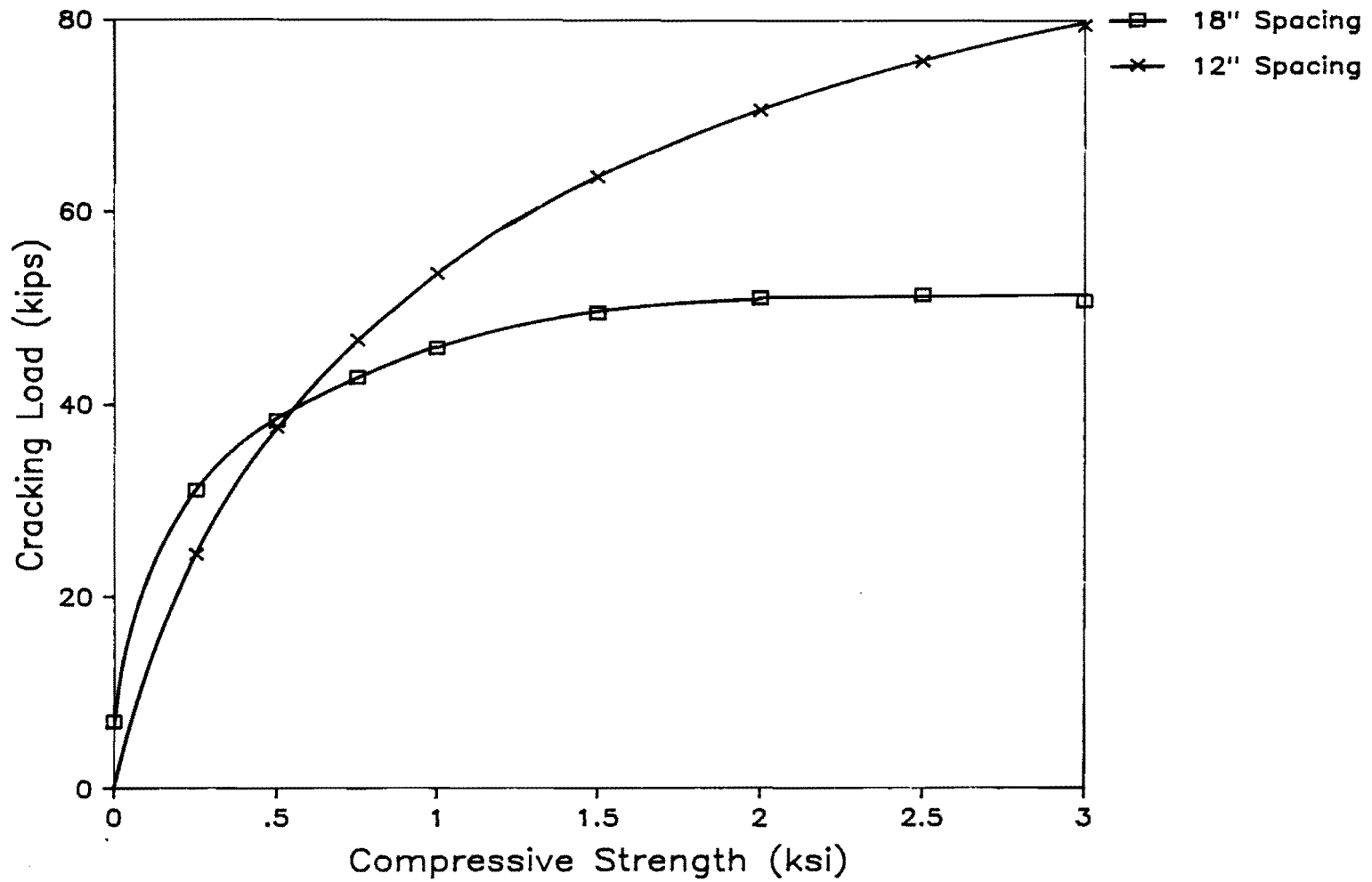


Fig C.3. Predicted cracking loads using Eq. C.1 for an 8 inch slab with 12 and 18 inch strand spacings.